

**Ultrasonic Impact Treatment of Traffic
Signal Mast Arm Welds**

by

Amanda Hope Palmatier, B.S.

Thesis

Presented to the Faculty of the Graduate School of
The University of Texas at Austin
in Partial Fulfillment
of the Requirements
for the Degree of

Master of Science in Engineering

The University of Texas at Austin

May 2005

**Ultrasonic Impact Treatment of Traffic
Signal Mast Arm Welds**

**Approved by
Supervising Committee:**

Supervisor: Karl H. Frank

Michael D. Engelhardt

Dedication

To my family:

I would not have succeeded without your continuous love and support. Thank you for restraining your requests for me to come home.

To my Austin family:

My time in Texas would have been wasted without you. Please try to restrain your requests for me to return.

Acknowledgements

I would like to thank the following people for all of the help that they have provided during the course of this research.

To Dr. Frank: Thank you for your guidance and mentoring. You have taught me so much more than what is covered in this thesis.

To Andy Creel: Thank you for all of your hard work. I would never have been able to conduct all my testing in a timely fashion without your help.

To Scott Walton, Jim Yang, Michael Smith, and Buck Witt: Thank you for your willingness to answer my questions.

To Blake Stasney, Mike Bell, Dennis Phillip and the rest of the FSEL staff: Thank you very much for your help during this project. You were always able to give me the assistance that I needed.

May 5, 2005

Abstract

Ultrasonic Impact Treatment of Traffic

Signal Mast Arm Welds

Amanda Hope Palmatier, M.S.E.

The University of Texas at Austin, 2005

Supervisor: Karl Frank

Ultrasonic Impact Treatment (UIT) has developed over the past few decades as a weld treatment with potential for great fatigue resistance enhancement. Prior research of traffic signal mast arm welds with UIT application indicates that UIT may significantly increase fatigue life of traffic signal structures. Currently UIT is being considered by the Texas Department of Transportation as part of the fabrication process of new traffic signal mast arms, as well as a potential retrofit for in-service traffic signal structures. This study was initiated to investigate UIT as a viable retrofit for in-service traffic signal structures, as well as to investigate aspects of UIT application specific to Texas traffic signal mast arm welds.

Table of Contents

CHAPTER 1 INTRODUCTION.....	1
1.1 Traffic Signal Mast Arms.....	1
1.2 Ultrasonic Impact Treatment (UIT).....	3
1.2.1 Previous Research on UIT Application to Mast Arm Welds.....	4
1.3 Scope of Work.....	8
CHAPTER 2 TEST SETUP.....	11
2.1 Test Setup Assumptions.....	11
2.2 Test Setup Design.....	13
2.3 Mast Arm Weld Molds.....	18
2.3.1 Equipment.....	18
2.3.2 Procedure.....	18
CHAPTER 3 UIT APPLICATION TO BOTH WELD TOES.....	20
3.1 Introduction.....	20
3.2 Background Information.....	22
3.3 Investigation Procedure.....	23
3.4 Investigation results.....	25
3.5 Conclusions and Recommendations.....	28

CHAPTER 4 GALVANIZATION REPAIR AFTER UIT APPLICATION.....	29
4.1 Introduction.....	29
4.2 Previous Research.....	30
4.3 Heat-Applied Zinc-Lead Solder Galvanization Repair Tests.....	32
4.3.1 Equipment	33
4.3.2 Test Setup.....	34
4.3.3 Pre-Treatment Static Tests	34
4.3.4 Heating and Galvanization.....	36
4.3.5 Post-Treatment Static Tests.....	37
4.4 Results.....	37
4.5 Discussion.....	44
4.5.1 Comparison to Previous Tests.....	45
4.5.2 Heat-Applied Galvanization Repair Problems.....	45
4.5.3 Non-Contact Thermometer Problems	46
CHAPTER 5 UIT APPLICATION DURING FABRICATION	47
5.1 Introduction.....	47
5.2 Training Session	48
5.3 Afternoon Fabrication Yard UIT Application Training	49
5.3.1 Test Setup.....	49
5.3.2 UIT Application Demonstration	54
5.3.3 Inspection by a TxDOT Inspector.....	60
5.3.4 Repair of Galvanizing	63
5.3.5 Removal of Mast Arm from Fixed Testing Stand.....	65
5.3.6 Trained Technician Treatment Times	66

5.4	Application of UIT by Trained Employees	66
5.4.1	Employee’s UIT Application Times	68
5.5	Discussion.....	69
5.5.1	Trained Applied Ultrasonics Technician Treatment vs Trained TransAmerican Employee Treatment	69
5.5.2	UIT Application Concerns.....	70
CHAPTER 6 FIELD UIT APPLICATION.....		71
6.1	Introduction.....	71
6.2	Location of Mast Arms.....	71
6.2.1	Traffic Control	75
6.2.2	UIT Application	75
6.2.3	Inspection	78
6.2.4	Application Times.....	78
6.2.5	Weather Conditions.....	79
6.3	Miscellaneous Observations.....	79
CHAPTER 7 FATIGUE TEST SETUP DETAILS.....		81
7.1	Introduction.....	81
7.2	Test Specimens.....	81
7.3	Test Setup Revisions	84

CHAPTER 8 UIT RETROFIT TEST RESULTS.....	86
8.1 Introduction.....	86
8.2 Static Tests.....	86
8.3 Dynamic Tests	92
8.4 Fatigue Test Results.....	98
8.5 Discussion.....	99
8.5.1 Field UIT Application vs. Fabrication Yard UIT Application.....	99
8.5.2 Effect of Base plate Thickness	101
8.5.3 Weld Toe Geometry	102
CHAPTER 9 CONCLUSIONS AND RECOMMENDATIONS.....	107
9.1 Conclusions.....	107
9.2 Recommendations for Further Research	108
APPENDIX A PREVIOUS RESEARCH	110
A.1 Previous Research Geometries	110
A.2 Previous Test Results.....	112

APPENDIX B LITERATURE REVIEW – PART 1: HISTORY OF ULTRASONIC IMPACT TREATMENT (UIT)	114
B.1 History of Ultrasonic Impact Treatment (UIT)	114
B.2 UIT Machine Composition	115
B.3 UIT Benefits.	117
B.4 Machine Specifications.....	117
B.4.1 Energy Transform	117
B.4.2 Pathways of Energy Transfer	118
B.4.3 Different UIT Machine Options Available	120
B.5 UIT Application Parameters	120
B.5.1 Frequency	121
B.5.2 Pin Diameter.....	121
B.5.3 Amplitude.....	121
B.5.4 Speed.....	122
B.5.5 Application Angle	122
B.5.6 Treatment Pressure	122
B.5.7 Application Movement.....	122
B.5.8 Number of Passes with the Ultrasonic Impact Tool.....	123
B.5.9 Multi-Pass Welds	123
B.5.10 UIT Application Groove Appearance	123
B.6 How to Choose UIT Application Parameters	124
B.6.1 Optimum Application Software	124
B.6.2 Single vs. Multi-Element Tool.....	124

B.7 Where UIT Equipment is Produced..... 125

**APPENDIX C LITERATURE REVIEW – PART 2: FATIGUE ENHANCEMENT
FROM UIT APPLICATION 126**

C.1 Introduction.... 126

C.2 Endurance Limit 126

C.2.1 Butt Welds..... 128

C.2.2 Fillet Welds 130

C.2.3 Cruciform Joints..... 133

C.3 Fatigue Life Improvement 134

C.3.1 Butt Welds..... 135

C.3.2 Fillet Weld..... 137

C.3.3 Cruciform Joints..... 138

C.4 Impact of UIT on Stress Range and Endurance Limit..... 140

C.5 Effect of Steel Grade on UIT..... 141

C.6 Long vs. Short Life..... 143

C.7 Fatigue Crack Initiation 144

C.7.1 As-Welded Steel Specimens 144

C.7.2 UIT Steel Specimens 144

C.8 UIT in Temperature Extremes 146

C.8.1 Cool Temperatures 146

C.8.2 Heated Conditions 147

C.9	UIT in a Corrosive Fatigue Environment	147
APPENDIX D LITERATURE REVIEW – PART 3: EFFECT OF UIT		148
D.1	Introduction.....	148
D.2	Weld Toe Geometry Improvement.....	148
D.3	Residual Stresses	150
D.3.1	Depth of Compressive Residual Stress	151
D.3.2	Cause of Compressive Stresses	152
D.3.3	Fatigue Crack Prevention.....	152
D.4	Structure and Mechanical Properties.....	153
D.4.1	Grain Size Reduction	153
D.4.2	Reduction in Grain Size Distribution.....	154
D.4.3	Grain Elongation	155
D.4.4	Creation of Cementite Along Pearlite Grain Boundaries.....	156
D.4.5	Steel Hardening	158
APPENDIX E LITERATURE REVIEW – PART 4: UIT VS. OTHER METHODS OF WELD TREATMENT		160
E.1	Introduction.....	160
E.2	Hammer and Shot Peening	162
E.2.1	Fatigue Crack Initiation from Hammer and Shot Peening.....	162
E.2.2	Extent of Compressive Layer for Hammer and Shot Peening	163
E.2.3	Fatigue Improvement from Hammer Peening.....	163
E.3	TIG Remelting	164
E.3.1	Fatigue Crack Initiation from TIG Only	164
E.3.2	Weld Toe Geometry Improvement from TIG Remelting	165

E.3.3 Hardness from TIG Remelting	165
E.3.4 Residual Stresses of TIG Remelting	165
E.3.5 Fatigue Improvement from TIG Remelting	166
E.4 TIG Remelting Followed By UIT	168
E.4.1 Fatigue Crack Initiation from TIG Followed by UIT	168
E.4.2 Fatigue Improvement from TIG Followed by UIT	168
E.5 Sand Blasting	169
E.5.1 Fatigue Strength Enhancement	169
E.6 Low Transformation Temperature Electrodes.....	170
E.6.1 Fatigue Improvement from LTTE3.....	170
E.7 Conclusion... ..	171
REFERENCES.....	172
VITA	175

CHAPTER 1

Introduction

1.1 TRAFFIC SIGNAL MAST ARMS

Previous research by Mark Koenigs at the University of Texas at Austin investigated traffic signal structure failures [28]. The traffic signal structures investigated by both Koenigs and the author are cantilever single mast arm traffic signal structures with round tapered poles. Traffic signal structures are comprised of two members: the vertical member, referred to as the mast, and the horizontal member, referred to as the mast arm. Figure 1.1.1 shows a typical single mast arm cantilever traffic signal structure.



Figure 1.1.1 Typical Cantilever Traffic Signal Structure

Traffic signal mast arm-base plate connections are particularly susceptible to fatigue [28]. The top of traffic signal mast arm welds experience fluctuating tensile stresses when wind and traffic gust loads cause the mast arm to oscillate, fatiguing the mast arm weld toe [28]. The mast arm fluctuates vertically under wind loads. Horizontal movement from wind loading is minimal [28]. The most common location of fatigue failure on traffic signal structures is the fillet-welded socket connection of the mast arm to the mast arm base plate [28]. The mast arm is welded to the base plate, and the base plate is in turn bolted to a built-up box, which is part of the mast. A typical base plate-to-mast bolted connection is shown in Figure 1.1.2.



Figure 1.1.2 Mast Arm Base Plate-to-Built-up Box Bolted Connection

The signal structure components are shop welded and then galvanized by the supplier. The components are then connected in the field using high strength bolts.

1.2 ULTRASONIC IMPACT TREATMENT (UIT)

Ultrasonic Impact Treatment (UIT) is a weld treatment that increases fatigue life of treated welds [3, 4]. UIT equipment is light [3, 11, 12, 16] and easy to learn [7, 17, 20]. UIT is applied to weld toes to improve weld toe profiles and induce a compressive residual stress [9, 19]. UIT requires a power generator, a water cooler, and the UIT generator, as explained in Appendix B. The UIT generator creates ultrasonic oscillations that pass through a waveguide to the UIT tool. The UIT tool operates at 27 kHz, creating a groove along the application line. The UIT tool can be either a single- or multi-pin tool, with pins of diameters ranging from 2 mm to 16 mm. The size of the pin dictates the diameter of the groove created. Figure 1.2.1 shows the UIT tool. UIT equipment is produced in the United States by Applied Ultrasonics, Inc. A review of research to date on the effects of UIT is included in Appendices B through E.



Figure 1.2.1 UIT Multi-Pin Tool With Two 2 mm Diameter Pins

1.2.1 Previous Research on UIT Application to Mast Arm Welds

Previous research at the University of Texas at Austin investigated the effects of UIT application to mast arm welds [28, 29, 30]. Fatigue tests were performed on mast arm welds with and without UIT. Mast arms had UIT application under both loaded and unloaded conditions. The test setup is described in Chapter 2.

Koenigs performed fatigue tests on similar mast arm specimens, both with and without UIT application along the mast arm weld toe [28]. These tests showed that UIT increases fatigue resistance of mast arms, but only when UIT is applied under loaded conditions.

Koenigs conducted tests in two phases [28]. Phase 1 tests included similar mast arms that had mast arm welds both with and without UIT application. All UIT applications to mast arm welds in Phase 1 were performed at zero load. All stresses are calculated at the mast arm weld toe. All mast arms of Phase 1 were tested at a stress range of 12 ksi. All but one mast arm of Phase 1 was tested at a maximum stress of 28.5 ksi. The one mast arm that was not fatigue tested at a maximum stress of 28.5 ksi was mast arm TX3x3/8 CP LMS. Mast arm TX3x3/8 CP LMS was similar to all other mast arms with UIT application of Phase 1, except that mast arm TX3x3/8 was fatigue tested at a maximum stress of 14 ksi instead of 28.5 ksi. The results of Phase 1 show that both mast arms with and without UIT tested at a maximum test stress of 28.5 ksi showed no improvement in fatigue life. However, the mast arm with UIT and a maximum test stress of 14 ksi showed a significant fatigue life improvement [28]. The test conditions and results for the Phase 1 tests are given in Appendix A. Figure 1.2.1.1 shows the S-N plot of the Phase 1 test specimens. Both axes of the plot are log scale. Specimens with UIT and tested at a maximum stress of 28.5 ksi are labeled “Phase 1 UIT – 28.5 ksi”. The one specimen with UIT and tested at a maximum

stress of 14 ksi is labeled “Phase 1 UIT – 14 ksi”. Figure 1.2.1.1 shows that the specimen “Phase 1 UIT – 14 ksi” had the greatest improvement in fatigue resistance.

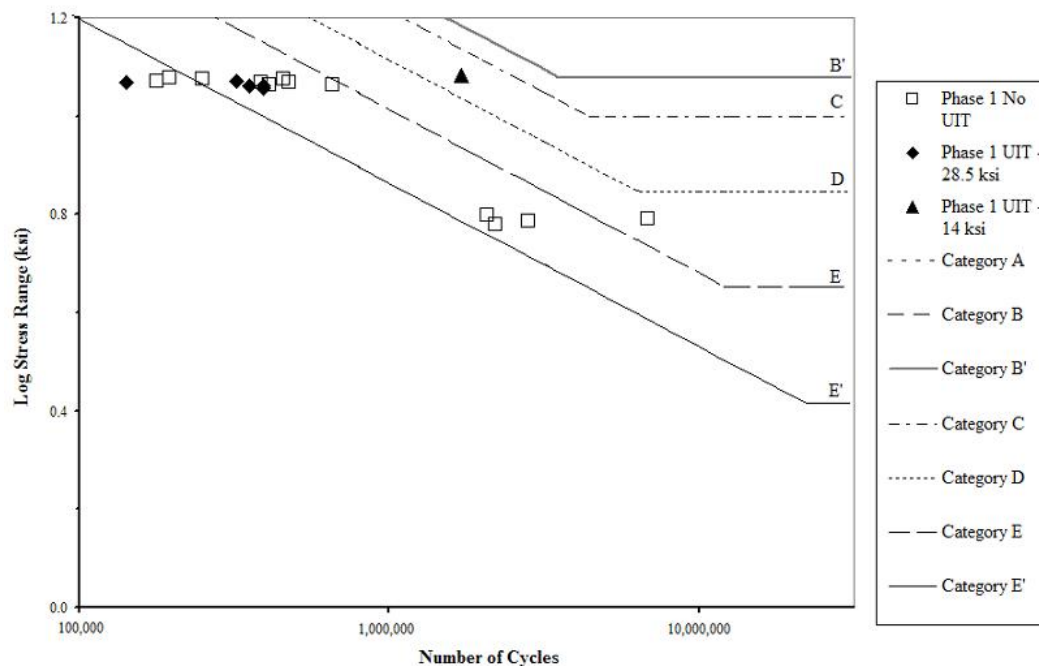


Figure 1.2.1.1 S-N Plot of Koenigs' Phase 1 Mast Arms With and Without UIT

Phase 2 of Koenigs' tests included mast arm specimens both with and without UIT. Since the mast arm in Phase 1 with the highest increase in fatigue life was the mast arm with maximum test stress closer to the treatment stress, Koenigs' Phase 2 test specimens with UIT application had UIT applied under a 16.5 ksi stress [28]. The test conditions and results for the Phase 2 tests are given in Appendix A. Figure 1.2.1.2 shows the S-N plot of the Phase 2 test specimens. Both axes of the plot are log scale. Specimens with UIT and tested at a stress range of 12 ksi are labeled “Phase 2 UIT – 12 ksi”. Specimens with UIT and

tested at a stress range of 20 ksi are labeled “Phase 2 UIT – 20 ksi”. All fatigue testing in Phase 2 had a maximum stress of 28.5 ksi. Figure 1.2.1.2 shows that mast arms with UIT applied at a 16.5 ksi stress had a significant improvement in fatigue resistance over mast arms with no UIT. The data for tests on mast arms with UIT application before hot-dip galvanization is not included, due to the negative effect that extreme heat has on UIT, which is discussed in Chapter 4.

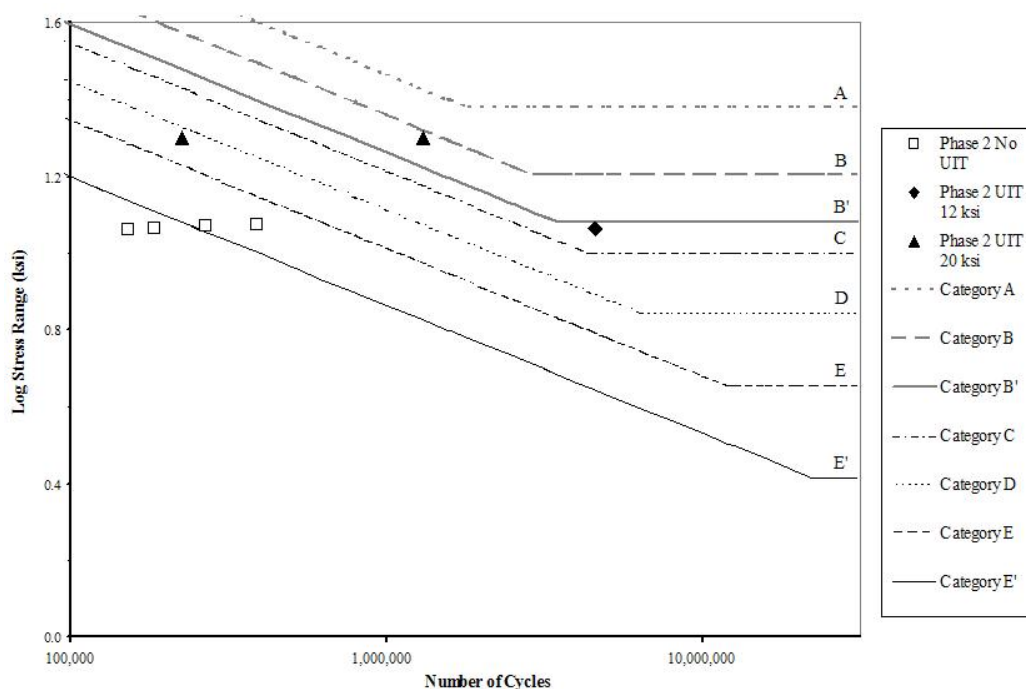


Figure 1.2.1.2 S-N Plot of Koenigs' Phase 2 Mast Arms With and Without UIT

Dylan Freytag conducted fatigue tests of mast arms from TransAmerican both with and without UIT were tested at the Ferguson Laboratories at the University of Texas at Austin [29, 30]. Mast arms from TransAmerican had UIT applied under loaded conditions at TransAmerican’s fabrication yard. The UIT application process is described in Chapter 6. Test setup is described in Chapter

2. Appendix A lists the fatigue results and test conditions of the mast arms from TransAmerican both with and without UIT application. Figure 1.2.1.3 shows the S-N plot of the test results from the TransAmerican mast arms. The mast arms from TransAmerican without UIT are labeled “TA”. The mast arms from TransAmerican with UIT applied under loaded conditions are labeled “TAU”. Figure 1.2.1.3 shows that mast arms with UIT applied under loaded conditions have an increase in fatigue life compared to mast arms with no UIT.

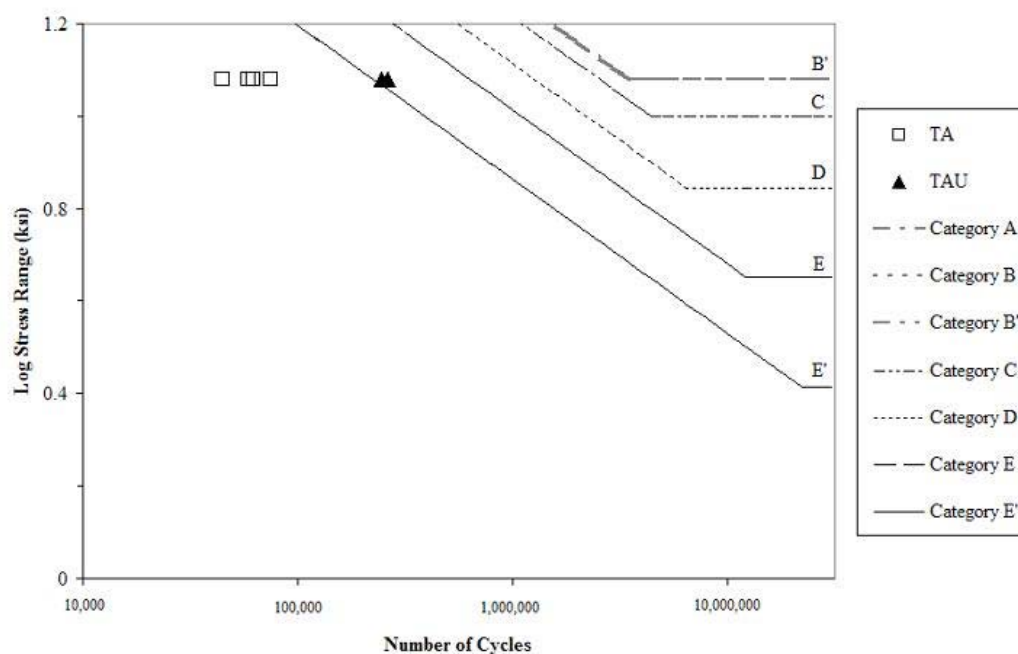


Figure 1.2.1.3 S-N Plot of TransAmerican Mast Arms With and Without UIT

Fatigue Provisions of 2001 AASHTO Highway Signs, Luminaires, and Traffic Signal Specifications classify mast-arm-to-flange plate socket connections, such as the fillet-welded connections under investigation, as Category E'. As shown in Figure 1.2.1.1, Figure 1.2.1.1, and Figure 1.2.1.3, most mast arms without UIT performed at or below fatigue Category E'. Some

mast arms without UIT performed at Category E. One mast arm without UIT had a fatigue resistance above Category D. Also, there is some variance in geometries that prevents accurate comparisons. The effect of baseplate thickness is discussed in Chapter 8. Figure 1.2.1.1 shows that mast arms with UIT applied under zero load with high maximum stress have no increase in fatigue life. Figure 1.2.1.1, Figure 1.2.1.2, and Figure 1.2.1.3 show that mast arms with UIT applied under loaded conditions have fatigue resistances at least above Category E', with improvements above Category D and even above Category B'. These improvements affirm the potential fatigue resistance improvement by UIT, and prompt the research conducted in the remainder of this thesis.

1.3 SCOPE OF WORK

Koenigs' and Freytag's research of TransAmerican's mast arms proved that mast arm fatigue lives improve when UIT is applied under loaded conditions [28, 29, 30]. Research shows that UIT applied in the fabrication yard and in the laboratory under loaded conditions increased fatigue lives of mast arms. The purpose of the current research is to further explore the intricacies of UIT application to mast arm welds.

Aspects of UIT application to mast arm welds that have not been adequately researched in previous papers to date include whether UIT application should include one or both toes of mast arm weld toes, and galvanization repair techniques (see Appendices B through E). Chapter 3 presents an investigation by the author of unusual fatigue cracking in two previously fatigue tested mast arm welds with UIT application, and presents UIT application to both mast arm weld toes as a solution to prevent future irregular fatigue cracking.

UIT application removes slag and galvanizing. UIT application to mast arm welds removes galvanizing, which creates a need for galvanization repair. Chapter 4 contains research by the author into Applied Ultrasonic's concerns of using heat-applied galvanization repair after UIT application.

One possible function of UIT that has not been explored in previous research is retrofit of existing mast arms to increase fatigue life. The Texas Department of Transportation (TxDOT) was very interested in the possibility of UIT retrofit for in-service mast arms. To investigate this possibility, the author fatigue tested two mast arms from the same intersection in Denton, TX with similar load histories. One mast arm was chosen arbitrarily to be the control specimen and was removed from the field without any alterations. The other mast arm was the experimental mast arm, and had UIT application as a retrofit under field conditions five months prior to removal from the field. After removal from the field, the Denton mast arms were shortened to 8 feet in length and transported to Ferguson Laboratories at the University of Texas at Austin for fatigue testing. Details of the UIT retrofit procedure are presented in Chapter 6. Descriptions of the mast arm geometries are detailed in Chapter 7. The test setup for the Denton mast arms, as well as for all fatigue tests of mast arms at the University of Texas, is described in Chapter 2. Chapter 8 presents the results from the fatigue tests, including S-N charts comparing the current research to previous data in order to draw conclusions on the effectiveness of UIT retrofit to in-service mast arms.

Based on the results of this and other research [28, 29, 30], UIT application may become a common addition to mast arms in Texas. Since UIT application to mast arms is a new process, Chapter 5 presents a critical review of UIT application at a fabrication plant. The review includes observations from the first day of UIT application training at a fabrication plant, including teaching and application times. Comparisons of UIT application at the fabrication yard and as

retrofit are included in Chapter 9. Chapter 9 also includes a synopsis of conclusions from Chapters 3 through 8, as well as recommendations for future research.

CHAPTER 2

Test Setup

2.1 TEST SETUP ASSUMPTIONS

All efforts were made to match the test setup that was used in Koenigs' research [28]. This was done to allow comparison between current tests and previous tests at the University of Texas at Austin.

Mast arms were shortened to approximately 85 inches in length before fatigue testing at Ferguson Laboratory at the University of Texas at Austin. The mast arm was shortened by making a cut at approximately 85 inches from the mast arm's base plate. A 1 inch thick end plate was welded to the cut end of the mast arm.

Using Koenigs' assumptions, the moment diagram for any cantilever traffic signal structure was greatly simplified to be represented as shown in Figure 2.1.1 [28]. In this figure, the mast-arm is simply a cantilevered beam. To transform this service loading into a testing apparatus, two mast-arms were tested back to back so that the structure could be modeled as a simply supported beam, as shown in Figure 2.1.2 [28]. In this test setup, the critical connection details and loading were both located in the center of the beam. The symmetry of the test setup allowed two specimens to be tested at once and did not require construction of a fixed support.



Figure 2.1.1 Moment Diagram Superimposed on Cantilever Mast Arm

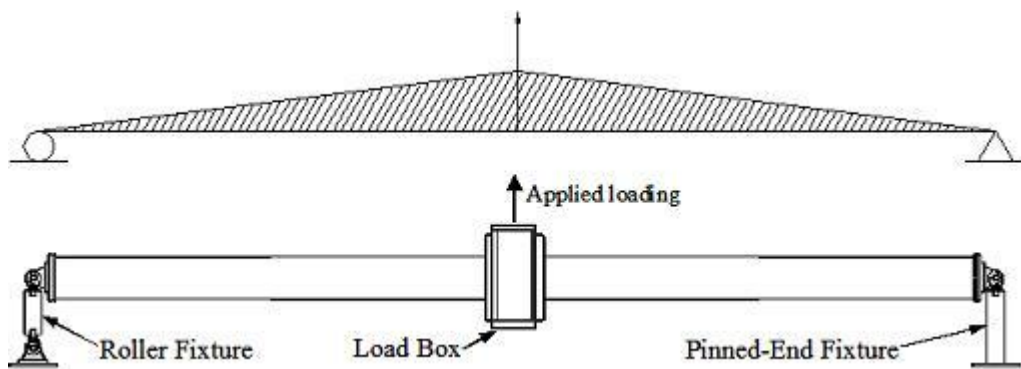


Figure 2.1.2 Test Setup Design with Simply Supported Beam Analogy [28]

2.2 TEST SETUP DESIGN

All tests were designed so the top of the mast arm and the actuator would remain in tension. The system was stable when the actuator was in tension, and unstable when the actuator is in compression. When the actuator went into compression the system became unstable and the test setup moved out of plane. If the actuator was allowed to run through compression cycles, lateral bracing would have been required.

The specimens were tested in pairs with the base plates bolted to a load box, and the end plates bolted to end restraints. The base plate was bolted to the load box using all-thread rods approximately 1 foot in length. The end plate was bolted to end restraints with high-strength steel bolts. Figure 2.2.1 shows the test setup with mast arms in place. The end restraint in the right of the photo allowed for rotation only of the mast arm end. The end restraint in the far left of the photo allowed for both rotation and translation of the mast arm end. Rotational freedom was provided by a lubricated ball clevis at each end.



Figure 2.2.1 Test Setup with Mast Arms

Each fixed end consisted of a riser section and one or two spherical rod eyes and clevises. The spherical rod eye allowed for corrections due to alignment imperfections. Figure 2.2.2 shows the end hardware that allowed for rotation only. This hardware consists of a single fixed riser section connected to a spherical rod eye and clevis. Figure 2.2.3 shows the end hardware that allowed for rotation and translation. This hardware consists of a single riser section between two spherical rod eyes and clevises.



Figure 2.2.2 End Restraint that Allows for Rotation Only



Figure 2.2.3 End Restraint that Allows for Rotation and Translation

The load box is visible between the two mast arms in Figure 2.2.1. The load box in this setup was drilled to accommodate different baseplate hole spacing. The load box was bolted to a 22 kip closed loop controlled loading actuator with a swivel. The ram used in this system was an MTS hydraulic actuator controlled by an MTS 407 Controller. Hydraulic pressure was provided by an external pump supplying 3000 psi constant pressure. An MTS 290 Hydraulic Service Manifold was connected between the pump and actuator.

The goal was to test the mast arms at a desired stress range. Usually fatigue tests are run under load control. However, the computer system running the fatigue tests worked best under displacement control, according to the head laboratory technician. Hence, tests were run under displacement control. Running the fatigue tests under displacement control had the added advantage of eliminating any dynamic amplification of loads. Displacements for the dynamic tests were determined during static tests.

Static tests started after specimens were secured in the test setup as described in Chapter 8. Strain gauges were attached at desired locations, which are described in Chapter 8. One strain gauge along the mast arm, located 3 inches from the base plate connection, collected data to confirm that the mast arm was experiencing the calculated strain range, and hence the calculated stress range. Additional strain gauges were applied at locations that may lead to increased understanding of mast arm fatigue behavior.

During the static tests, mast arms were subjected to a simple up and down load pattern from a load of 0 kip to the maximum load and back to 0 kip in 1 kip increments. During the static test, displacements and strains were measured. Static tests also include measurements at the minimum load.

The dynamic test was run under displacement control. The displacements corresponding to the calculated maximum and minimum loads were determined during static tests. The mast arms were subjected to sinusoidal cyclic loading between the maximum and minimum displacement. The frequency of the cyclic loading varied depending on the geometries of the mast arms. The specifics of previous dynamic tests are included in Appendix A. The specifics of the current research's dynamic tests are included in Chapter 8.

The dynamic tests were run to failure. Failure was defined as a 5% drop in load carrying capacity.

After one mast arm specimen failed, the test was stopped. The mast arm that failed was repaired to allow continuation of testing under the same load conditions until failure of the second mast arm specimen. When the first mast arm failure could not be repaired, an acceptable replacement was found. The most common acceptable replacements were previously failed mast arms from the same test series that were repaired after failure.

2.3 MAST ARM WELD MOLDS

In order to measure the long leg, short leg, and global angle of mast arm welds, molds of the welds were made. Once the mold has been cast, the weld geometry was measured using specialty measuring equipment described in Chapter 8.

2.3.1 Equipment

All molds consisted of Silastic M and its corresponding catalyst, both produced by Dow Corning. The Silastic M was a white, silly-putty-like substance. The catalyst was a blue liquid. A Styrofoam cup, a plastic spoon, and electronic scale were also needed for preparation of the mold.

Wax-based sculpting clay, clay-sculpting tools, a Plexiglas plate, a rag, and a cutting tool were needed to prepare the dam that contains the mold.

2.3.2 Procedure

First, the area to have a mold taken was cleaned with acetone and a rag. Next, three pieces of wax-based sculpting clay were cut with the cutting tool on the Plexiglas plate. The wax-based sculpting clay is cut into approximately 2" x

2" x 1/4" pieces. These three pieces of clay were used as three walls to contain the mold material. The base plate of the weld area created the fourth wall, and the mast arm was the floor. The sculpting tool was used to smooth the clay against the mast arm and base plate.

Silastic M and the catalyst were mixed in the Styrofoam cup in a 10:1 Silastic M-to-catalyst ratio. Molds of mast arm welds commonly require about 150 g of Silastic M and 15 g of catalyst. The mixture was mixed until no white streaks existed in the mixture.

When the mold was mixed and the clay dam was in place, the mold mixture was poured into the dam. It took at least 16 hours for the material to set completely. Figure 2.3.2.1 shows a complete clay dam filled with the molding material for a mast arm weld.



Figure 2.3.2.1 Clay Dam Filled with Molding Material

CHAPTER 3

UIT Application to Both Weld Toes

3.1 INTRODUCTION

UIT should be applied so that it creates a groove with a width that indents approximately half upon the weld metal and half upon the base metal heat affected zone (HAZ). When the groove width is not applied evenly, the width should cover more of the base metal HAZ than the weld metal [9].

Previous test results show that welds in steel treated with UIT have had fatigue crack initiation in the UIT application line [5, 6, 12, 15, 28]. Fatigue crack initiation has mainly occurred at the mast arm weld toe, and the fatigue crack propagation has mainly been through the HAZ of the mast arm base metal [28, 29, 30]. Koenigs' and others' tests with UIT application to the base plate-mast arm weld at the University of Texas at Austin have only applied UIT to the mast arm weld toe of the base plate-mast arm weld in tests to date [28, 29, 30]. UIT has only been applied to the mast arm weld toe of the base plate-mast arm weld because previous tests have found this location to be the site of the majority of mast arm failures [28, 29, 30]. Tests at the University of Texas at Austin have had all but two mast arms fail along the UIT application of the mast arm weld toe [28, 29, 30]. Two mast arms had fatigue crack initiation along the untreated base plate weld toe [29]. In other words, two mast arms treated with UIT along the mast arm weld toe had fatigue cracks in the untreated base plate weld toe, as shown in Figure 3.1.1.



Figure 3.1.1 Fatigue Crack Along Un-Treated Base Plate Weld Toe [29]

The untreated base plate weld toe fatigue cracks were first thought to generate from the roots of the welds and extend to the base plate weld toes. After UIT was performed it was assumed that the weak plane was from the root of the weld to the base plate weld toe. After examination by the author, however, it was determined that fatigue crack initiation was at the untreated weld toe, not at the root.

3.2 BACKGROUND INFORMATION

Freytag performed fatigue tests in the test setup described in Chapter 2 [29]. Two mast arms in Freytag's fatigue tests, TXuALGP and TXuBLGP, developed fatigue cracks at the untreated weld toe. These mast arms were 10 inches in diameter, and were cut to a testing length of approximately 86 inches from an original length of 36 feet. An end plate was welded to the cut end. The nominal thickness of the mast arms was ¼", and they were made of A572 Gr. 50 steel. The fillet weld connecting the mast arm to the base plate had been treated along the mast arm weld toe with UIT by a trained Applied Ultrasonics technician under loaded conditions.

The designations TXuALGP and TXuBLGP are part of a labeling system created by Koenigs. TXuALGP and TXuBLGP were tested together because they have the same specifications: they were both manufactured in Brenham, TX, both have a pole wall thickness of 0.239 inches, and both connection details are an unstiffened socket connection with galvanization prior to UIT.

The mast arms were cycled between a minimum stress of 16 ksi and a maximum stress of 28 ksi for a stress range of 12 ksi at the mast arm weld toe. The specifics of the test are included in Appendix A. The fatigue lives of the two mast arms are given in Table 3.2.1. TXuBLGP failed first at 246,045 cycles with fatigue cracking along the treated mast arm weld toe in the UIT application area. This failure was the same as all other failures in similar mast arms with UIT application fatigue tested at the University of Texas at Austin [28, 29, 30]. TXuBLGP underwent weld repair along the fatigue crack, and the test was restarted. TXuALGP failed at 263,044 cycles in the untreated base plate weld toe. Failure along the untreated base plate weld toe had not occurred in any other fatigue tests of similar specimens [28, 29, 30]. The TXuALGP fatigue crack is shown in Figure 3.1.1. TXuBLGP was reexamined by Freytag at this point, and a

fatigue crack at the untreated base plate weld toe was discovered. This crack emerged during the additional 17,000 cycles of loading after the weld repair.

Table 3.2.1 Fatigue Lives of Test Specimens [29]

Specimen Label	Fatigue Life
TXuALGP	263,044
TXuBLGP	246,045

3.3 INVESTIGATION PROCEDURE

The author examined Freytag's mast arm fatigue cracks that initiated in the base plate weld toe. First, the mast arm of sample TXuALGP was shortened to a length of 6 inches from the base plate. Next, three cross-section samples were cut from TXuALGP. Two samples, labeled A and B were taken from the horizontal axis, and the third sample, labeled C, was taken from the top of the specimen along the vertical axis, as shown in Figure 3.3.1 and Figure 3.3.2.

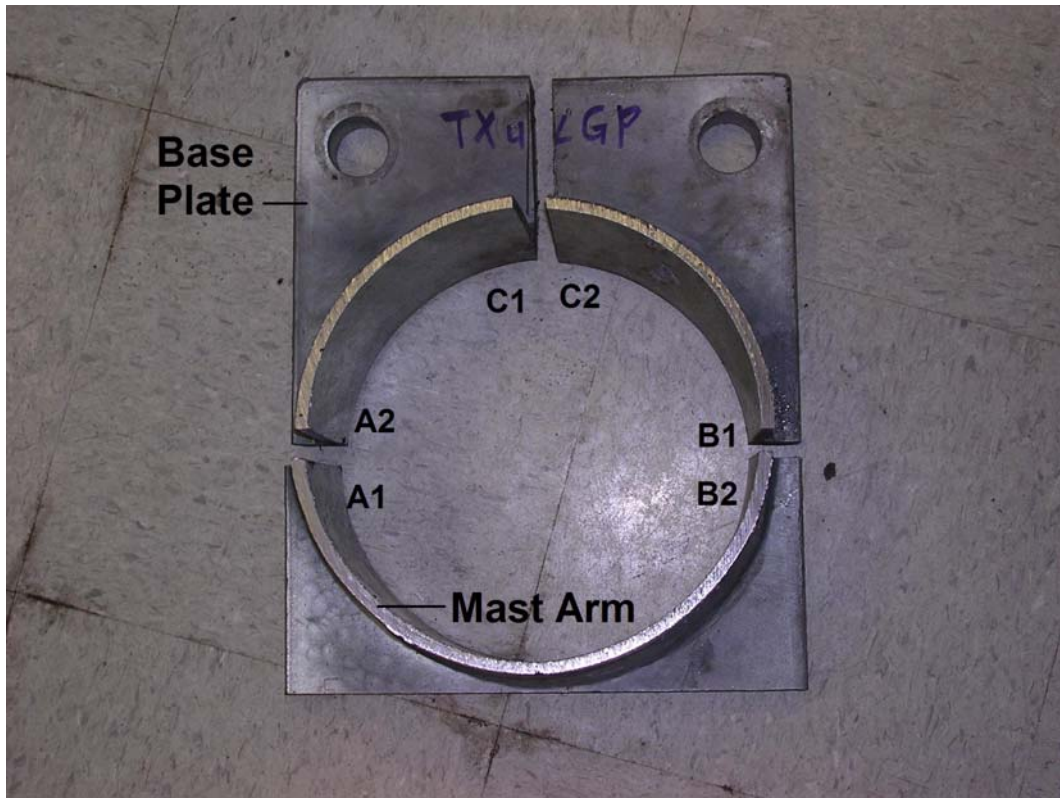


Figure 3.3.1 Top View of TXuALGP, Indicating Location of Test Samples

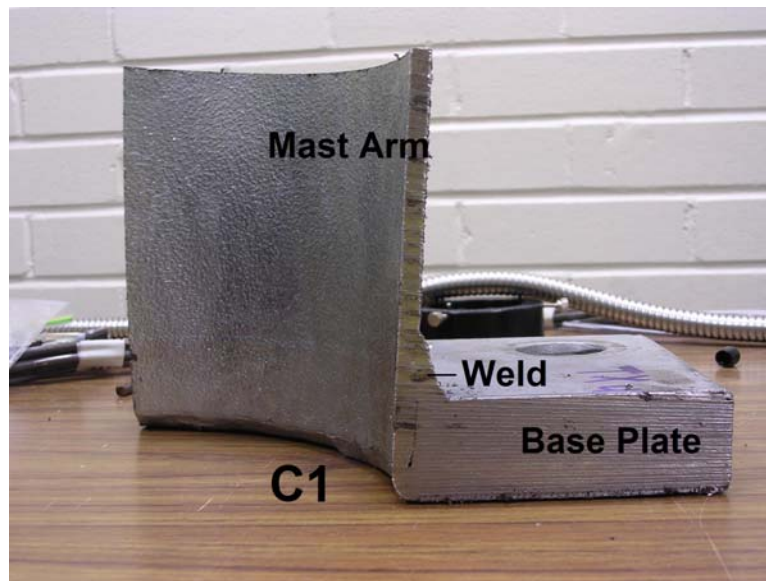


Figure 3.3.2 Cross-section Side View of C Sample Location

Next, the surfaces of the cross-section samples A, B, and C from TXuALGP were sanded on a circular power sander with 100-grit sandpaper. Afterwards the samples were polished with an air powered pneumatic grinder using progressively finer grades of sand paper.

All 3 cross-section samples from TXuALGP were inspected on both the left and right profile under a microscope. The microscope used for the investigation was the LW Scientific, Inc. Inspection System IS-2Z with Alpha-1501 dual gooseneck light guide at magnifications of 20x and 90x.

3.4 INVESTIGATION RESULTS

TXuALGP vertical cross-section sample C is the only sample that shows the fatigue crack at the base plate weld toe. Although TXuALGP horizontal cross-section samples A and B do not show the fatigue crack at the base plate

weld toe, they do show that there is an incomplete connection between the mast arm and the base plate, or a “gap”, as shown in Figure 3.4.1.

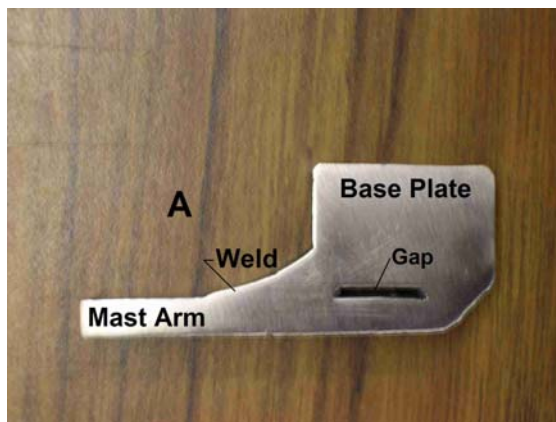


Figure 3.4.1 Right Profile of TXuALGP Horizontal Cross-section A (A2)

Closer inspection of the TXuALGP vertical cross-section, C, shows that the unusual fatigue crack originated from the base plate weld toe, as shown in Figure 3.4.3, and not the root of TXuALGP as originally hypothesized. Figure 3.4.5 shows the 90x magnification of TXuALGP vertical cross-section left profile C1 at the base plate weld toe where there is slag visible at the base plate weld toe, which may have contributed to the fatigue crack initiation. As is visible in Figure 3.4.3, at no time does the fatigue crack intersect the gap that exists between the mast arm and the base plate.

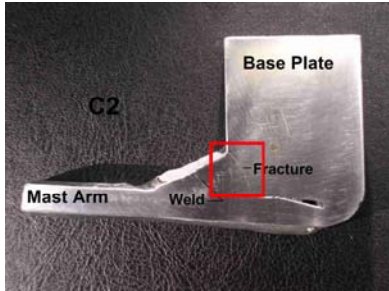


Figure 3.4.2 Section C2

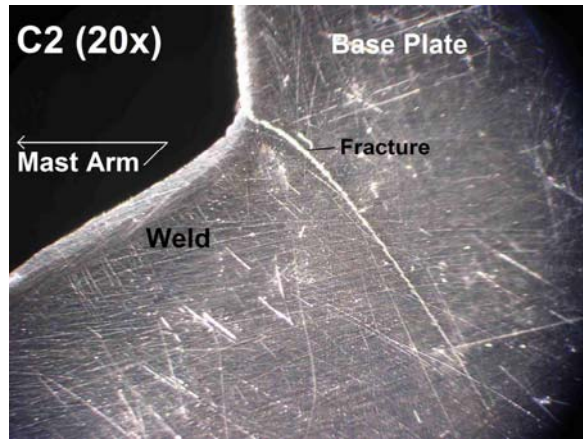


Figure 3.4.3 20x Magnification of C2

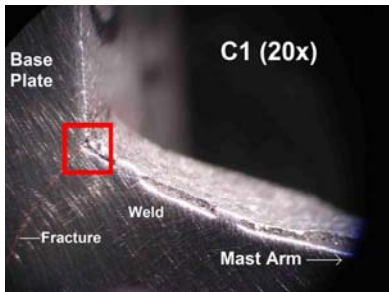


Figure 3.4.4 Section C1 (20x)

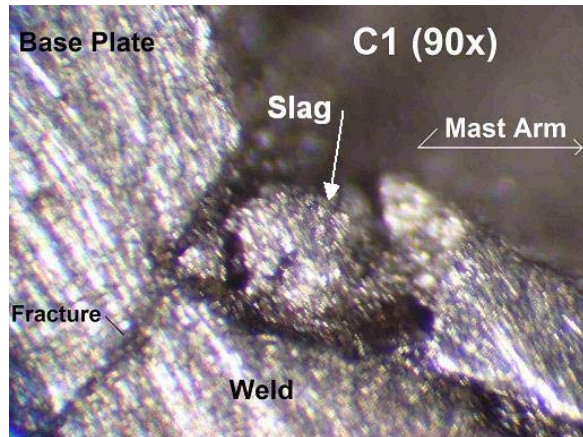


Figure 3.4.5 90x Magnification of C1

3.5 CONCLUSIONS AND RECOMMENDATIONS

Figure 3.4.1 shows that the hole cut in the base plate to accommodate the mast arm was cut too large, resulting in an incomplete connection of the mast arm to the base plate. This may have weakened the mast arm-base plate connection and may have lead to the fatigue crack initiation at the base plate weld toe. However, fatigue crack initiation at the base plate weld more likely occurred due to poor welding, as indicated by the slag especially visible in Figure 3.4.5.

It is also possible that the base plate weld toe fatigue crack initiation was due to the increased strength the mast arm weld toe after UIT application. UIT application to the mast arm weld toe had the potential to create enough compressive stress at the weld toe to make the base plate weld toe the new weakest point. Previous tests on specimens of A572 Grade 50 steel with no welds showed that when the base metal was treated with a 3 mm diameter pin size multi-pin UIT tool a peak compressive residual stress was generated near the sample surface that exceeded the yield stress of the parent metal [13]. Since previous research on various metals has shown an increase fatigue strength of fillet welds of 46% - 192% [3, 9, 10, 12, 26], it is not unreasonable to conclude that UIT increased the strength of the mast arm weld toe past the yield strength of the parent metal, making the mast arm weld toe no longer the weakest point. To prevent base plate weld toe failure, UIT at both the mast arm and the base plate weld toes is recommended.

CHAPTER 4

Galvanization Repair After UIT Application

4.1 INTRODUCTION

UIT application removes galvanization in the treated area. One use of UIT is application to mast arm welds. Removal of galvanization during UIT application creates a need for galvanization repair after UIT application to mast arm welds. There are three methods of galvanization repair. The first method of galvanization repair is a cold-spray zinc-lead paint. Previous test results show that mast arms with cold-spray zinc-lead paint galvanization repair after UIT application behave the same in fatigue as mast arms with UIT application that do not undergo any galvanization repair. The second method of galvanization repair is hot-dip galvanization, which involves dipping the entire mast arm in a hot galvanization bath. Previous tests by Koenigs show that hot-dip galvanization after UIT application undoes UIT benefits [28]. The third method of galvanization repair uses a zinc-lead solder. The zinc-lead solder is applied at the working temperature of 600°F to 750°F, at which point the solder melts and solidifies to repair the galvanization.

Previous tests show that when UIT peened welds are exposed to temperatures above 300°C (572°F), the fatigue life of the treated welds is the same as for untreated welds [7, 28]. This test examines the effects of heat-applied solder galvanization repair on the fatigue life of UIT peened mast arm welds. All efforts were made to match previous experiments on similar non-treated and ultrasonic impact treated mast arms.

4.2 PREVIOUS RESEARCH

Mikheev et al. conducted tests of butt joints in high strength steel that were heated to 300°C (572°F) after UIT application. Fatigue test results showed that when high strength steel samples were subjected to 300°C temperatures after UIT application and before fatigue testing, there was no increase in fatigue life. The results of tests on treated and untreated specimens occupied a single scatter region characteristic of several fatigue tests of such welds [7]. The extreme temperature may have relaxed the favorable residual compressive stresses that UIT had induced in the surface layer of the specimens, resulting in no fatigue enhancement.

Koenigs tested the effects of UIT both when UIT is applied before hot-dip galvanization, and when UIT is applied after hot-dip galvanization. Representatives from Applied Ultrasonics warned that the heat incurred during the hot-dip galvanization process, when performed after UIT application, would undo the benefits of UIT. An attempt was made to compensate for the heat influence of hot-dip galvanization on mast arm welds after UIT application. After a trained technician performed the standard UIT application under loaded conditions using the 3mm diameter pins in the multi-pin tool along the toe of the socket weld, the same settings were used for an additional treatment to an area around the socket weld. The resulting condition of the socket weld after the heat affected area treatment is shown in Figure 4.2.1.



Figure 4.2.1 UIT Application to Both Weld Toes and the HAZ on TXuCLGP

After UIT application under loaded conditions to both the weld toe and the HAZ by a trained technician, the mast arms were unloaded and shipped to United Galvanizing in Houston, TX. United Galvanizing performed hot-dip galvanizing. Mast arm welds that had UIT application prior to hot-dip galvanizing performed very poorly in fatigue, indicating that the hot-dip galvanizing process negated any improvement induced by UIT [28]. In contrast, when mast arms are hot-dip galvanized before UIT application, there is significant improvement in the fatigue life of any weld. Hence, UIT has great fatigue benefits, which are undone by extreme heating during hot-dip galvanization.

4.3 HEAT-APPLIED ZINC-LEAD SOLDER GALVANIZATION REPAIR TESTS

The author fatigue tested two mast arms with UIT applied under loaded conditions at the University of Texas at Austin. The purpose of these fatigue tests was to determine the effect of heat-applied galvanization repair to mast arms with UIT application. The mast arms were previously untested mast arms from Koenigs' tests [28]. Koenigs' previous tests of mast arms with UIT applied at Ferguson Laboratory under a 16.5 ksi stress are summarized in Appendix A. Koenigs' results show that mast arms with UIT applied at a stress of 16.5 ksi and tested at a 12 ksi stress range at the mast arm weld toe, with a maximum testing stress of 28.5 ksi, had fatigue lives of at least 4,545,952 cycles, with an average fatigue life of 4,553,401 cycles [28]. For heat-applied galvanization repair to have no negative effects on the mast arms with UIT application to be tested, fatigue testing at a 12 ksi stress range with a maximum test stress of 28.5 ksi should produce fatigue lives of at least 4,553,401 cycles.

The two mast arms tested by the author after heat-applied galvanization repair were mast arm specimens TXuCLGP and TXuDLGP. Both mast arms had been previously shortened to 83" in length, with a 10" x 10" x 1" end plate welded to the end. Mast arm TXuCLGP had an average outer diameter of 9.875 inches, and mast arm TXuDLGP had an average outer diameter of 10.073 inches. Both mast arms had a wall thickness of 0.1793 inch, and they were made of A572 Gr. 50 steel. Both base plates had dimensions of 12" x 18" x 1.25". The fillet weld connecting the mast arm to the base plate had been treated along the mast arm weld toe and HAZ with UIT by a trained Applied Ultrasonics technician under a stress of 16.5 ksi.

The designations TXuCLGP and TXuDLGP are part of a labeling system created by Koenigs. TXuCLGP and TXuDLGP were tested together because they have the same specifications: they were both manufactured in Brenham, TX, both

have a pole wall thickness of 0.179 inches, and both connection details are an unstiffened socket connection with galvanization prior to UIT [28].

4.3.1 Equipment

All temperatures were recorded using the ST Pro Series Professional noncontact thermometer, produced by Raytek. The noncontact thermometer uses a laser point sighting system to locate the position of the reading. The display shows 1% accuracy. According to the thermometer's literature, an infrared thermometer measures the surface temperature of an opaque object. The major difficulty in using the noncontact thermometer is determining the correct emissivity. Emissivity is a term used to describe the energy-emitting characteristics of materials. Most painted surfaces have an emissivity of 0.95. Inaccurate readings can result when measuring a shiny or polished metal surface, such as galvanized steel. The emissivity of galvanized steel as provided by Raytek is 0.88. However, by comparing measurements from a thermal couple to measurements from the noncontact thermometer, the emissivity of specimens TXuCLGP and TXuDLGP was determined to be 0.98.

All heat-applied solder galvanization repair was applied using Gal-Viz. Gal-Viz is a self-fluxing solder alloy for repairing damaged galvanized materials, produced by J.W. Harris, Inc. Gal-Viz is applied to metal at a working temperature of at least 600°F. Current TxDOT specifications allow the mast arm metal to reach temperatures between 600°F and 750°F during heat-applied solder galvanization repair. J.W. Harris, Inc. literature for Gal-Viz instructs the user to rub the Gal-Viz rod on the heated metal. When the Gal-Viz rod melts, the temperature of the metal is correct. This conveniently worked as a check for the

non-contact thermometer, which fluctuated rapidly throughout the heating process.

4.3.2 Test Setup

Mast arms TXuCLGP and TXuDLGP were tested in the test setup described in Chapter 2. Mast arms TXuCLGP and TXuDLGP were cycled between a minimum stress of 16 ksi and a maximum stress of 28 ksi for a stress range of 12 ksi.

4.3.3 Pre-Treatment Static Tests

First, the mast arms were subjected to a static test to determine the deflections corresponding to the previously calculated stress ranges. The stress range is 12 ksi to match stress ranges from previous tests of comparable mast arms, both with and without UIT application. The maximum load was 11.31 kip, corresponding to a 28 ksi stress at the mast arm weld toe. The minimum load was 6.46 kip, corresponding to a 16 ksi stress at the mast arm weld toe. The data from the static tests are shown in Table 4.3.3.1.

Table 4.3.3.1 Load and Displacement Data from Pre-Treatment Static Test

Load (kip)	Displacement (inch)
11.31	1.08
11.31	1.08
11.31	1.08
6.46	0.63
6.46	0.64
6.46	0.64

Next, the mast arm was loaded to the maximum load of 11.31. The temperature was measured with a non-contact thermometer prior to heating at five locations on each mast arm. All five temperature reading locations were 1.5 inches from the mast arm weld toe. Two temperature reading locations were at either end of the UIT application line along the weld toe. Three temperature reading locations were at the middle most area of UIT application. The locations of the temperature reading locations are shown in Figure 4.3.3.1. The average temperatures at each location are shown in Table 4.3.3.2.



Figure 4.3.3.1 Location of the Middle-Most Temperature Reading Locations (Blue Circles Labeled D2, D3, and D4; The Endmost Temperature Reading Locations are Not Visible in this Picture)

Table 4.3.3.2 Temperatures at Five Locations Along the UIT Application of Mast Arms TXuCLGP and TXuDLGP at Different Times During Heat-Applied Galvanization Repair

Location	Unheated Temperature (°F)	Galvanization Temperature (°F)	After Galvanization Temperature (°F)	(15 min.) After Temperature (°F)
C1	75.5		252	125
C2	68.8		200	135
C3	74.6	770	260	165
C4	74.5		276	162
C5	75.2		213	156
				(5 min.)
D1	70		161	89
D2	68		244	199
D3	71.8	650	242	221
D4	70.8		171	160
D5	70.1		102	96

4.3.4 Heating and Galvanization

After room temperature readings were recorded, a torch was used to heat the area for the heat-applied solder alloy galvanization repair. Gal-Viz, which is described in the Equipment section, was used as the heat-applied galvanization repair. Readings of the mast arm surface temperature during heating were taken, which are also recorded in Table 4.3.3.2. It was arbitrarily decided that mast arm TXuCLGP would be heated to the maximum temperature allowed for heat-applied galvanization repair (750°F), and that mast arm TXuDLGP would be heated to the minimum temperature allowed for heat-applied galvanization repair (600°F), in an attempt to cover the extremes of possible field conditions.

4.3.5 Post-Treatment Static Tests

The mast arms were allowed to cool for 2 hours after heat-applied galvanization repair, and then the static test was run again. The static test took deflection readings at maximum and minimum loads. The controller was under deflection control. The mast arm cooled to 81°F before static tests began. The results of the static test after heat-applied galvanization repair are shown in Table 4.3.5.1. From this data the average maximum and minimum displacements were determined. These maximum and minimum displacements were used as the deflection control parameters for dynamic test.

Table 4.3.5.1 Load and Displacement Data from Post-Treatment Static Test

Load (kip)	Displacement (inch)
11.312	1.1019
11.31	1.0965
11.31	1.0965
6.461	0.6542
6.461	0.6549
6.461	0.6542

4.4 RESULTS

The failure parameters for the mast arms with UIT application followed by heat-applied galvanization repair were determined as 5% change in the loads, as shown in Table 4.4.1. These failure parameters were programmed into the controller that controlled the 22 kip closed loop loading actuator. The mast arm typically fails by fatigue cracking that causes the mast arm to lose 5% of its load carrying capacity. Hence, failure is generally when the mast arm's load carrying

capacity drops below the load limit, the maximum load limit is also set in case of equipment failure.

Table 4.4.1 Failure Parameters for TXuCLGP and TXuDLGP

	Load (kip)	Displacement (inch)
Maximum	11.88	1.153
Minimum	6.14	0.622

The controller first reported failure after 85,214 cycles. Mast arms TXuCLGP and TXuDLGP were visually inspected for cracks, and none were detected. At this point the controller had unknowingly been re-set, probably due to a brownout. When the test was restarted, the re-set controller misread data and induced a deflection of 2.5 inches in tension, which caused a massive fracture along the mast arm weld toe of TXuDLGP. A picture of this failure after grinding to remove the galvanization is shown in Figure 4.4.1 and Figure 4.4.2. Figure 4.4.2 shows the extreme angle created in the base plate of TXuDLGP during failure.



Figure 4.4.1 Top View of Crack Along the Mast Arm Weld Toe of TXuDLGP



Figure 4.4.2 Side View of Mast Arm TXuDLGP After Cracking

Due to the extreme cracking and base plate bending, TXuDLGP could not be repaired, and hence could not be replaced in the test setup to continue fatigue tests. Mast arm TXuBLGP was determined to have almost identical dimensions and fabrication conditions as TXuDLGP, and therefore was an acceptable replacement for mast arm TXuDLGP in the test setup. TXuBLGP was put into the test setup in place of mast arm TXuDLGP on the North end of the test setup. In this way tests could continue until TXuCLGP failed.

The controller first reported failure for mast arm TXuCLGP at 101,865 cycles. A picture of mast arm TXuCLGP at this point is shown in Figure 4.4.3. Visual inspection revealed no fatigue cracks. However, the thick galvanization repair along the weld toe prevented good inspection. Since no fatigue cracks were visible in TXuCLGP, the controller was reset, and dynamic testing continued.



*Figure 4.4.3 Mast Arm TXuCLGP After 1st Controller-Reported Failure
(101,865 cycles)*

The controller reported failure again for mast arm TXuCLGP only 7,546 cycles later at 109,411 cycles. A picture of mast arm TXuCLGP at this point is shown in Figure 4.4.4. Visual inspection revealed cracking in the thick galvanization repair. Galvanization was removed with a screwdriver in the area of the cracked galvanization. However, the local galvanization removal did not reveal any cracks in the mast arm weld toe or surrounding metal. Since no fatigue cracks were visible in TXuCLGP, the controller was reset, and dynamic testing continued.



*Figure 4.4.4 Mast Arm TXuCLGP After 2nd Controller-Reported Failure
(109,411 cycles)*

The controller reported a third and final failure for mast arm TXuCLGP 8,050 cycles later at 117,461 cycles. Visual inspection showed extensive cracking in the thick galvanization repair. Galvanization removal with a screwdriver of the cracked galvanization repair revealed visible cracking along TXuCLGP's mast arm weld toe. Removal of the entire thick galvanization repair with a screwdriver revealed the extent of fatigue cracking along TXuCLGP's mast arm weld toe, as shown in Figure 4.4.5. Figure 4.4.6 shows the fatigue crack on TXuCLGP's mast arm weld toe along the UIT application after highlighting.



Figure 4.4.5 Mast Arm TXuCLGP After 3rd Controller-Reported Failure (117,461 cycles) and After Removal of All the Thick Galvanization Repair



Figure 4.4.6 Highlighted Fatigue Crack on Mast Arm TXuCLGP Weld Toe Along the UIT Application

4.5 DISCUSSION

The first controller-reported failure occurred at 85,214 cycles. At this point no fatigue cracking was visible in the thick galvanization repair on either TXuCLGP or TXuDLGP. TXuDLGP cracked under the following 2.5 inch displacement. It is interesting that TXuDLGP failed first, because mast arm TXuDLGP had heat-applied galvanization repair at the minimum heat of about 600°F, while mast arm TXuCLGP had heat-applied galvanization repair at the maximum heat of about 750°F. Hence, increasingly higher temperatures above 600°F cannot be said to have increasingly negative effects on UIT application. Until more tests are conducted, it can only be said that temperatures in excess of 572°F have negative effects on UIT application [7].

An extreme crack occurred in TXuDLGP, visible in Figure 4.4.1 and Figure 4.4.2, after an accidental one-time displacement of 2.5 inches. This crack cannot be classified as a fatigue crack under the 12 ksi stress range fatiguing conditions. It is impossible to say what effect the 2.5 inch displacement after 85,214 cycles had on mast arms TXuCLGP and TXuDLGP. From the extreme failure the 2.5 inch displacement induced in TXuDLGP, the 2.5 inch displacement obviously had a life-shortening effect on both TXuCLGP and TXuDLGP. Hence, the number of cycles recorded at failure for TXuCLGP and TXuDLGP are conservative.

Mast arm TXuCLGP first showed visible fatigue cracks along the UIT application line at the mast arm weld toe after 117,461 cycles. However, it is more likely that mast arm TXuCLGP failed after 101,865 cycles when the controller first reported failure, despite no visual confirmation. The thick galvanization repair hindered visual confirmation. The thick galvanization repair may have also hindered visual confirmation of any fatigue cracking in TXuDLGP along the UIT application line in the mast arm weld toe at 85,214 cycles before

the 2.5 inch displacement that caused extensive cracking. Hence, the thick heat-applied galvanization repair hinders accurate visual inspections for important fatigue crack initiation. Even when cracks in galvanization repair were observed, it was impossible to tell if fatigue cracking existed without removing the galvanization entirely.

4.5.1 Comparison to Previous Tests

Koenigs' previous tests of comparable UIT peened mast arms from the same manufacturer with the same specifications tested under the same conditions as the author's tests of TXuCLGP and TXuDLGP, but without heat-applied galvanization repair, show fatigue lives of at least 4,545,952 cycles, with an average fatigue life of 4,553,401 cycles [28]. Specimens from the same test group without UIT had average fatigue life of 332,798 cycles, with a minimum of 151,679 cycles and a maximum of 657,716 cycles [28]. For the heat-applied galvanization repair to have definitely had no negative effect on the UIT application of TXuCLGP and TXuDLGP mast arm weld toes, TXuCLGP and TXuDLGP should have experienced fatigue lives of at least 4,545,952 cycles. Since mast arms TXuDLGP and TXuCLGP had fatigue lives of 85,214 cycles and 117,461 cycles respectively, it can be concluded that heat-applied galvanization repair undoes the benefits of UIT. Mast arms treated with UIT under loaded conditions and then exposed to heat-applied galvanization of at least 600°F have no improvement in fatigue life.

4.5.2 Heat-Applied Galvanization Repair Problems

One problem with the heat-applied galvanization repair is that it is easily removed. Flaking of the heat-applied galvanization repair leads to cracks in the

galvanization during fatigue testing. This indicates that the galvanization would flake off in the field and leave the mast arm weld toe susceptible to corrosion.

4.5.3 Non-Contact Thermometer Problems

One possible source of error is reading the noncontact thermometer. While torch heating the mast arms, the non-contact thermometer gave wildly fluctuating readings, and did not give steady temperature readings. Temperatures taken after torch heating fluctuated more slowly, but were not steady either.

CHAPTER 5

UIT Application During Fabrication

5.1 INTRODUCTION

Traffic signal mast arms baseplate connections are particularly susceptible to fatigue. The top of traffic signal mast arm welds experience fluctuating tensile stresses when wind and traffic gust loads cause the mast arm to oscillate. It has been postulated that UIT application to mast arm weld toes during the fabrication process will delay fatigue crack initiation [28]. Successful UIT application during the fabrication process will extend fatigue lives of traffic signal mast arm welds in the field. Since mast arm welds are the weakest spot in the traffic signal structure [28], increased weld life translates into increased traffic signal life.

Previous tests show that if hot-dip galvanization is used, UIT must be applied after hot-dip galvanization, since temperatures above 300°C have proven to undo the benefits of UIT, probably because extreme heat relaxes the beneficial compressive stresses induced by UIT [7, 16]. Hence, UIT is applied last during the fabrication process at the fabrication plant. Galvanization removed during UIT application is repaired with a zinc-rich paint, which has no effect on the UIT, as discussed in Chapter 7 [3, 7].

Previous research claims that UIT is light, quiet, and easy to learn [3, 11, 12, 16, 19, 20]. Critical areas under scrutiny during UIT application at the fabrication plant are: time lost due to training workers, time lost during the UIT application, and efficiency of the treated poles. This chapter investigates the first two issues by documenting the application of UIT to fabricated mast arms at the

TransAmerican Power Products facility. The observations of that first time use of UIT are documented in this chapter.

5.2 TRAINING SESSION

UIT training took place at the TransAmerican Power Products, Inc. fabrication yard, located at 2427 Kelly Lane, Houston, TX 77066. The observed training began on October 12, 2004. UIT training covers application technique and basic theory behind UIT. UIT training was lead by a trained Applied Ultrasonics technician. Applied Ultrasonics is currently the only UIT producer in the US.

During the morning training of October 12, 2004, the Applied Ultrasonics technician met with the Vice President of TransAmerican, TransAmerican's Quality Control person, two TxDOT inspectors, and the author. The two workers that would actually perform the treatment were not present at this morning presentation. Since everyone in the group, with the exception of the Quality Control person, was familiar with UIT, the Applied Ultrasonics technician presented a shortened version of the UIT background information presentation. UIT training for a group that is not familiar with the process that lasted one and a half hours usually lasts the entire morning of a daylong UIT training.

The UIT presentation introduced the concept of increasing fatigue life, using UIT, showed the equipment and proper application settings and techniques, and stressed that already cracked materials cannot be treated. The TransAmerican Quality Control person, the only person at the presentation not familiar with UIT, asked many questions, and the Applied Ultrasonics technician had no problem answering all the questions. The TransAmerican Quality Control person has an

extensive background on other weld fatigue life improvements, and after the presentation he understood UIT to be a process similar to shot peening.

5.3 AFTERNOON FABRICATION YARD UIT APPLICATION TRAINING

The UIT application training took place in the TransAmerican yard over a few days. The first day is documented in this section.

5.3.1 Test Setup

Since UIT is the last step in the fabrication process, the mast arms to be treated were already galvanized and stockpiled in the TransAmerican fabrication yard. Figure 5.3.1.1 shows the stockpiled mast arms in the fabrication yard.



Figure 5.3.1.1 Stockpiled Mast Arms at the TransAmerican Fabrication Yard

A crane moved mast arms in the TransAmerican yard from their stockpiled location to the fixed testing stand. The mast arms were stockpiled near the fixed testing stand, so that the crane did not have to move, only rotate, during transportation of the mast arms.

TransAmerican had a fixed testing stand made of steel that was connected to a concrete slab. The fixed testing stand had holes in it to allow for the different size base plates that TransAmerican fabricated and tested on site. It took a total of 3 people to connect the mast arm to the test stand. Figure 5.3.1.2 shows the mast arm being bolted into place.



Figure 5.3.1.2 Mast Arm Being Connected to Fixed Testing Stand

Previous research by Koenigs shows that UIT application is most effective when applied under an imposed stress of 16.5 ksi at the treated weld toe [28]. The mast arms at TransAmerican have UIT applied under a 16.5 ksi bending stress to simulate the stress in the arm under static service loading. There are two sets of design specifications by TxDOT for cantilever traffic signal structures: structures that are designed to survive a maximum of 100 mph winds, and structures that are

designed to survive a maximum of 80 mph winds. TxDOT inspectors decided to use the specifications for structures designed to survive a maximum of 100 mph winds when determining the load to place at the mast arm end that would induce a 16.5 ksi stress at the weld toe of a 20 foot mast arm. A 500-pound weight was applied to the end of all 20 foot mast arms before UIT application at the TransAmerican fabrication yard to produce the nominal 16.5 ksi stress at the weld toe.

After the mast arm was bolted to the fixed testing stand it was loaded by crane with a 500-pound circular weight, as shown in Figure 5.3.1.3 and Figure 5.3.1.4. Figure 5.3.1.3 shows the crane as it moved a 500-pound circular weight to the end of the mast arm to induce dead load. Figure 5.3.1.4 shows personnel securing the 500-pound weight in place. Figure 5.3.1.5 shows a close-up of the 6 inch extension at the end of the mast arm that was used to support the 500-pound circular weight during UIT application.



Figure 5.3.1.3 Crane Moving the 500-Pound Circular Weight to the Mast Arm
End



Figure 5.3.1.4 Placing the 500-Pound Circular Weight on the End of the Mast Arm



Figure 5.3.1.5 Mast Arm with 6-Inch Extension at the End for the 500-Pound Circular Weight

Figure 5.3.1.6 shows the entire UIT application set-up in the TransAmerican fabrication yard prior to UIT application.



Figure 5.3.1.6 Entire Loaded and Fixed Mast Arm UIT Setup

5.3.2 UIT Application Demonstration

UIT application began after the mast-arm was secured in the loading setup and loaded with the 500-pound weight. The Applied Ultrasonics trained technician demonstrated the UIT application procedure by applying UIT to the TransAmerican mast arm. The TransAmerican workers who were being trained observed the example application.

First, the power generator was turned on. The power generator supplied power to the UIT generator. Next, the water pump was turned on to cool the UIT generator. As explained in Appendix B, the UIT generator produces the ultrasonic oscillations that are utilized by the UIT tool to treat the steel weld. Then the UIT generator was turned on to maximum power, which corresponded to 80 volts. The UIT tool used 10 amps, so the power applied during UIT application was 800 watts. The UIT generator was set at maximum power for all mast arm applications. Figure 5.3.2.1 shows the UIT generator and the water pump. Figure 5.3.2.2 shows the UIT generator, the UIT tool, and the power generator.

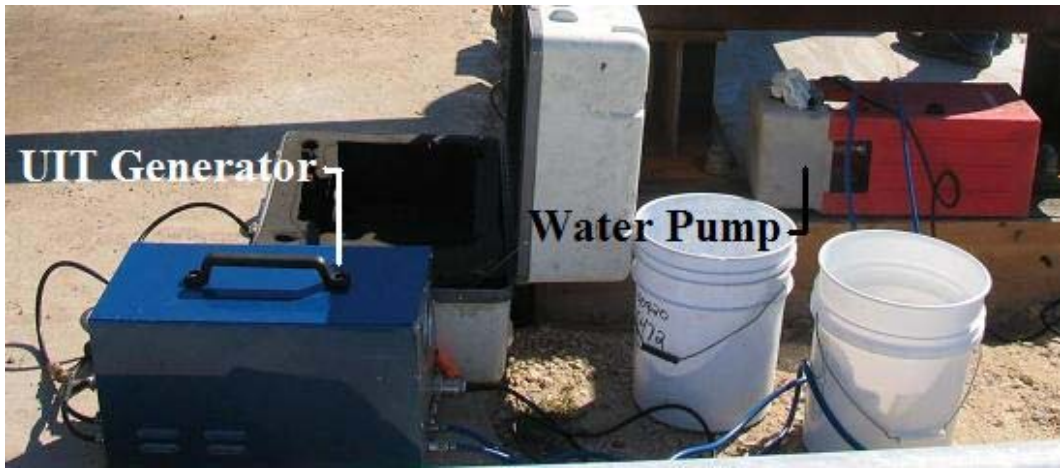


Figure 5.3.2.1 UIT Generator (Blue Box on Left) and Water Pump (Red Box on Right)

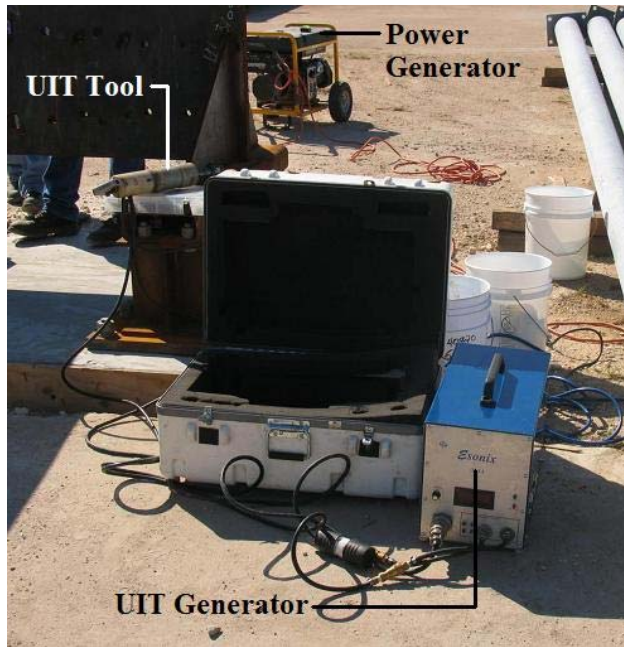


Figure 5.3.2.2 Front View of the UIT Tool, Power Generator, and UIT Generator

The technician applied UIT to both toes of the mast arm-base plate weld. The Applied Ultrasonics technician expressed that it is irrelevant which weld toe is treated first. Both weld toes were treated with UIT following the same procedure. UIT was applied to the mast arm weld toe with the multi-pin UIT tool held at a 45° angle from the mast arm. The angle that the UIT tool is held against the weld toe during application can range from 30° to 60°, but an effort to keep the tool at 45° to the weld toe should be made. The UIT application followed the weld toe so as to create a smoother transition from the weld to the mast arm or base plate. A maximum of four passes was made with the UIT tool. UIT with a 3 mm diameter pin should create about a 1/8" (3mm) impression at the weld toe. In general, the groove created by UIT is expected to be about the size of the treatment pin.

The UIT tool used during application was a 3 mm diameter multi-pin head on the tool, with two 3 mm pins installed. Applied Ultrasonics has found that two pins perform better than three or four 3 mm diameter pins during application to 10-inch diameter mast arm weld toes. The reason that two pins give superior UIT application is that the small diameter of the mast arm prevents three or more pins from coming into contact during application. A flat plate, for example, would probably get superior UIT application from three or four 3 mm diameter pins in the multi-pin tool because all of the pins would be able to contact the steel during treatment. Figure 5.3.2.3 shows UIT application.



Figure 5.3.2.3 Application of UIT to a Mast Arm Weld Toe

The UIT was applied with a steady, yet light, pressure on the UIT tool. The application technique did not require a hard push. The UIT tool was moved over the length of the mast arm weld toe to be treated. The 3 kg (6.6 pound) weight of the tool and the action of the tool itself created the necessary contact force. The length of the UIT application along the mast arm weld toe extended 90° from the top vertical of the mast arm in each direction. Hence, the entire top 180° of the mast arm weld toes was treated with UIT. In other words, since the mast arm had a 10 inch diameter, the mast arm had a weld toe circumference of 31.4 inches. The topmost 15.7 inches of the 31.5-inch mast arm weld toe was peened with UIT. The bottom 180° of the mast arm does not need UIT application because previous tests indicate that fatigue cracking does not occur in where the mast arm is in compression, namely, the bottom of the mast arm [28].

Figure 5.3.2.4 shows the mast arm-baseplate connection before UIT application. Figure 5.3.2.5 shows a completed, 180° application of UIT to the weld toe on the arm. Notice in Figure 5.3.2.5 that the treated area is shiny due to

galvanization flaking off during treatment to reveal the un-galvanized steel underneath. In Figure 5.3.2.5 the groove produced by the 3 mm diameter pins of the multi-pin UIT tool is also visible. Figure 5.3.2.6 shows application of UIT to the top weld on the baseplate.



Figure 5.3.2.4 Mast Arm-Baseplate Weld Connection Before UIT Application



Figure 5.3.2.5 Completed Mast Arm Weld Toe UIT



Figure 5.3.2.6 Application of UIT to Baseplate Weld Toe

5.3.3 Inspection by a TxDOT Inspector

After the example UIT application by the trained technician, a TxDOT inspector inspected the groove produced by UIT application. One hindrance to perfect UIT application is when existing galvanization on the mast arm weld toe does not flake off from UIT application, or flakes off and then gets between the UIT tool pins and the mast arm weld metal. Pieces of galvanization can result in a barrier between the UIT tool and the metal to be treated. According to the Applied Ultrasonics technician, during past UIT applications, pieces of galvanization have prevented proper impact of the weld metal by the UIT tool. If either the galvanization does not flake off during treatment, or galvanization that has flaked off gets between the UIT tool and the area of treatment, gaps in proper UIT application will occur. The UIT application area must be cleared of any remaining galvanization after UIT application for inspection for incomplete treatment. The trained technician suggested using a screwdriver to remove galvanization after UIT application, if a screwdriver is available. Oil cannot be used to remove galvanization after UIT application, because oil will interfere with application of the zinc-rich paint to repair the area after UIT application. TxDOT inspectors recommend using a wire brush for galvanization removal after UIT application. Figure 5.3.3.1 shows galvanization being removed with a wire brush.



Figure 5.3.3.1 Removal of Galvanization with a Wire Brush

After all galvanization was removed from the UIT application area, and the UIT application was complete, the UIT application depth was measured. Proper UIT application with 3 mm diameter pins in a multi-pin UIT tool usually produces a 1/8" (3 mm) diameter groove along the treated weld toe. The width of the UIT application groove and the maximum depth of the UIT application groove were difficult to measure. The depth of the UIT application groove can be measured either with a weld undercut measuring device, or by rolling a single 3 mm diameter pin from the UIT tool in the UIT application groove. Rolling the 3 mm diameter pin from the UIT tool in the UIT application groove is a good check of the UIT application groove's depth and width when more sophisticated tools are not available. Figure 5.3.3.2 shows the measurement of the UIT application

groove using an undercut measuring device. Figure 5.3.3.3 shows a 3 mm diameter pin from the UIT tool rolled in the UIT application groove.



Figure 5.3.3.2 Measurement of UIT Application Groove Using an Undercut Measuring Device

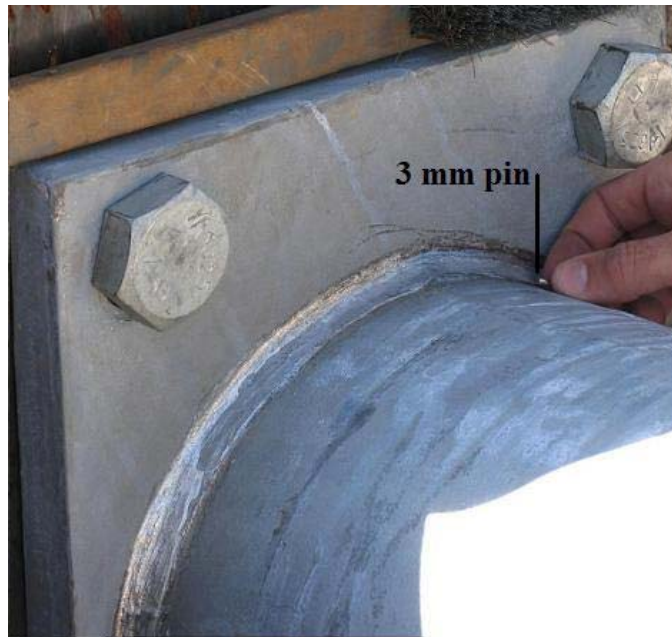


Figure 5.3.3.3 Measurement of UIT Application Groove by Rolling a 3 mm Diameter Pin from the UIT Tool in the UIT Application Groove

5.3.4 Repair of Galvanizing

After satisfactory inspection of the UIT application by a TxDOT inspector, a zinc-rich paint repair was applied in two coats by the TxDOT inspector. The first coat was allowed to dry before the second coat was applied. The zinc-rich paint used at the TransAmerican fabrication yard by TxDOT inspectors was Rust-oleum Cold Galvanizing compound, which contained 93% pure zinc. Figure 5.3.4.1 shows the paint being applied. Figure 5.3.4.2 shows the area of UIT application while the paint is drying. Figure 5.3.4.3 shows a completed UIT application after repair is completely dried.



Figure 5.3.4.1 Application of Zinc-Rich Paint



Figure 5.3.4.2 Drying Zinc-Rich Paint



Figure 5.3.4.3 Mast Arm Weld After Completion

5.3.5 Removal of Mast Arm from Fixed Testing Stand

After both weld toes have had UIT application and been painted, the crane removed the 500-pound weight from the end of the mast arm. The crane then secured the mast arm in the test setup as three people removed the bolts from the testing stand. Two people aided the crane by guiding the un-bolted mast arm as the crane moved the mast arm from the testing stand to a storage area.

The finished mast arm treated in the demonstration was labeled for reference on what a correct UIT application and paint to a mast arm weld should look like, and was set aside for future reference.

5.3.6 Trained Technician Treatment Times

Table 5.3.6.1 lists the times for each phase of UIT application to a mast arm weld during the training demonstration

Table 5.3.6.1 Description of Phases of UIT Application

Phase	Description	Time (min)
1	Move the mast arm with crane from stockpile to fixed testing stand, bolt the mast arm to the fixed testing stand, and apply the 500-pound circular weight with the crane to the end of the fixed mast arm.	15
2	UIT application to the mast arm weld toe.	6
3	UIT application to the base plate weld toe.	5
4	Inspection of both mast arm and base plate weld toes, removal of galvanization flakes and remaining galvanization, touch-up of UIT application, and application of zinc-rich cold-spray galvanization repair.	15
5	Unbolting the mast arm with UIT application and moving the mast arm by crane to a new stockpiled location.	4
Extra	Discussion and breaks.	7
	Total:	53

5.4 APPLICATION OF UIT BY TRAINED EMPLOYEES

The TransAmerican employees that were trained to apply UIT at the fabrication yard were present during the UIT application by the Applied Ultrasonics technician, but the employees were often not in the best position to view the UIT application technique. The employees that were being trained to apply UIT to the mast arm welds at the fabrication yard practiced first on a test plate weld. The test plate weld consisted of a small section of a base plate-mast arm connection. Figure 5.4.1 shows an employee practicing on the test plate.



Figure 5.4.1 Employee Applying UIT to a Test Plate Weld

After the employees became comfortable with the UIT process, they started UIT application to a loaded mast arm weld in the setup. During the UIT application by the employee, the Applied Ultrasonics technician and Vice President of TransAmerican often had to stop the employee to show him by example the correct UIT application techniques. During the employee's first UIT application of a mast arm weld he made many more passes than was necessary, did not always hold the tool at 45° , and was not able to keep the treatment along the weld toe. Figure 5.4.2 shows an employee applying UIT to the weld toe. The Uit tool is almost vertical, not at the desired 45° angle.



Figure 5.4.2 Employee’s First UIT Application to a Mast Arm Weld

5.4.1 Employee’s UIT Application Times

The employee’s UIT application to a mast arm weld involved the same phases as the Applied Ultrasonics technician, as listed in **Error! Reference source not found..** The approximate times for the employee’s UIT application are listed in Table 5.4.1.1. Phases such as UIT application to the mast arm weld toe and the baseplate weld toe overlapped at times, so times are approximate.

Table 5.4.1.1 Employee’s First UIT Application to a Mast Arm Weld Times

	Phase 1	Phase 2	Phase 3	Phase 4	Phase 5	Extra	Total
Time (min)	7	35	35	20	5	20	102

By the end of two days of training the employees, TransAmerican employees could complete three to four UIT applications and paint repairs to mast

arms per day. However, by two weeks later, the employees were able to complete 10 to 15 UIT applications per day, according to a Houston TxDOT inspector.

5.5 DISCUSSION

5.5.1 Trained Applied Ultrasonics Technician Treatment vs Trained TransAmerican Employee Treatment

It is visible in Figure 5.4.2 that the TransAmerican employee held the UIT multi-pin tool at an extreme angle to the weld toe, not at the recommended 30° to 60°. The employee used more than the recommended two 3 mm diameter pins in the multi-pin UIT tool. The shiny areas visible in Figure 5.4.2 show that the employee's UIT application strayed from the weld toe into the baseplate, mast arm, and weld metal by many millimeters. Excess UIT application is not in accordance with approved UIT application techniques, and the effects of excess UIT application is unknown. However, since compressive stresses and plastic deformation definitely take place, even in areas of excessive UIT application, it can be assumed that poor UIT application that results in excess UIT application area will still enhance the fatigue life of the mast arm weld. The UIT application by the Applied Ultrasonics technician, on the other hand, was in perfect accordance with the Applied Ultrasonics UIT application guidelines. The bolts attaching the mast arm to the testing setup hampered both the employee and Applied Ultrasonics technician during UIT application.

Treatment by the Applied Ultrasonics technician from start to finish took less than an hour, and would have been less if the focus had been pure UIT application instead of instruction. Treatment by an employee on his first day of training can last for one to two hours, although the employee will have UIT

application times comparable to a trained Applied Ultrasonics technician after a few weeks. The TransAmerican employee did not understand English, which slowed the learning process at TransAmerican. A possible way to increase employee productivity would be to teach the UIT application technique in the employee's native language. Another possible way to expedite employee learning of UIT application is to have the employees being trained attend the morning presentation on UIT. By attending the morning UIT presentation, the employees being trained may feel more comfortable with the UIT tool when they begin their hands-on training.

5.5.2 UIT Application Concerns

A concern with UIT raised by the TxDOT inspectors is under-treatment. A concern that UIT needs to be applied entirely around the pole was raised, since cracks will find the new weakest spot in a connection. Since the mast arm-base plate connection is in compression on the bottom half of the mast arm, crack initiation in this area is not of concern.

Proper application of UIT requires that all galvanizing is removed during UIT application. Occasionally, UIT application does not remove galvanizing correctly. The problem of flaking galvanizing interfering with UIT application may be prevented by removing galvanizing prior to UIT application.

CHAPTER 6

Field UIT Application

6.1 INTRODUCTION

Previous research by Freytag has shown that UIT application during the fabrication process increases fatigue life of mast arms [29, 30]. Since UIT increases the fatigue life of mast arms when UIT is applied to new mast arms under loaded conditions in the fabrication yard, TxDOT considered the possibility that UIT would increase fatigue life of in-service mast arms with UIT applied as a retrofit. This chapter details the UIT retrofit process.

6.2 LOCATION OF MAST ARMS

Two mast arms on the corners of I-35E and Bonnie Brae Rd in Denton, TX had UIT retrofit. The two mast arms from Denton that underwent UIT retrofit are Mast arm 1 and Mast arm 2. Mast arm 1 is on the Northeast corner of the North intersection, and Mast arm 2 is on the Southwest side of the South intersection. The mast arms from the South intersection were removed 5 months after UIT retrofit for the tests of Chapter 7 and 8. From the South intersection, only Mast arm 2, on the Southwest side of the intersection, had UIT retrofit. The mast arm on the Northeast side of the South intersection did not have UIT retrofit, and was used as a control in the fatigue testing of Chapters 7 and 8. Figure 6.2.1 shows a satellite photo of the intersection. The North and South intersections where Mast arms 1 and 2 are located are marked in Figure 6.2.1.



Figure 6.2.1 Satellite Image of the Intersections Being Treated with UIT

The location of the mast arms for UIT retrofit was chosen due to a recent mast arm failure nearby. The recent mast arm failure indicated to TxDOT that the intersection of I-35E and Bonnie Brae St. experienced high winds. High wind loads create more fatigue cycles for mast arms than normal wind loads.

Mast arm 1 is 24 feet in length with a 7.5 inch diameter mast arm and end plate bolt spacing of 6" x 10". Figure 6.2.2 shows mast arm 1. Mast arm 2 is 28 feet in length with a 8 inch diameter mast arm and end plate bolt spacing of 7" x 11". Figure 6.2.3 shows Mast arm 2. Both mast arms have been in service for approximately 10 years.



Figure 6.2.2 Mast Arm 1 on the Northeast Corner of the North Intersection of I-35E and Bonnie Brae St. in Denton, TX



Figure 6.2.3 Mast Arm 2 at the Southwest Corner of the South Intersection of I-35E and Bonnie Brae St. in Denton, TX

As is visible in Figure 6.2.2, Mast arm 1 has 2 sets of lights. The first set of lights, closest to the mast, has 3 lights. There are 2 signs next, and then a 5 light signal structure. Finally, at the end of the mast arm is a rectangular horizontal plate, to reduce galloping.

As is visible in Figure 6.2.3, Mast arm 2 has a street sign right next to the mast, followed by a one-way sign. Next is a 3 light signal structure, followed by another sign. At the end of Mast arm 2 is a 5 light signal structure. Not visible is the horizontal rectangular plate behind the 5 light signal structure to reduce galloping on Mast arm 2. This plate is called a “damping plate”, or “sign blanks”. The damping plate on Mast arm 2 is shown in Figure 6.2.4.



Figure 6.2.4 Horizontal Damping Plate on Mast Arm 2

6.2.1 Traffic Control

Traffic was constant and heavy, but not congested. Traffic did not have to be stopped because the bucket truck could park partially on the grass or out of the way of traffic. Traffic cones were used at each site.

6.2.2 UIT Application

UIT was applied to both the end plate-mast arm weld and the baseplate-mast weld. UIT retrofit in Denton was part of a two-day UIT retrofit by TxDOT. Mast arms in other cities had UIT retrofit to select mast arms the day before UIT retrofit in Denton. The recommendation of UIT application to both toes had not yet been implemented in TxDOT procedure during the first day of UIT retrofit. The Applied Ultrasonics technician was first informed of the recommendation to apply UIT to both toes while in Denton. It was decided that the Applied Ultrasonics technician would apply UIT to one mast arm weld toe for Mast arm 2, following the same treatment parameters that were used in the other cities, and apply UIT to both mast arm weld toes for Mast arm 1. A multi-pin UIT tool with 3 mm diameter pins was used at all sites.

Figure 6.2.2.1 and Figure 6.2.2.2 show the UIT application to the Mast arm 1 weld toe. Figure 6.2.2.3 shows the UIT application to the Mast 2 weld toe. Both applications covered the area of the mast or mast arm in tension. The UIT application is visible because it is shinier than the non-treated areas. Notice the large bolts in Figure 6.2.2.1 that hinder UIT application.

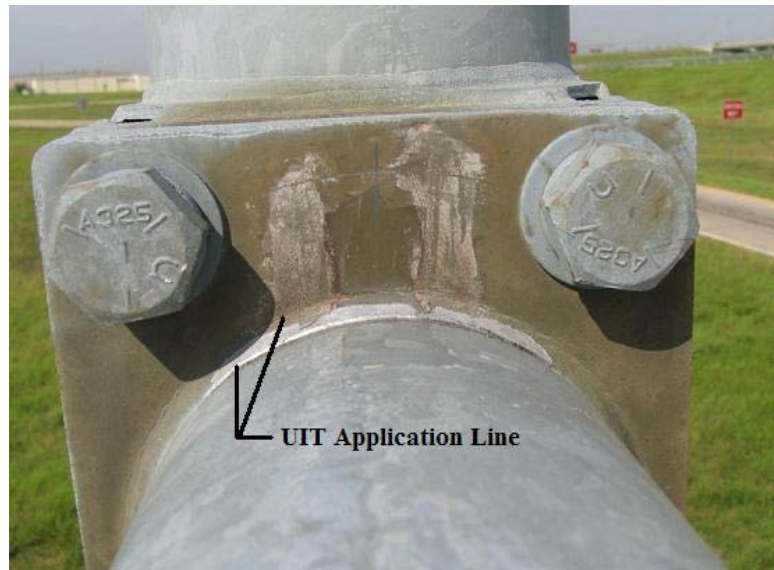


Figure 6.2.2.1 Mast Arm 1 After UIT Application.

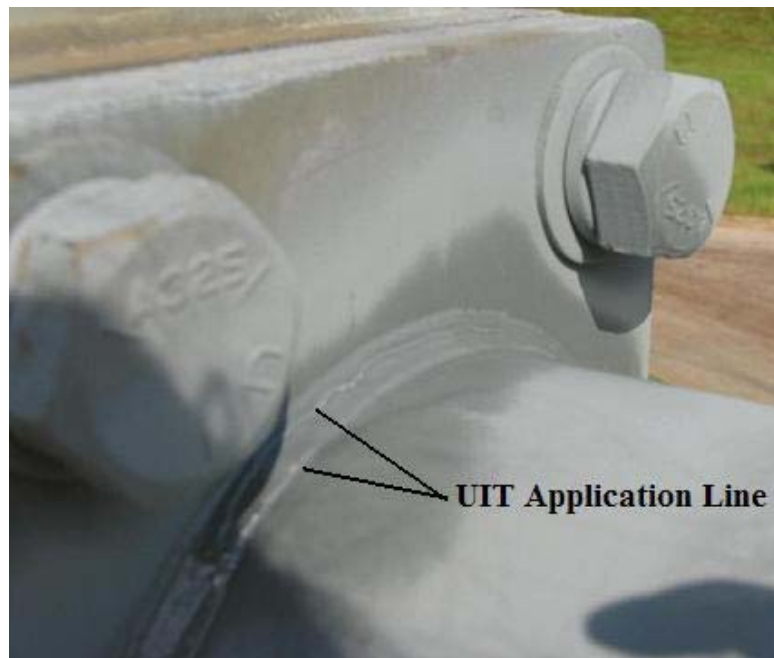


Figure 6.2.2.2 Mast Arm 1 After UIT Application and Spray-on Galvanization Repair



Figure 6.2.2.3 UIT Application at the bottom of Mast 2

First, the technician applied UIT to the base plate-mast arm weld toe. Next, the trained technician descended to apply UIT at the base plate-mast weld toe. To save time, the TxDOT inspector used the bucket truck to inspect the UIT application at the base plate-mast arm weld toe while the base plate-mast UIT application was performed. After satisfactory inspection by the TxDOT inspector, the TxDOT inspector applied two coats of a zinc-rich paint.

Finally the TxDOT inspector descends to inspect the base plate-mast weld UIT application and apply the zinc-rich paint. To save time, while the TxDOT inspector was inspecting and painting, if there were more masts and mast arms to be treated, the bucket truck was moved to the next UIT application location.

6.2.3 Inspection

The TxDOT inspector looked for a continuous application of UIT, meaning that the visible application was an unbroken line from start to finish. The TxDOT inspector also visually confirmed that the UIT extended 45 degrees in both directions from the top of the weld. Mast arms only received UIT application to the top 90° of the mast arm weld toe, and for Mast arm 1 only one toe was treated at the time of these application. Based on later laboratory tests, application to both weld toes has been recommended.

After inspection confirmation that the UIT application was satisfactory, the TxDOT inspector then used a flat-head screwdriver to scrape away galvanization loosened by the UIT application. Once the UIT application area was free of flaked galvanization and debris, the TxDOT inspector applied 2 coats of zinc-rich paint. The paint was Rust-oleum Cold Galvanizing compound, 93% pure zinc.

6.2.4 Application Times

The UIT applications of Mast arm 1 and 2 began at 10:17 am and finished at 11:11 am. The application times are shown in Table 6.2.4.1. The average time from arrival to site to departure of site is approximately 35 minutes. Total time at a site is not always just the addition of total times at the masts and the mast arms, since UIT application to the mast base begins while painting was applied to the mast arm.

Table 6.2.4.1 UIT Application Times

Location	Time (min)					Total Time
	Setup	UIT Application	Inspection and weld cleaning	Galvanization repair	Clean up	
Mast arm 1	11	6	2	3	2	24
Mast 1	-	6	3	4	0	13
					Total	33
Mast arm 2	5	6	2	3	2	18
Mast 2	-	7	3	4	4	18
					Total	36

6.2.5 Weather Conditions

According to Accuweather.com, on Thursday, September 23, 2004, at 10 AM it was 75°F with dewpoint at 63°F and 65% relative humidity with winds at 6 mph from the SSE. By 11 AM the temperature was 81 °F with dewpoint at 64°F, 57% relative humidity and winds out of the S at 9 mph.

6.3 MISCELLANEOUS OBSERVATIONS

Morning operations were stalled for 2 hours because the bucket truck was 2 hours late getting to the site due to trouble locating a generator.

The bolts used on Mast arm 2 interfered with UIT application, as visible in Figure 6.2.2.2. The technician applied UIT as best as possible, and the TxDOT inspector found the application to be adequate. The UIT should be applied at a 45° angle, however this was not always possible and the UIT was applied as closely to a 45° angle as possible. The TxDOT inspector suggested using the UIT tool with a 15° angle that is also available, but it was decided that technicians in the field would be unlikely to switch to a 15° angle UIT tool so the straight UIT

machine was used, in an effort to simulate actual field applications as accurately as possible.

The most common problem during the UIT applications was keeping the power generator running. It was discovered after UIT application that the power generator was on an angle, which caused the engine to flood. The power generator, the UIT generator, and the water cooler stayed in the truck during UIT application. The UIT tool has a 50-foot cord, as visible in Figure 6.2.2, which facilitated application to the mast arm welds.

The TxDOT inspector also had slight problems applying the zinc-rich paint in the field due to excessive wind, but this never slowed treatment for more than a minute.

CHAPTER 7

Fatigue Test Setup Details

7.1 INTRODUCTION

To determine the effectiveness of UIT retrofit, two mast arms with similar load histories were chosen for testing. One mast arm had UIT retrofit, and one did not. The mast arms with similar load histories were removed from the field and tested by the author in Ferguson Laboratories at the University of Texas at Austin. It was impossible for TxDOT to find two mast arms at the same location with similar load histories with the same geometric properties. It was decided that two mast arms at the same location with similar load histories would better reflect the effect of UIT retrofit than two mast arms with the same geometric properties with different load histories at different locations.

7.2 TEST SPECIMENS

The mast arm specimens to test UIT retrofit effectiveness were taken from the South intersection of I-35E and Bonnie Brae St. in Denton, TX. Figure 6.1.1 in Chapter 6 shows a satellite photograph of the intersection. The mast arm from the Southwest corner of the South intersection was treated in the field UIT as described in Chapter 6. This mast arm was removed from the field 5 months after UIT application, and will be referred to as mast arm DU. The “D” refers to “Denton” and the “U” refers to “UIT”. The mast arm from the Northeast corner of the South intersection was not treated by UIT. The untreated mast arm from the Northeast corner will be referred to as mast arm DN. The “D” refers to “Denton” and the “N” refers to “No UIT”.

Mast arm DU was a 24-foot mast arm with thickness of 0.152 inch after removal of galvanization, and a diameter of $7\text{-}\frac{1}{8}$ inch at the end plate. Mast arm DN was a 28-foot mast arm with thickness of 0.148 inch after removal of galvanization, and a diameter of $7\text{-}\frac{5}{8}$ inch at the end plate. Figure 7.2.1 shows the dimensions of the mast arm DU baseplate, and Figure 7.2.2 shows the dimensions of the mast arm DN baseplate.

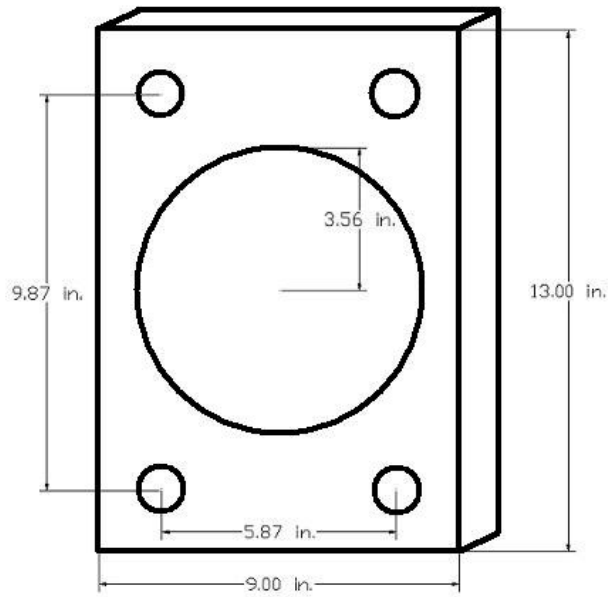


Figure 7.2.1 DU Mast Arm Baseplate Dimensions

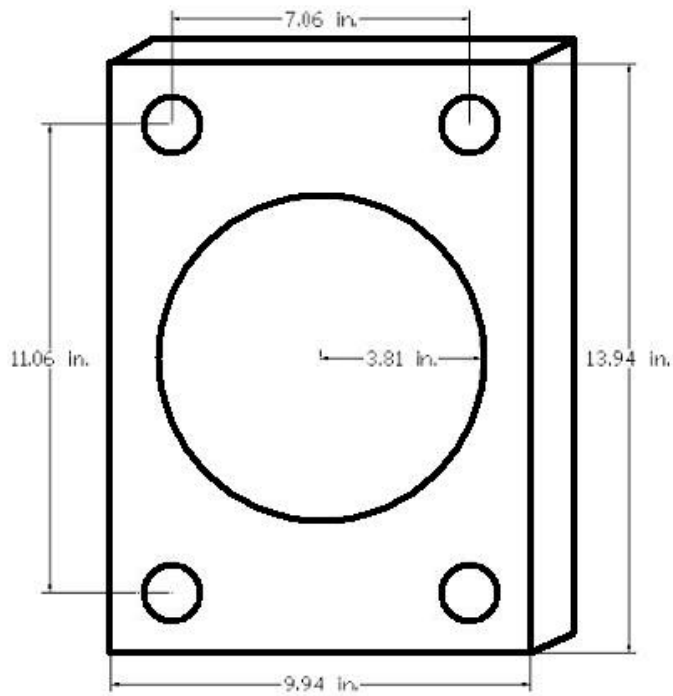


Figure 7.2.2 DN Mast Arm Baseplate Dimensions

7.3 TEST SETUP REVISIONS

As visible in Figure 7.2.1 and Figure 7.2.2, the mast arm DU baseplate and the mast arm DN baseplate have different bolthole spacing. Hence, the load box had two different bolthole spacing on either side. However, the bolthole spacing for each side of the load box had the same center, so as to not impose different moments on the mast arms in the test setup.

The mast arms were cut down to 85" to fit into the test setup, and had 10" x 10" x 1" steel end plates welded to the ends. The mast arm specimens were then connected to the load box by approximately 1 foot long all-thread rods. Mast arm DU required 1" all-thread rods, and mast arm DN required 1-1/4" all-thread rods. In order to eliminate the concern of prying of the baseplate onto the load box, washers were placed on the all-thread rod between the baseplate and the load box. Aside from preventing prying, the washers also provided a known load path between the base plate and the load box. With the washers in place, the load was being transferred directly at the bolthole of the baseplate, and not at any other locations around the baseplate. This eliminated any rocking of the baseplates due to out of flatness of the plates. Also, the washers were cut at angles to allow the angled mast arms to be horizontal at zero load when connected to the load box. A picture of the baseplate connected to the load box with the beveled washers is shown in Figure 7.3.1. Notice in Figure 7.3.1 that the top washer between the baseplate and the load box is longer than the bottom washer. The washers are beveled to match the angle of the baseplate.



*Figure 7.3.1 Beveled Washers Connecting the Mast Arm Baseplate to the Load
Box*

CHAPTER 8

UIT Retrofit Test Results

8.1 INTRODUCTION

The two mast arms described in Chapter 7 were tested by the author at Ferguson Laboratory at the University of Texas at Austin to determine the effectiveness of UIT retrofit. This chapter describes the test procedure and result of the two mast arms from Denton described in Chapter 7.

8.2 STATIC TESTS

Static tests were performed prior to dynamic testing of specimens DU and DN. All tests were cycled between a minimum and maximum displacement that corresponded to the loads that would induce the desired stresses at the mast arm weld toes. Desired loads were calculated using the same equations and assumptions that Koenigs and Freytag used for their tests on similar mast arms [28, 29, 30]. Loads were calculated from the dimensions of the mast arm at the mast arm weld toe. Using the outer diameter, D_o , and inner diameter, D_i , the moment of inertia at the weld toe, I , can be calculated from the equation: $I = \pi/64*(D_o^4 - D_i^4)$. Knowing the desired maximum and minimum stresses, and the distance from the centroid to the extreme fiber, $c = D_o/2$, the moment at the weld toe, M , can be calculated from the equation: $M = \sigma*I/c$. Using this data along with the length of the moment arm (the distance from the end support to the weld toe), l , the loads, P , corresponding to the desired stress can be calculated by the equation: $P = 2*M/l$.

The outer diameter of the test specimens was measured using either outer diameter calipers or measuring tape. The inner diameter was assumed to be the

difference of the outer diameter and twice the thickness, t , which can be described by the equation: $D_i = D_o - 2*t$. The thickness was measured from scrap pieces of the shortened specimens before calculations were made. The thickness was measured with digital calipers after removal of galvanizing with nitric acid.

The desired stress range for the smaller specimen DU was 12 ksi with a minimum stress of 16 ksi. The calculated minimum load was 2.30 kip and the maximum load was 4.03 kip. The result was a lower stress range on specimen DN, the untreated specimen. Table 8.1.1 shows the test loads and nominal stress ranges.

Table 8.2.1 Specimens DU and DN Geometric Properties and Calculated Loads, Stresses, and Strains

	Specimen	
	DU	DN
Diameter _{outer} (in.)	7.5267	7.9626
Diameter _{inner} (in.)	7.2227	7.6666
thickness (in.)	0.152	0.148
Length (in.)	88.5	88.5
I (in ⁴)	23.95	27.75
P _{min} (kip)	2.30	2.30
P _{max} (kip)	4.03	4.03
stress _{min} (ksi)	15.99	14.6
stress _{max} (ksi)	28.02	25.6
stress _{range} (ksi)	12.03	11.0

After specimens DU and DN were secured in the test setup, the mast arms were subjected to static loading from 0 kip to the maximum load of 4.03 kip and back to 0 kip in 1 kip increments. During the static test, displacements and strains

were measured. The static test also included measurements at the minimum load of 2.30 kip.

Strain gauges were attached at the top of the mast arm 3 inches from the weld, and at the mid-height of the baseplate on either side. Locations of the strain gauges are shown in Figure 8.1.1.

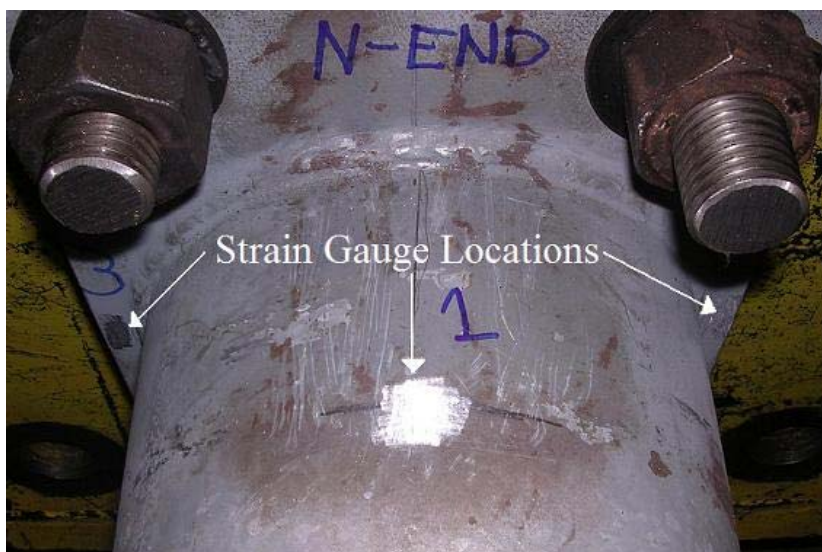


Figure 8.2.1 Locations of Strain Gauges

The results of the strain measurements at 3 inches from the mast arm-base plate weld were within 7.8% of the expected strains for the DU specimen, and within 15.8% of the expected strains for the DN specimen. Figure 8.2.2 is a plot of load vs. strain for the DU static test, showing both measured and expected strains. Figure 8.2.3 is a plot of load vs. strain for the DN static test, showing both the measured and expected strains. Since the strain gauges were attached 3 inches from the mast arm weld toe, expected strains were calculated using the moment arm and diameter at a the location of the strain gauge. These variations in strain were similar to those experienced by Koenigs for similar mast arms [28].

Variations between calculated and measured strains can be explained by improper placement of strain gauges, as well as assumption errors in the calculations.

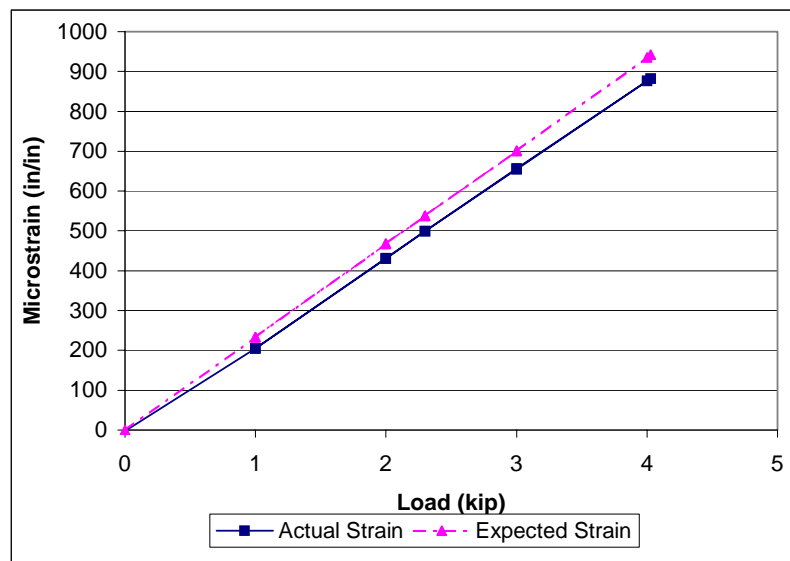


Figure 8.2.2 Actual and Expected Strain at 3 Inches from the Mast Arm Weld Toe of Specimen DU

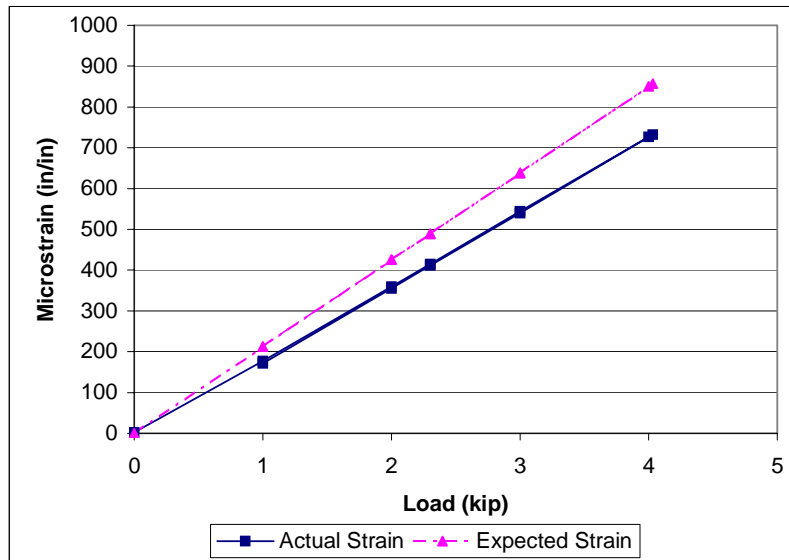


Figure 8.2.3 Actual and Expected Strain at 3 Inches from the Mast Arm Weld Toe of Specimen DN

Although base plate effects are not accounted for in this thesis, research is beginning at the University of Texas at Austin into the effects of base plate thickness on mast arm fatigue life. In an effort to gather information for future research, strains were also measured along the mid-height of the baseplate during static tests. Figure 8.2.4 shows the strains on both the East and West side of the mid-height of the DU baseplate. Figure 8.2.5 shows the strains on both the East and West side of the neutral axis of the DN baseplate. Notice that the DU baseplate has strains ranging to 225 in/in at 4.03 kip, while the DN baseplate has strains ranging to only about 61 in/in at 4.03 kip. The DU baseplate was only 1 inch thick, while the DN baseplate was $1\text{-}\frac{5}{16}$ inches thick. The additional $\frac{5}{16}$ inches on the DN baseplate adds stiffness to the baseplate that may increase the fatigue life of the mast arm weld. Current knowledge of the effect of baseplate thickness is discussed further in Section 8.4.2.

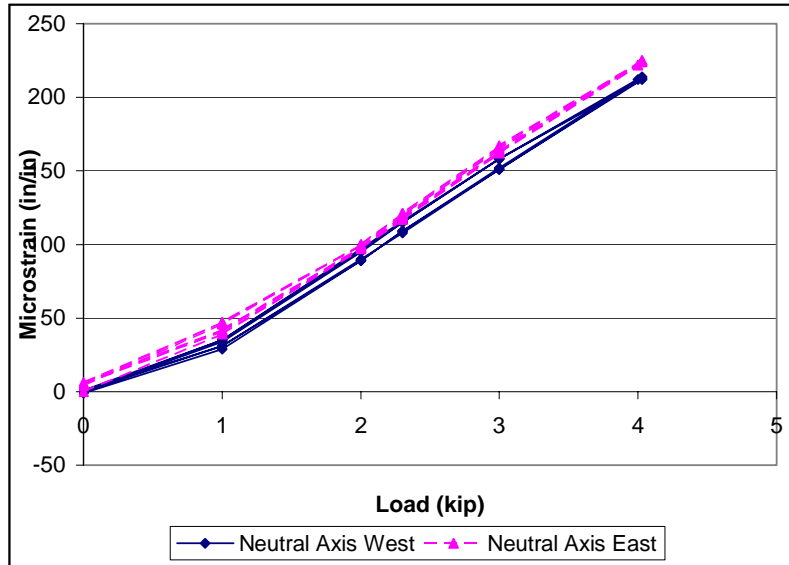


Figure 8.2.4 Strain at the Mid-Height of Baseplate DU

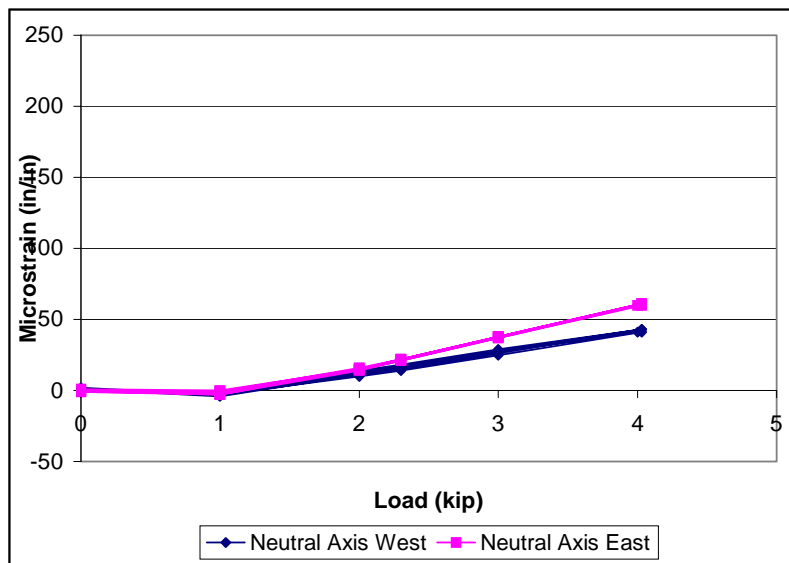


Figure 8.2.5 Strain at the Mid-Height of Baseplate DN

8.3 DYNAMIC TESTS

The dynamic loads were based on specimen DU's geometry and the desired stress range of 12 ksi, from a minimum stress of 16 ksi to a maximum stress of 28 ksi at the mast arm weld toe. The dynamic test was performed under displacement control. The displacements for the dynamic test were determined during static tests. There were three phases to the dynamic testing. The first dynamic test phase, Phase 1, cycled both uncracked mast arms DU and DN from 2.30 kip to 4.03 kip. The second dynamic test phase, Phase 2, cycled the uncracked DN mast arm, and the DU mast arm after weld repair from 2.30 kip to 4.03 kip. The third dynamic test phase, Phase 3, cycled the still uncracked DN mast arm, and the DU mast arm after weld repair and the addition of a stiffener, from 2.30 kip to 4.03 kip.

Table 8.2.1 gives the maximum and minimum loads and deflections during all three phases of dynamic testing. The differences in displacements are due to changes in stiffness of the repaired specimens. Limits were determined to be approximately a 5% addition to the maximum load and deflection and approximately a 5% drop from the minimum load and deflection.

Table 8.3.1 Maximum and Minimum Loads and Deflections During Dynamic Testing

Phase:	Phase 1		Phase 2		Phase 3	
Duration (cycles):	0 - 90,680		90,680 - 116,876		116,876 - 224,905	
	Min	Max	Min	Max	Min	Max
Load (kip)	2.30	4.03	2.30	4.03	2.30	4.03
Deflection (in)	3.175	3.625	3.091	3.543	2.832	3.216

The testing conditions of Phase 1 lasted until mast arm DU developed fatigue cracking that lowered applied loads below the limits at 90,680 cycles. A close-up of the fatigue cracks in the DU mast arm weld toe along the UIT application line is shown in Figure 8.3.1. Figure 8.3.2 shows the entire fatigue crack on mast arm DU after highlighting with a red marker.



***Figure 8.3.1 Close-up of Fatigue Crack on Specimen DU Mast Arm Weld Toe
Along the UIT Application Line (90,680 cycles)***



***Figure 8.3.2 Highlighted Fatigue Crack on Specimen DU Mast Arm Weld Toe
Along the UIT Application Line (90,680 cycles)***

The fatigue crack in specimen DU was repaired by grinding away the galvanizing and re-welding the fatigue crack. The mast arms were then cycled between maximum and minimum load at 0.08 Hz to determine the displacements for Phase 2 of the dynamic test.

The testing conditions of Phase 2 lasted until a new fatigue crack on mast arm DU occurred through the weld repair at 116,876 cycles. A close-up of the second fatigue crack in the DU mast arm weld toe through the weld repair is shown in Figure 8.3.3.



***Figure 8.3.3 Close-up of Fatigue Crack on Specimen DU Mast Arm Weld Toe
Along the Weld Repair (116,876 cycles)***

After the failure of the weld repair on mast arm DU, it was decided to add a stiffener to mast arm DU, to prevent further fatigue cracking. Figure 8.3.4 shows the stiffener added to mast arm DU before Phase 3 dynamic testing.



Figure 8.3.4 Stiffener Added to Mast Arm DU After 116,876 Cycles

The testing conditions of Phase 3 lasted until mast arm DN developed a fatigue crack at 224,905 cycles. A close-up of the fatigue crack in the DN mast arm weld toe is shown in Figure 8.3.5. Figure 8.3.6 shows the entire fatigue crack on mast arm DN after highlighting with a red marker.



Figure 8.3.5 Close-up of Fatigue Crack Along Mast Arm Weld Toe of Specimen DN (224,905 cycles)



Figure 8.3.6 Highlighted Fatigue Crack Along Mast Arm Weld Toe of Specimen DN (224,905 cycles)

8.4 FATIGUE TEST RESULTS

Since mast arms DU and DN did not have the same mast arm thickness, mast arm diameter, baseplate thickness, bolthole spacing, or any other comparable characteristics, the best way to compare the fatigue test results is by plotting results on a S-N chart. Figure 8.4.1 shows a S-N chart of DU and DN on the same plot, along with AASHTO fatigue Categories. Both axes are log scales.

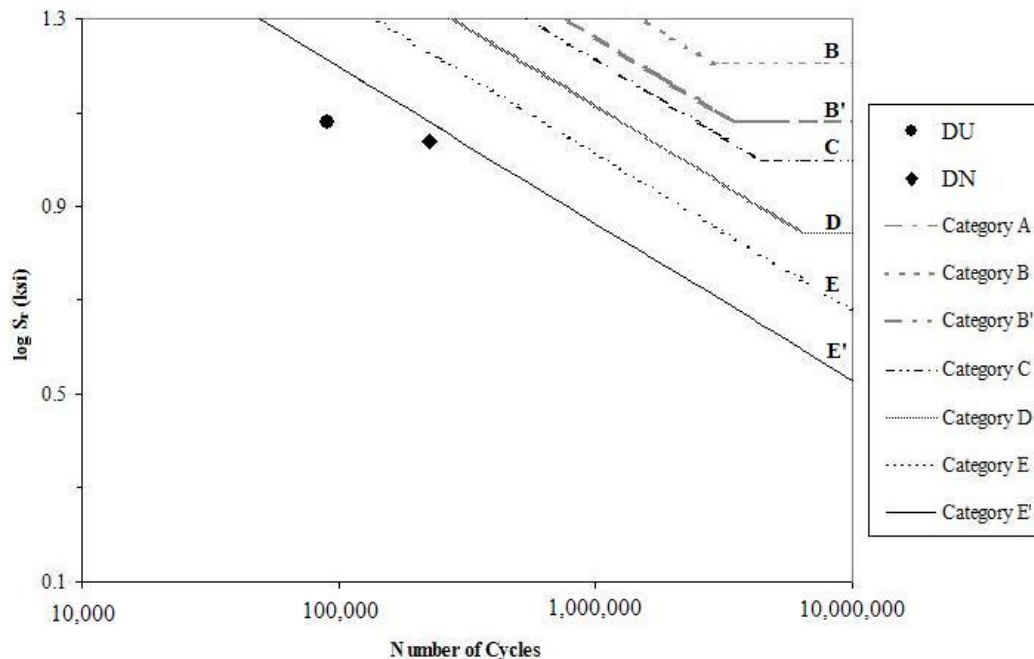


Figure 8.4.1 S-N Plot of DU, DN, and AASHTO Fatigue Categories

Figure 8.4.1 shows that neither mast arm DU nor mast arm DN reached Fatigue Category E'. The S-N plot for mast arm DU and DN also shows that DU had a slightly better fatigue resistance than DN. These results show that UIT retrofit does not improve fatigue life.

8.5 DISCUSSION

The results from the fatigue tests of DU and DN show that mast arms that have been in the field for 10 years under higher-than-average wind loads do not benefit from UIT retrofit. However, differences in geometries introduce variables that make a direct comparison impossible.

8.5.1 Field UIT Application vs. Fabrication Yard UIT Application

Fatigue testing by Freytag was conducted at Ferguson Laboratories at the University of Texas at Austin on mast arms from TransAmerican facility [29, 30]. Tests included mast arms with and without UIT. Mast arms with UIT had UIT applied at TransAmerican's facility. Table 8.5.1.1 lists the fatigue results of the mast arms from TransAmerican and Denton, TX. Mast arms with UIT application at the fabrication yard are labeled TAU. Mast arms without UIT from TransAmerican are labeled TA. Figure 8.5.1 shows the S-N plot comparing mast arms with UIT applied in the fabrication yard to mast arms with UIT retrofit in the field.

Table 8.5.1.1 Test Results for TA Series, TAU Series, DU, and DN

Specimen Name	Stress Range (ksi)	Mast Arm D _o (in.)	Number of Cycles	UIT?	Base Plate thickness (in.)
TA A	12	10	75,121	No	1.25
TA B	12	10	59,196	No	1.25
TA C	12	10	44,771	No	1.25
TA D	12	10	62,026	No	1.25
TAU A	12	10	263,044	Yes	1.25
TAU B	12	10	246,045	Yes	1.25
DU	12	7.5	90,680	Yes	1
DN	10.9	8	224,905	No	1.625

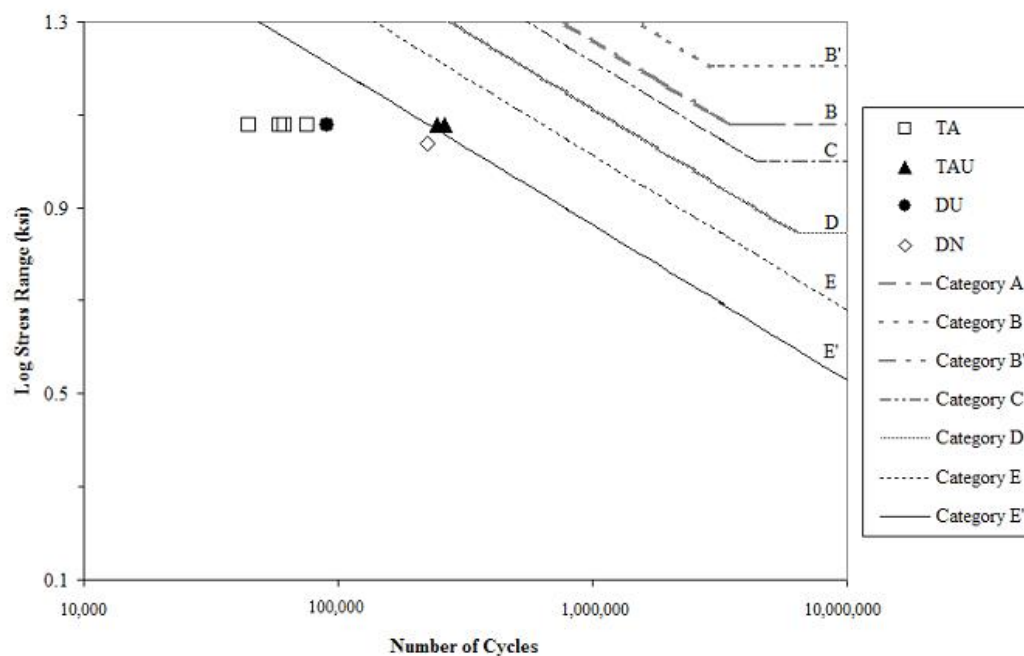


Figure 8.5.1 S-N Plot for DU, DN, and the TAU Series

As can be seen in Table 8.5.1.1 and Figure 8.5.1, UIT application at the fabrication yard increased fatigue life of TransAmerican mast arms to above Category E'. Mast arm DU, with field UIT application, did not see the same improvement in fatigue life as the TAU specimens at the same stress range. However, since geometric properties vary between the specimens, a direct comparison cannot be made. More tests, involving specimens with the same geometries, should be conducted to allow for accurate comparisons.

It is also worth noting that both TAU specimens developed unusual fatigue cracking along the untreated weld toe. This unusual crack development was discussed in Chapter 3. From the investigations of TAU specimens' fatigue cracks, it has been recommended to apply UIT to both weld toes to prevent unusual fatigue cracking in the future.

8.5.2 Effect of Baseplate Thickness

Previous tests by Koenigs compared the fatigue resistance of mast arm welds on 1.5 inch baseplates with the fatigue resistance of mast arm welds on 2 inch baseplates. Both baseplate sets had holes for the mast arm. Tests confirmed that the 0.5 inch increase in baseplate thickness increased fatigue resistance. The 1.5 inch baseplate specimens had a fatigue Category of E, while the 2 inch baseplate specimens had fatigue Categories ranging from D to B', which is a significant increase in fatigue performance.

Koenigs studied the effect of baseplate thickness on socket weld stress concentration factors using Finite Element Analysis (FEM) [31]. Three baseplate thickness were analyzed: 1.50 inch, 2.00 inch, and 12.00 inch. Results show that increasing the thickness of a relatively thin baseplate is the most effective. Increasing the baseplate thickness from 1.50 inch to 2.00 inch decreases the stress concentration factor by 24%, while increasing the baseplate thickness from 1.50 inch to 12.00 inch reduces the stress concentration factor by 48%.

Although the exact effects of baseplate thickness for mast arms are not yet known, it is safe to assume that thicker baseplates lead to increased fatigue resistance of mast arm weld toes. As visible in Figure 8.2.4 and Figure 8.2.5, the 1 inch base plate experienced microstrains of 225 in/in at a 4.03 kip load, while the 1.625 inch base plate only experienced a microstrain of 61 in/in at the same load. The increased bending of DU's baseplate, as evidenced by the large strain at the mid-height, increased the bending strain in the mast arm weld toe during loading. Bending effects may have compounded any fatigue effects specimen DU's mast arm weld toe experienced, and lead to a decreased fatigue life.

8.5.3 Weld Toe Geometry

Another important factor in fatigue resistance of a weld is weld toe geometry. Previous research shows that UIT increases the toe radius and introduces an undercut for softer metals [9]. UIT improvements on weld toes lower the stress concentration at the weld toe [19].

TxDOT specifications for mast arm weld toes are found in document MA-C-96: Standard Assembly for Traffic Signal Support Structures. The dimensions for the standard mast arm-baseplate weld are shown in Figure 8.5.3.1, which is taken from TxDOT document MA-C-96. As shown in Figure 8.5.3.1, the long leg of the weld should be $\frac{7}{16}$ " , and the short leg should be $\frac{1}{4}$ " , giving a global angle of 30° .

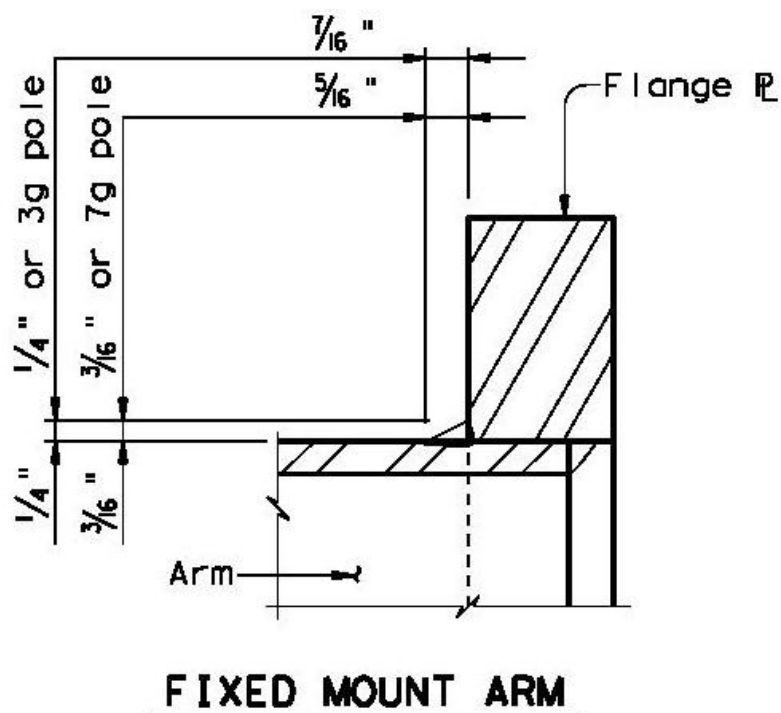


Figure 8.5.3.1 Standard Mast Arm-Baseplate Weld Dimensions from TxDOT Document MC-C-96

Molds were made of the mast arm weld profile for mast arm DU both before and after UIT application. A mold of the mast arm weld for mast arm DN was also made. The molds were made as described in Chapter 2. Figure 8.5.3.2 shows a typical weld, pointing out the locations of the long and short leg. All measurements of the weld legs were made with the Mitutoyo Profile Projector, Model PJ250. The Profile Projector projected a 10x magnification of the weld mold onto a screen with cross hairs. From this projection, a digital readout with accuracy of 0.0001 inch was adjusted to give the lengths of the weld legs.

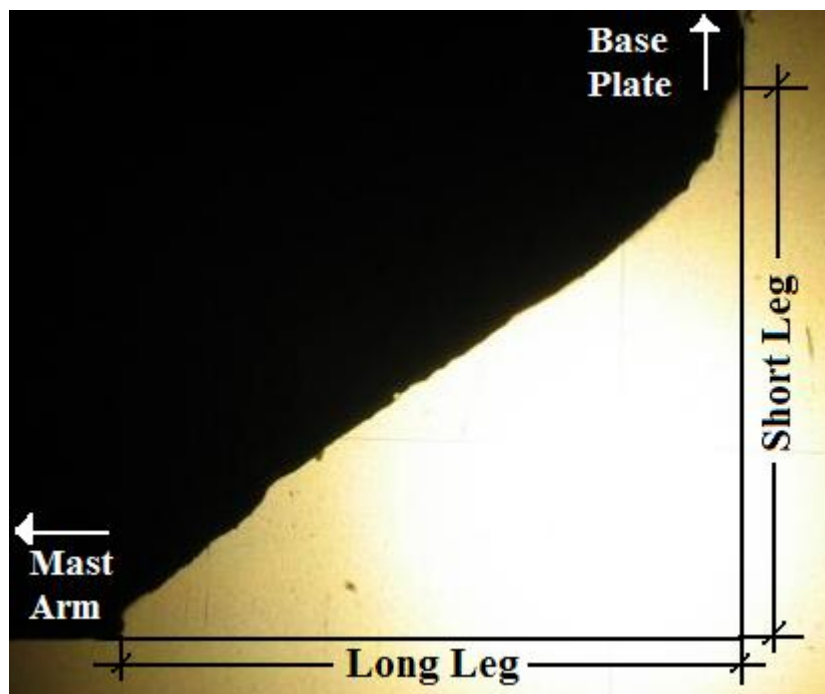


Figure 8.5.3.2 Typical Weld Leg Locations

Figure 8.5.3.3 shows the weld profile of mast arm DU before UIT application at 10x magnification. Figure 8.5.3.4 shows the weld profile of mast

arm DU after UIT application at 10x magnification. Comparison of Figure 8.5.3.3 and Figure 8.5.3.4 clearly show a change in weld toe profile. As mentioned in previous research, the weld toe profile after UIT application has a visibly increased toe radius.



Figure 8.5.3.3 10x Magnification of Mast Arm Weld DU Before UIT

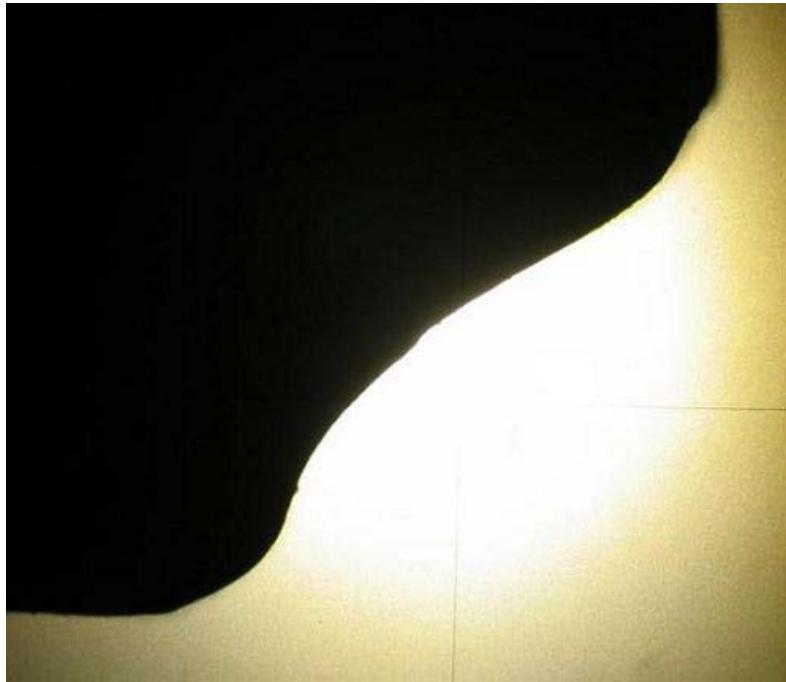


Figure 8.5.3.4 10x Magnification of Mast Arm DU Weld After UIT

The weld toe geometries for specimens DU and DN, as well as the standard mast arm-base plate weld toes geometries, are listed in Table 8.5.3.1. The global angle is the angle between the long leg and the hypotenuse, taken as the arctangent of the short leg/long leg.

Table 8.5.3.1 Weld Toe Geometries

Weld	Average Values		
	Short Leg (in.)	Long Leg (in.)	Global Angle (°)
DU Before UIT	0.312	0.412	37
DU After UIT	0.318	0.338	43
DN	0.344	0.386	42
Specification	0.250	0.438	30

Mast arm DU before UIT had weld geometry closest to the specifications. The DU short leg was about 0.06 inch longer than specifications, and the long leg was about 0.02 inches shorter than specification before UIT application. UIT did not change the length of DU's short leg, but UIT application only decreased the length of the long leg, as expected. The length of DU's long leg decreased from 0.02 inches shorter than specifications to about 0.10 inch too short. As a result, the DU's global angle increased from 7.4° above specification to 13.6° above specification.

Figure 8.5.3.5 shows the weld profile of DN at 10x magnification. Both DU and DN had short legs that were longer than specification, and long legs that were shorter than specification. Comparison of the weld profile of DU after UIT with the weld profile of DN shows distinctly different weld profiles. Weld quality on mast arms should be investigated.



Figure 8.5.3.5 10x Magnification of Mast Arm DN

CHAPTER 9

Conclusions and Recommendations

9.1 CONCLUSIONS

- UIT application to mast arm weld toes has fatigue cracking initiate at the treated mast arm weld toe, and propagate into the parent material in almost all fatigue tests of mast arms with UIT application [28, 29, 30]. However, two mast arms with UIT application at the mast arm weld toe had fatigue crack initiation at the untreated base plate weld toe [29]. Since the untreated base plate weld toe is a possible site of fatigue crack initiation it is suggested to treat both weld toes of mast arm-base plate welds.
- UIT peened mast arm welds that have heat-applied solder galvanization repair at temperatures of 600°F to 750°F have significantly lower fatigue lives than comparable UIT peened and un-treated mast arms that did not have heat-applied galvanization repair. This low fatigue life may be due to a one-time large displacement of 2.5 inches, but it is more likely that temperatures above 572°F relieve the beneficial compressive stresses induced by UIT [7].
- UIT applied in the fabrication yard have to new mast arms improves fatigue resistance. Data from fatigue tests of UIT retrofit in the field is inconclusive due to differences in geometries of test specimens.
- Magnification of weld profiles and measurements of weld geometries from the Denton mast arms show that at least some welds that are in the field differ from specifications.

9.2 RECOMMENDATIONS FOR FURTHER RESEARCH

- Fatigue life varied greatly with difference in mast arm and base plate geometry. One possible difference in geometry that may affect fatigue life is base plate thickness. A better understanding of the influence of base plate thickness on fatigue resistance would clarify the effects of UIT and allow a better comparison between the test results of mast arms DU and DN.
- The two mast arms from Denton that were included in this thesis were not comparable due to difference in mast arm and base plate geometry. Replications of this test, with comparable mast arms, would expand on the knowledge gained in this thesis.
- Current UIT application occurs while mast arm weld toes experience a stress of 16.5 ksi, as per Koenigs' tests [28]. More research into the best treatment stress may further improve the benefits of UIT application to the mast arm weld toes.
- Weld quality effects fatigue crack initiation, and hence fatigue life of mast arms. The effects of UIT on different weld qualities have not been investigated to date. Research to date has only investigated the effects of UIT on welds that meet welding specifications. Research of the effects of UIT on welds that do not meet welding specifications would increase the understanding of the effect of UIT as a retrofit process to imperfect welds.

APPENDIX A

Previous Research

A.1 PREVIOUS RESEARCH GEOMETRIES

Table A.1.1 Geometric Properties of Koenigs' Phase 1 Test Specimens

Specimen Name	D _o (in)	Pole Wall Thickness (in.)	End Plate Thickness (in)
VALu A	9.958	0.171	1.5
VALu B	9.969	0.17	1.5
VALu C	9.979	0.17	1.5
VALu D*	10	0.172	1.5
TXu A	9.969	0.23	1.5
TXu B	9.948	0.23	1.5
TXu C	9.969	0.234	1.5
TXu D	9.948	0.233	1.5
VAL 3x3/8 A	9.969	0.169	1.5
VAL 3x3/8 B	9.958	0.17	1.5
TX 3x3/8 A	9.938	0.233	1.5
TX 3x3/8 B	9.969	0.234	1.5
VALu EP	10.031	0.175	1.5
VALu FP	9.979	0.176	1.5
TXu EP	9.979	0.236	1.5
TXu FP	9.969	0.239	1.5
VAL 3x3/8 CP	10	0.171	1.5
TX 3x3/8 CP LMS	9.917	0.227	1.5

Table A.1.2 Geometric Properties of Koenigs' Phase 2 Tests

Specimen Name	D _o (in.)	Pole Wall Thickness (in.)	End Plate Thickness (in.)
VALNu A	9.948	0.17	1.5
VALNu B	9.979	0.171	1.5
VALNu G A	10.01	0.173	1.5
VALNu G B	10	0.175	1.5
VALNu PR A	9.99	0.174	1.5
VALNu PR B	9.979	0.175	1.5
VALNu GP A	9.979	0.174	1.5
VALNu GP B	9.969	0.173	1.5
VALNu CP	9.979	0.171	1.5

Table A.1.3 Geometric Properties of TransAmerican Tests

Specimen Name	Mast Arm D _o (in)	Pole Wall Thickness (in)	End Plate Thickness (in.)
TA A	10	0.25	1.25
TA B	10	0.25	1.25
TA C	10	0.25	1.25
TA D	10	0.25	1.25
TX u A L GP	10	0.25	1.25
TX u B L GP	10	0.25	1.25

A.2 PREVIOUS TEST RESULTS

Table A.2.1 Koenigs' Phase 1 Test Results

Specimen Name	Controlling Stress Range (ksi)	Cycles at Failure	Crack Location(s)	UIT Application Stress (ksi)	Maximum Stress (ksi)
VALu A	11.9	249,446	Toe of socket weld	None	28.5
VALu B	11.9	453,948	Toe of socket weld	None	28.5
VALu C	6.29	2,072,592	Toe of socket weld	None	28.5
VALu D*	6.2	6,856,881	Run Out - no cracking	None	28.5
TXu A	6	2,199,343	Toe of socket weld	None	28.5
TXu B	6.1	2,816,706	Toe of socket weld	None	28.5
TXu C	11.8	177,596	Toe of socket weld	None	28.5
TXu D	12	194,694	Toe of socket weld	None	28.5
VAL 3x3/8 A	11.7	386,253	Termination of stiffener	None	28.5
VAL 3x3/8 B	11.6	410,410	Termination of stiffener	None	28.5
TX 3x3/8 A	11.7	473,735	Toe of socket weld & Termination of stiffener	None	28.5
TX 3x3/8 B	11.6	657,716	Termination of stiffener	None	28.5
VALu EP	11.4	393,767	Toe of socket weld	0	28.5
VALu FP	11.5	353,103	Toe of socket weld	0	28.5
TXu EP	11.8	320,915	Toe of socket weld	0	28.5
TXu FP	11.7	141,155	Toe of socket weld	0	28.5
VAL 3x3/8 CP	11.5	393,767	Termination of stiffener	0	28.5
TX 3x3/8 CP LMS	12.1	1,707,128	Toe of socket weld & Termination of stiffener	0	14

Table A.2.2 Koenigs' Phase 2 Test Results

Specimen Name	Controlling Stress Range (ksi)	Cycles at Failure	Crack Location(s)	UIT Application Stress (ksi)	Maximum Stress (ksi)
VALNu A	11.9	389,428	Toe of socket weld	None	28.5
VALNu B	11.8	265,540	Toe of socket weld	None	28.5
VALNu G A	11.6	183,132	Toe of socket weld	None	28.5
VALNu G B	11.5	151,679	Toe of socket weld	None	28.5
VALNu PR A*	11.6	4,557,126	Run Out - no cracking	16.5	28.5
VALNu PR B*	11.5	4,557,126	Run Out - no cracking	16.5	28.5
VALNu GP A	11.6	4,545,952	Toe of socket weld	16.5	28.5
VALNu GP B	19.91	224,240	Toe of socket weld	16.5	28.5
VALNu CP	19.95	1,301,077	Toe of socket weld	16.5	28.5

Table A.2.3 TransAmerican Test Results

Specimen Name	Stress Range (ksi)	No. of cycles	UIT Application Stress (ksi)	Maximum Stress (ksi)
TA A	12	75,121	None	28
TA B	12	59,196	None	28
TA C	12	44,771	None	28
TA D	12	62,026	None	28
TX u A L GP	12	263044	16.5	28
TX u B L GP	12	246045	16.5	28

APPENDIX B

Literature Review – Part 1: History of Ultrasonic Impact Treatment (UIT)

B.1 HISTORY OF ULTRASONIC IMPACT TREATMENT (UIT)

The beneficial effects of ultrasound on mechanical properties of steel and metal alloys were first published in the late 1950's and early 1960's by many authors [20]. Proof of ultrasound's valuable enhancements to steels and alloys prompted research to create a tool that applied ultrasound directly to welds. Scientists were challenged to produce a manageable tool that utilized the benefits of ultrasound on metals. Difficulties included power needs, size constraints, mobility, and the dual need for a waveguide with rigid constraint while providing a deforming element that allowed for treatment of uneven welds [1].

By the 1970's, E. Statnikov introduced the ultrasonic impact tool for strengthening welds and reducing residual stresses [2]. E. Statnikov originally intended the ultrasonic impact tool for use on naval ships in the Soviet Union. Research has shown that the ultrasonic impact tool relaxes residual stresses by at least 50% in steel at depths of up to 12 mm [1], and increases the fatigue strengths of welded joints by improving weld toe geometry, removing defects, and introducing beneficial residual stresses [3, 4]. Statnikov's tool optimized power, weight, and size characteristics of the ultrasonic equipment, as well as developed an effective connections scheme providing moving constraint between a deforming element and a waveguide [1]. Northern Scientific & Technological Company (NSTC) of Russia [3], in association with Paton Welding Institute in

Kiev, Ukraine [5] have made significant further developments on the ultrasonic impact tool.

Research on ultrasonic impact treatment (UIT), specifically the effectiveness of treatment and comparisons with different weld treatments, has been carried out in Russia [6, 7], Ukraine [8], France [9, 10], China [4, 11], Norway [3], Finland [12], and the US [5, 13, 14, 15, 16]. After many decades of testing, IIW UIT Specification was issued in 1996 [17]. E. Statnikov was awarded a U.S. patent for UIT on January 15, 2002 [18].

B.2 UIT MACHINE COMPOSITION

Figure B.2.1 shows the UIT tool. The UIT equipment is composed of:

- Ultrasonic Generator
- Ultrasonic Transducer (Magnetostriction or Piezoelectric Transducer)
- UIT tool
- Cooling tank (not shown) [10, 19]

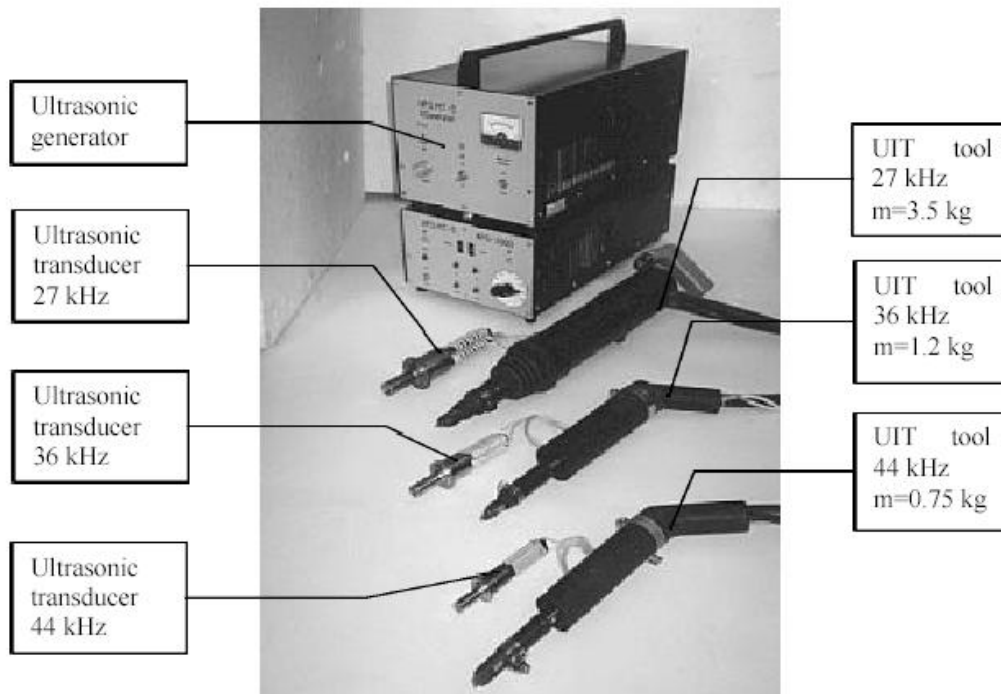


Figure B.2.1 UIT Equipment, Including UIT Generator, Transducer, and Tool

[17]

The peening unit, referred to as an ultrasonic peening gun or the UIT tool, consists of the acoustic system, shell, and holder, and is designed to give a high treatment velocity and a strong peening force [11].

Ultrasonic impact treatment of the metal or weld surface consists of a rounded pin at the end of the tool vibrating at an ultrasonic frequency in a direction perpendicular to the treated surface [7]. The ultrasonic impact tool can be hand-applied, or mounted on metal machining equipment.

B.3 UIT BENEFITS

The main benefits of UIT are increases of fatigue life, endurance limit, and fatigue strength for welded joints, especially in high strength steels. UIT is a beneficial treatment for any weld, regardless of the weld shape [9, 19].

UIT has advantages over many other weld and metal fatigue life improvement techniques. One of the UIT advantages is its easy application to hard-to-access areas [1]. Another important UIT attribute is that UIT is a relatively quiet technique [3, 11, 12, 16, 19, 20] that is light [3, 11, 12, 16], does not produce the excessive shaking associated with most peening techniques [3, 12, 16, 20] and is easy to learn [7, 17, 20].

UIT can be applied at any time during the life of a metal structure: during fabrication, in use, or as repair. Because UIT induces compressive stresses, UIT can even be applied on welds with initial cracks [9, 14, 17, 18, 19, 21]. Ideal candidates for UIT include new and existing bridges [14]. UIT has been shown to work effectively on a wide range of metals, including low-carbon steel, low-alloy steel, and high strength steel. UIT has also been shown to effectively improve fatigue characteristics on a wide range of welded joints, including butt, fillet, non-load carrying longitudinal, cruciform, transverse, and tube welds.

B.4 MACHINE SPECIFICATIONS

B.4.1 Energy Transform

There are two general types of ultrasonic transducers that can be used for UIT: magnetostrictive and piezoelectric. Both accomplish the same task of converting alternating electrical energy to vibratory mechanical energy but do it in a different way.

Magnetostrictive transducers are generally less efficient than the piezoelectric ones. Magnetostrictive transducers require a dual energy conversion from electrical to magnetic and then from magnetic to mechanical. Magnetic hysteresis effects also detract from the efficiency of the magnetostrictive transducer. In addition, the magnetostrictive transducer for UIT needs water-cooling. The equipment in this case is relatively heavy and expensive.

Piezoelectric transducers convert alternating electrical energy directly to mechanical energy through the piezoelectric effect in which certain materials change dimension when an electrical charge is applied to them. Piezoelectric transducers incorporate stronger, more efficient, and highly stable ceramic piezoelectric materials, which can operate under high temperature and stress conditions.

The efficiency of the modern piezoelectric transducers is 98% as compared to only 25% to 30% for typical magnetostrictive transducers. Piezoelectric transducers are reliable today and can reduce the energy costs for operation by as much as 60% [22].

Many tests did not include the type of ultrasonic transducer used, most likely because the researchers did not know what they were using due to proprietary rights at the time the tests were conducted. The few tests that included the type of ultrasonic transducer used list both magnetostrictive transducers [10, 19] and piezoelectric transducers [4, 11]

B.4.2 Pathways of Energy Transfer

UIT benefits steel and alloys through a multi-phase conversion of energy. First, the ultrasonics transducer undergoes forced harmonic oscillations. These harmonic oscillations flow through a concentrator of oscillating velocity, the

waveguide. The waveguide then impacts upon an indenter, often in the form of one or multiple small pins with a diameter that can range from 2 to 16 mm. The indenter pins impact upon the metal specimen surface, transferring the oscillating velocity to the surface metal of the specimen to be treated. The oscillations in the treated metal are transformed into force impulses during the impact of the indenter pins on the surface of the treated metal [1, 17].

Impacts of indenter pins upon the treated metal specimen create one of four possible interactions between the indenter and the metal.

1. Ultrasonic Periodic Impact. In this case, the indenter induces plastic deformation of the metal, which always occurs, but with the added result of exciting ultrasonic periodic stress waves in the treated metal. Hereafter, both the indenter and treated metal oscillate at the same frequency, and are in continuous contact during treatment.
2. Ultrasonic Non-Periodic Impact. Similar to Ultrasonic Periodic Impact, with the difference of non-periodic stress waves in the treated material, as opposed to periodic stress waves. The result of ultrasonic non-periodic impact is that the indenter rebounds of the metal specimen during treatment.
3. Single contacts of the indenter with a rebound off the metal specimen. This causes propagation of single stress pulses in the treated specimen.
4. A combination of the forced oscillations of the indenter both impacting and rebounding off the surface of the treated metal. The combination of these two events can have features of random and controlled events. The nature of these events

depends on the algorithm of oscillating system excitation and impact control. [17, 23]

The energy of force pulses and oscillations during indenter impact on the treated metal specimen is sequentially utilized for: plastic deformation of the metal surface, saturation of the near-surface layer of the treated metal with plastic deformations, oscillations and pulsed deflection of the treated layer during the impact, and creation of ultrasonic stress waves and force pulses in the volume of treated material [17].

B.4.3 Different UIT Machine Options Available

A variety of UIT machines have been developed for tools that oscillate at frequencies of 27, 36, and 44 Hz, while a 55 Hz UIT machine is currently under development [21]. The higher frequency UIT tools decrease in weight and have increasing treatment speed with increasing frequency. The benefit of higher frequency UIT tools will be increased ease of use and speed of application. There are currently prototypes of UIT tools with a working frequency of 36 and 44 kHz [17], although there are no published results on any tests of these prototypes.

B.5 UIT APPLICATION PARAMETERS

Manufacturers of UIT machines often include their own specifications of operating parameters. UIT machines have been created in China, Russia, Ukraine, Canada, and the United States. Operating parameters that have been used in research over the past few decades are listed in the following subsections.

B.5.1 Frequency

The most common ultrasonic frequency of the UIT tool used in research is close to 27 kHz, and has been used on tests in the US [5, 13, 20], France [9], Finland [12], Russia [17], and the Ukraine [19]. One test conducted in Russia in 2000 reported using a tool frequency of 21 kHz [6]. Another variation of frequency was a reported 27.5 kHz [7]. The Applied Ultrasonics specifications expect a tool frequency to be 26.9 to 27.2 kHz [1].

B.5.2 Pin Diameter

The majority of UIT application is done with a multi-pin tool, although a single-pin version is available. The single pin UIT tool consists of a 16 mm diameter element [7]. The multi-pin tool has settings for pins ranging from 2 to 5 mm diameter [17]. Although many tests did not specify the pin size, most tests did use the multi-pin tool. Tests that did specify the size pin used utilized the 3 mm diameter pin [3, 5, 12, 15, 16] or the 5 mm diameter pin [15, 16]. Only one pin size is used at a time. Not a single report included how many pins were used on the multi-pin tool.

Comparison of fatigue curves for the as-welded joints and welded joints treated by UIT using various parameters shows that the maximum effect is obtained by treatment using a 3 mm multi-pin tool [15, 16].

B.5.3 Amplitude

The most common amplitude is 30 μm [1, 12, 19]. One test used an amplitude of 20 μm [6], while another used an amplitude closer to 15 μm [24]. Although most tests did not specify what amplitude they used during UIT

application, Applied Ultrasonics specifies an amplitude of 35-40 μm when applying UIT with their tool [17].

B.5.4 Speed

Most tests that specified the speed of the tool during application reported a treatment velocity of 0.5 m/min [1, 7, 11, 19]. One test reported an application velocity of 0.42 m/min [12], while Applied Ultrasonics specifications recommend treatment speed of 0.3 m/min [17].

B.5.5 Application Angle

When treating a weld toe, the UIT pins are held approximately normal to the weld face and inclined at 45° to the base metal surface [11].

B.5.6 Treatment Pressure

All sources recommend not applying any more pressure during application than what is supplied by the UIT tool itself. The average weight of the 27 kHz UIT tool is about 3 kgf. It is recommended not to apply more than 3 kgf in addition to the 3 kgf from the weight of the hand-held tool [12, 19].

B.5.7 Application Movement

UIT is used with translational or reciprocal movement of the tool along the weld toe until specified geometry of the treatment area is formed [17].

B.5.8 Number of Passes with the Ultrasonic Impact Tool

Tests ranged from a single pass with the UIT tool [19] to 10 passes per specimen [13]. Yet another test used two passes with the UIT tool on specimens to obtain a smooth weld toe geometry [11]. The average number of passes, however, ranges from 3-5, with no more than 4 usually needed [5, 13]. Although the number of passes with the UIT tool varies, the researchers generally agreed to continue treatment until the desired effect on the weld toe geometry was visible [17].

B.5.9 Multi-Pass Welds

When making multi pass welds, slag removal is necessary after each pass. UIT removes slag during application [17]. Hence, the UIT tool is desirable for slag removal during multi-pass welding. UIT reduces labor consumption when forming multi-layer welds by up to 20% [1]. Reduction in labor consumption depends on weld metal strength.

B.5.10 UIT Application Groove Appearance

Typically, the width of the groove is up to 2 diameters of the indenter pins. The width of the groove created by UIT should be applied so that approximately half of the groove's width indents upon the weld metal and half indents upon the base metal HAZ. When the groove width is not applied evenly, the width should cover more of the base metal HAZ than the weld metal. It is recommended that 30%-60% of the groove's width indent upon the weld metal, and 40%-70% of the groove's width indent upon the base metal HAZ [9]. The maximum depth of the groove from the surface of the base metal is generally 0.6 mm, but varies with the weld quality and the strength of the welded joint material [9].

The groove's cross-sectional dimensions and the relation between its transverse length across the weld and the base metal are determined by the radius of the indenter, the angle at which the tool is located to the base metal surface and an oscillation angle of the tool relative to its axis in the groove's cross-sectional plane [9].

B.6 HOW TO CHOOSE UIT APPLICATION PARAMETERS

Each producer of the UIT tool includes their own specifications on how to set the parameters of the tool when treating a specimen. These specifications are based on the welded joint type, the strength of the parent material, and fatigue test conditions.

The indenter size and treatment parameters are selected based on the strength of the treated material to obtain the specified level of plastic deformation to induce the desired favorable residual compressive stresses, and the depth thereof.

B.6.1 Optimum Application Software

There is software available for Ultrasonic Peening Optimum Application. This program outputs a maximum possible increase in fatigue life of structural elements with minimum labor- and power-consumption. This software was developed based on original predictive model [22].

B.6.2 Single vs. Multi-Element Tool

The multi-pin tool is more frequently used in UIT application than the single-pin tool. The cyclic lifetime of butt joints in carbon steel after ultrasonic

impact treatment by a single-element tool was 10-20 or more times higher than that of the original samples tested under corresponding repeated varying stress levels, while the cyclic lifetime of butt joints in carbon steel after ultrasonic impact treatment by a multi-element tool was 4-5 times higher than that of the original samples [7]. However, this data cannot be interpreted to mean that the single element tool is more effective than the multi-element tool. The reason for not drawing a decisive conclusion is that the size pin of the multi-pin tool was not reported in these tests, and it has been well documented that the size of the pin diameter greatly impacts the fatigue life increase [15, 16].

B.7 WHERE UIT EQUIPMENT IS PRODUCED

Known UIT tools have been produced at:

1. Applied Ultrasonics, P.O. box 100422, Birmingham, Alabama, 35210, USA
2. Tianjin University, Tianjin 300072, China
3. Northern Scientific and Technology Company, NSTC, 6 Voronin St., Severodvinsk, Arkhangelsk Region, 164500, Russia
4. The E.O. Paton Electric Welding Institute, 11 Bozhenko St., Kiev, 252650, Ukraine
5. Integrity Testing Laboratory, Inc. 80 Esna Park Drive, Units 7-9, Markham, Ontario, L3R 2R7, Canada.

APPENDIX C

Literature Review – Part 2: Fatigue Enhancement from UIT Application

C.1 INTRODUCTION

Research has shown that UIT increases fatigue life, fatigue strength, and applicable stress ranges, as well as retards fatigue crack initiation for many steel grades and weld types in a variety of temperatures and environments. The degree of improvement depends on the fatigue conditions, the type of weld, and the type of parent metal used.

C.2 ENDURANCE LIMIT

Pulsating loads determine fatigue. The endurance limit is the maximum stress to which a material can be subjected to in fatigue for an indefinite service life. It is common practice to accept the assumption that carrying a certain load for several million cycles of stress reversals indicates that the load can be carried for an indefinite amount of time [25].

Conventional endurance limits use S-N curves. Figure C.2.1 shows an endurance limit determined from a S-N curve. In Figure C.2.1, the endurance limit is determined as the stress at which the S-N curve plateaus.

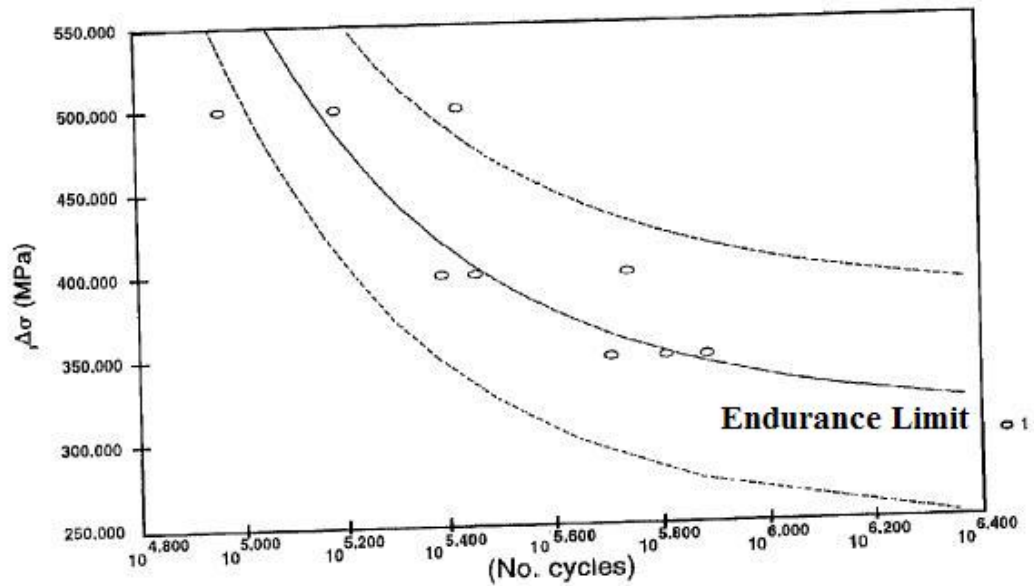


Figure C.2.1 Woehler's Curve; S-N Curve Showing Endurance Limit [10]

Endurance limit can also be determined from a set of specimens under the same fatigue conditions by calculating the mean value between the fatigue strength corresponding to the specimen whose life is just greater than 2×10^6 cycles and the fatigue strength corresponding to the specimen whose life is just less than 2×10^6 [11]. A graphical representation of this definition of endurance limit is shown in Figure C.2.2.

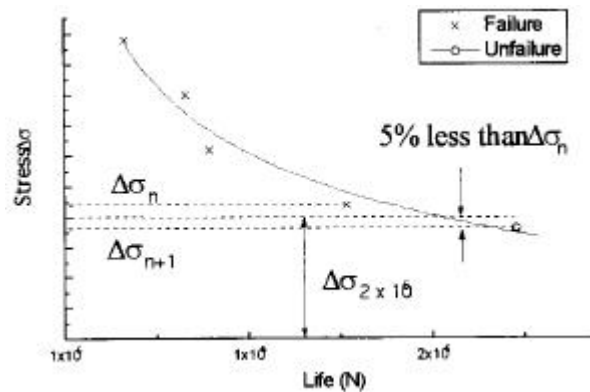


Figure C.2.2 Determination of Endurance Limit at 2×10^6 cycles [11]

C.2.1 Butt Welds

This section shows the results of four types of metals with butt welds that underwent fatigue testing to determine their endurance limits before and after UIT application. Table C.2.1.1 shows the material properties of the base metals used for the fatigue tests. Table C.2.1.2 shows the fatigue testing conditions of the butt welds, including the stress ratio, R . R is the ratio between the minimum and maximum stresses that the specimens are subjected to during fatigue testing [12]. $R = \sigma_{\min}/\sigma_{\max}$. Although UIT application parameters were rarely listed in full for any research, Table C.2.1.3 lists any UIT parameters given for each fatigue test specimen. Table C.2.1.4 lists the endurance limits at 2×10^6 cycles for the butt welded specimens tested, including percent improvement of endurance limit. Table C.2.1.5 lists the reference number of the papers that each fatigue test can found in, for easy reference.

As can be seen in Table C.2.1.4, UIT increases the endurance limit of all butt welds tested, by 27% to 85%.

Table C.2.1.1 Material Properties of Butt Weld Specimens

ID #	Material Properties			
	Material	σ_y (MPa)	σ_u (MPa)	δ (%)
1	Q235B steel	267.4	435.5	26
	J422 electrode	350	460	22
2	E690 steel	763	836	16
3	Low-carbon steel	233	405	
4, 5, 6, 7	High-strength steel	738	836	

Table C.2.1.2 Fatigue Testing Conditions of Butt Weld Specimens

ID #	Fatigue Testing Conditions	
	Test	R (stress ratio)
1	Tensile loading	0.1
2	Tensile loading, frequency = 30 Hz	0.1
3	Constant amplitude loading	0
4	Constant amplitude loading	-1
5	Constant amplitude loading	-1
6	Constant amplitude loading	0
7	Constant amplitude loading	0.6

Table C.2.1.3 UIT Application Conditions for Butt Weld Specimens

ID #	Any UIT Application Information Given
1	Application angle = (treated weld toe) normal to weld face and 45° to base metal surface, velocity = 0.5 m/min, and 2 passes of UIT tool
2	Frequency of 27 kHz, travel speed varied from 0.1 to 0.5 m/min, 3 passes with the UIT tool.
3, 4, 5, 6, 7	Frequency of 27 kHz, single pass, moving along the weld toe at 0.5 m/min.

Table C.2.1.4 Endurance Limit of Butt Welds Before and After UIT Application

ID #	Endurance Limit (MPa)		
	As-Welded	After UIT	Improvement (%)
1	148.5	234	57
2	129	224	74
3	140	220	57
4	80	140	75
5	70	130	85
6	110	140	27
7	340	440	30

Table C.2.1.5 Butt Weld Specimens' References

ID #	Reference
1	11
2	10
3, 4, 5, 6, 7	19

C.2.2 Fillet Welds

This section shows the results of five types of metals with fillet welds that underwent fatigue testing to determine their endurance limits before and after UIT application.

Table C.2.2.1 shows the material properties of the base metals used for the fatigue tests. Table C.2.2.2 shows the fatigue testing conditions of the fillet welds, including the stress ratio, R. Although UIT application parameters were rarely listed in full for any research, Table C.2.2.3 lists any UIT parameters given for each fatigue test specimen. Table C.2.2.4 lists the endurance limits at 2×10^6 cycles for the fillet-welded specimens tested, including percent improvement of

endurance limit. Table C.2.2.5 lists the reference number of the papers that each fatigue test can found in, for easy reference.

As can be seen in Table C.2.2.4, UIT increases the endurance limit of all fillet welds tested, by 30% to 200%.

Table C.2.2.1 Material Properties of Fillet Weld Specimens

Material Properties				
ID #	Material	σ_y (MPa)	σ_u (MPa)	δ (%)
1	S355 J0, t = 8 mm	355	490-630	20
2	S355 J0, t = 5 mm	355	490-630	20
3	E460 steel	543	589	25
4, 5, 6	High-strength steel	738	836	
7	Usiform 355 t = 6 mm	355	500	
8	Usiform 700 t = 5 mm	700	800	
9	TMCP steel	420		

Table C.2.2.2 Fatigue Testing Conditions of Fillet Welded Specimens

Fatigue Testing Conditions		
ID #	Test	R (stress ratio)
1, 2	Constant amplitude axial loading at frequency = 5 Hz	0.1
3	Four point bending, frequency of 30 Hz	0.1
4	constant amplitude loading	-1
5	constant amplitude loading	0
6	constant amplitude loading	0.6
7, 8	Four point loading	0.1
9	Four point bending, local span of 250 mm and support span of 500 mm, frequency = 7 Hz	0.1

Table C.2.2.3 UIT Application Parameters for Fillet Welded Specimens

ID #	Any UIT Application Information Given
1, 2	3 mm diameter pin in multi-pin UIT tool, 27 kHz, treatment speed of .42 m/min.
3	Frequency of 27 kHz, travel speed varied from 0.1 to 0.5 m/min, 2 passes with the UIT tool
4, 5, 6	Frequency of 27 kHz, single pass, moving along the weld toe at 0.5 m/min.
7, 8	Frequency of 27 kHz, 6.35 mm diameter pins in a multi-pin UIT tool, treatment speed of at least 0.3 m/min
9	Treatment speed between 0.3 to 0.7 m/min, Frequency of 27 kHz, no more than four passes, held tool at angle of 40o - 60o to the plate surface

Table C.2.2.4 Endurance Limits of Fillet Welded Specimens Before and After UIT Application

ID #	Endurance Limit (MPa)		
	As-Welded	After UIT	Improvement (%)
1	148.5	234	57
2	172	115	50
3	160	110	45
4	40	120	200
5	100	230	130
6	200	260	30
7	320	480	50
8	370	620	67
9	178	351	97

Table C.2.2.5 Fillet Welded Specimens' References

ID #	Reference
1, 2	12
3	10
4, 5, 6	19
7, 8	9
9	26

C.2.3 Cruciform Joints

This section shows the results of one type of metal with cruciform joints that underwent fatigue testing to determine their endurance limits before and after UIT application. Table C.2.3.1 shows the material properties of the base metals used for the fatigue tests. Table C.2.3.2 shows the fatigue testing conditions of the cruciform joints, including the stress ratio, R. Although UIT application parameters were rarely listed in full for any research, Table C.2.2.3 lists any UIT parameters given for each fatigue test specimen. Table C.2.3.4 lists the endurance limits at 2×10^6 cycles for the cruciform joint specimens tested, including percent improvement of endurance limit. Table C.2.3.5 lists the reference number of the papers that each fatigue test can found in, for easy reference.

As can be seen in Table C.2.3.4, UIT increases the endurance limit of all cruciform joints tested, by 64% to 71%.

Table C.2.3.1 Material Properties of Cruciform Joints

ID #	Material Properties			
	Material	σ_y (MPa)	σ_u (MPa)	δ (%)
1, 2	Q235B steel	267.4	435.5	26

Table C.2.3.2 Fatigue Testing Conditions for Cruciform Joints

Fatigue Testing Conditions		
ID #	Test	R (stress ratio)
1	Four-point bending	0.25
2	Four-point bending	-0.5

Table C.2.3.3 UIT Application Parameters for Cruciform Joints

ID #	Any UIT Application Information Given
1, 2	Application angle = (treated weld toe) normal to weld face and 45° to base metal surface, velocity = 0.5 m/min, and 2 passes of UIT tool

Table C.2.3.4 Endurance Limit of Cruciform Joints Before and After UIT Application

Endurance Limit (MPa)			
ID #	As-Welded	After UIT	Improvement (%)
1	142.5	234	64
2	165	282	71

Table C.2.3.5 Cruciform Joint Specimens' References

ID #	Reference
1, 2	11

C.3 FATIGUE LIFE IMPROVEMENT

Fatigue life is the number of cycles a specimen can undergo in fatigue before fatigue cracking propagates to the point that the specimen's load carrying capacity is significantly decreased. Fatigue lives can be determined for different

stress ranges, different maximum stresses, and different failure criterion, such as size of fatigue crack or a pre-determined drop in loads at constant deflection-controlled fatigue testing.

C.3.1 Butt Welds

This section shows the results of two types of metals with butt that underwent fatigue testing to determine their fatigue lives before and after UIT application. Table C.3.1.1 shows the material properties of the base metals used for the fatigue tests. Table C.3.1.2 shows the fatigue testing conditions of the cruciform joints, including the stress ratio, R , and the failure criterion, when given. Although UIT application parameters were rarely listed in full for any research, Table C.3.1.3 lists any UIT parameters given for each fatigue test specimen. Table C.3.1.4 lists the fatigue lives, in millions of cycles, for the butt weld specimens tested, including percent improvement of fatigue life. Table C.3.1.5 lists the reference number of the papers that each fatigue test can found in, for easy reference.

As can be seen in Table C.3.1.4, UIT increases the fatigue life of all butt welds tested, by 17 to 36.2 times.

Table C.3.1.1 Material Properties of Butt Weld Specimens

ID #	Material Properties			
	Material	σ_y (MPa)	σ_u (MPa)	δ (%)
1, 2	carbon steel			
3, 4	Q235B steel	257	436	26

Table C.3.1.2 Fatigue Test Conditions of Butt Weld Specimens

Fatigue Testing Conditions			
ID #	Test	R (stress ratio)	Failure Criterion
1, 2	Cyclic cantilever bending	0.1	Fatigue crack depth of 3.5 - 4 mm
3, 4	Fatigue Tested in Tension	0.1	Fatigue crack depth of 3.5 - 4 mm

Table C.3.1.3 UIT Application Parameters to Butt Weld Specimens

ID #	Any UIT Application Information Given
1, 2, 3, 4	Single element UIT tool w/pin diameter = 16 mm, frequency = 27.5 kHz

Table C.3.1.4 Fatigue Lives of Butt Weld Specimens Before and After UIT Application

Fatigue Life (10^6 Cycles)				
ID #	Stress Range (MPa)	As-Welded	After UIT	Improvement
1	168	0.063	1.068	x 17.0
2	150	0.098	2.000+	x 20.4
3	189	0.571	20.670+	x 36.2
4	207	0.328	10.47	x 31.9

Table C.3.1.5 Butt Welded Specimens' References

ID #	Reference
1, 2	7
3, 4	4

C.3.2 Fillet Weld

This section shows the results of two types of metals with fillet welds that underwent fatigue testing to determine their fatigue lives before and after UIT application. Table C.3.2.1 shows the material properties of the base metals used for the fatigue tests. Table C.3.2.2 shows the fatigue testing conditions of the cruciform joints, including the stress ratio, R, and the failure criterion, when given. Although UIT application parameters were rarely listed in full for any research, Table C.3.2.3 lists any UIT parameters given for each fatigue test specimen. Table C.3.2.4 lists the fatigue lives, in millions of cycles, for the fillet weld specimens tested, including percent improvement of fatigue life. Table C.3.2.5 lists the reference number of the papers that each fatigue test can found in, for easy reference.

As can be seen in Table C.3.2.4, UIT increases the fatigue life of all fillet welds tested, by 8.1 to 40.1 times.

Table C.3.2.1 Material Properties of Fillet Weld Specimens

Material Properties				
ID #	Material	σ_y (MPa)	σ_u (MPa)	δ (%)
1	ASTM A-572	345		
2	Q235B	267	436	26

Table C.3.2.2 Fatigue Testing Conditions of Fillet Weld Specimens

Fatigue Testing Conditions			
ID #	Test	R (stress ratio)	Failure Criterion
1	Sinusoidal loading, frequency = 20 Hz, 130 MPa stress range	0.5	Fatigue cracks and complete failure
2	Fatigue tested in tension	0.1	Fatigue crack depth of 3.5 - 4 mm

Table C.3.2.3 UIT Application Parameters for Fillet Welded Specimens

ID #	Any UIT Application Information Given
1	Multiple passes, no other information provided
2	Single element UIT tool with pin diameter = 16 mm, frequency = 27.5 kHz

Table C.3.2.4 Fatigue Lives of Fillet Welded Specimens Before and After UIT Application

ID #	Max Stress (MPa)	Fatigue Life (10^6 Cycles)		
		As-Welded	After UIT	Improvement
1	130	0.547	4.454	x 8.1
2	180	0.275	11.020+	x 40.1

Table C.3.2.5 Fillet Weld Specimens' References

ID #	Reference
1	27
2	4

C.3.3 Cruciform Joints

This section shows the results of one type of metal with cruciform joints that underwent fatigue testing to determine their fatigue lives before and after UIT application. Table C.3.3.1 shows the material properties of the base metals used for the fatigue tests. Table C.3.3.2 shows the fatigue testing conditions of the cruciform joints, including the stress ratio, R, and the failure criterion, when given. Although UIT application parameters were rarely listed in full for any research, Table C.3.3.3 lists any UIT parameters given for each fatigue test

specimen. Table C.3.3.4 lists the fatigue lives, in millions of cycles, for the cruciform joint specimens tested, including percent improvement of fatigue life. Table C.3.3.5 lists the reference number of the papers that each fatigue test can found in, for easy reference.

As can be seen in Table C.3.3.4, UIT increases the fatigue life of all cruciform joints tested, by 19.5 to 41.7 times.

Table C.3.3.1 Material Properties of Cruciform Joint Specimens

Material Properties				
ID #	Material	σ_y (MPa)	σ_u (MPa)	δ (%)
1, 2	Q235B steel	267.4	435.5	26

Table C.3.3.2 Fatigue Testing Conditions for Cruciform Joint Specimens

Fatigue Testing Conditions			
ID #	Test	R (stress ratio)	Failure Criterion
1	Four-point bending	0.25	Fatigue cracking
2	Four-point bending	0.5	Fatigue cracking

Table C.3.3.3 UIT Application Parameters for Cruciform Joint Specimens

ID #	Any UIT Application Information Given
1, 2	Application angle = (treated weld toe) normal to weld face and 45° to base metal surface, velocity = 0.5 m/min, and 2 passes of UIT tool

Table C.3.3.4 Fatigue Lives for Cruciform Joint Specimens

ID #	Max Stress (MPa)	Fatigue Life (10^6 Cycles)		
		As-Welded	After UIT	Improvement
1	211	0.24	10+	x 41.7
2	235	0.512	10+	x 19.5

Table C.3.3.5 Cruciform Joint Specimens' References

ID #	Reference
1, 2	11

C.4 IMPACT OF UIT ON STRESS RANGE AND ENDURANCE LIMIT

For both butt and fillet welds, the level of improvement in fatigue life due to UIT varies with applied stress range. UIT improves fatigue life more for a lower stress range than for a higher stress range. For example, the fatigue life of the transverse butt joints welded with an E5105 electrode in Q235B steel samples (Chinese specification) at a stress range of 207 MPa increases fatigue life by over 31 times after UIT application, while at a stress range of 189 MPa the fatigue life increases by over 35 times [4].

Although UIT is more effective at lower stress ranges, UIT also increases the stress range a welded connection can experience without failure. Many tests were performed at higher stress ratios for the peened specimens than for the as-welded specimens [4, 15, 16, 26]. For example, fatigue tests on Q235B (Chinese specification) butt weld specimens were fatigue tested at stress ranges from 153 MPa to 207 MPa for the as-welded condition, but due to the increase in endurance limit from UIT application, specimens with UIT application were fatigue tested at stress ranges from 189 MPa to 261 MPa, which were at higher stress ranges than

the as-welded specimens could be tested [4]. Therefore, UIT application raises the stress range at which a specimen can be tested. However, UIT application increases fatigue life more for lower stress ranges than the higher stress ranges. At any stress range, UIT application increases fatigue life when compared to the as-welded condition.

C.5 EFFECT OF STEEL GRADE ON UIT

In addition to higher strength steels having higher yield and ultimate strengths to begin with, UIT increases fatigue strength more for higher strength steels than for lower strength steels. As can be seen from Figure C.5.1, higher strength steels have higher fatigue strength of welded joints after the application of UIT. These tests did not specify the size, fatigue testing conditions, nor UIT application parameters for the results given. However, the results compare the effect of UIT on different strength steels. Hence, the strengths of the steels and fatigue strength increase after UIT application are listed in Table C.5.1. Figure C.5.1 gives a graphic representation of the increase in fatigue strength of different strength steel specimens under assumedly comparable fatigue conditions.

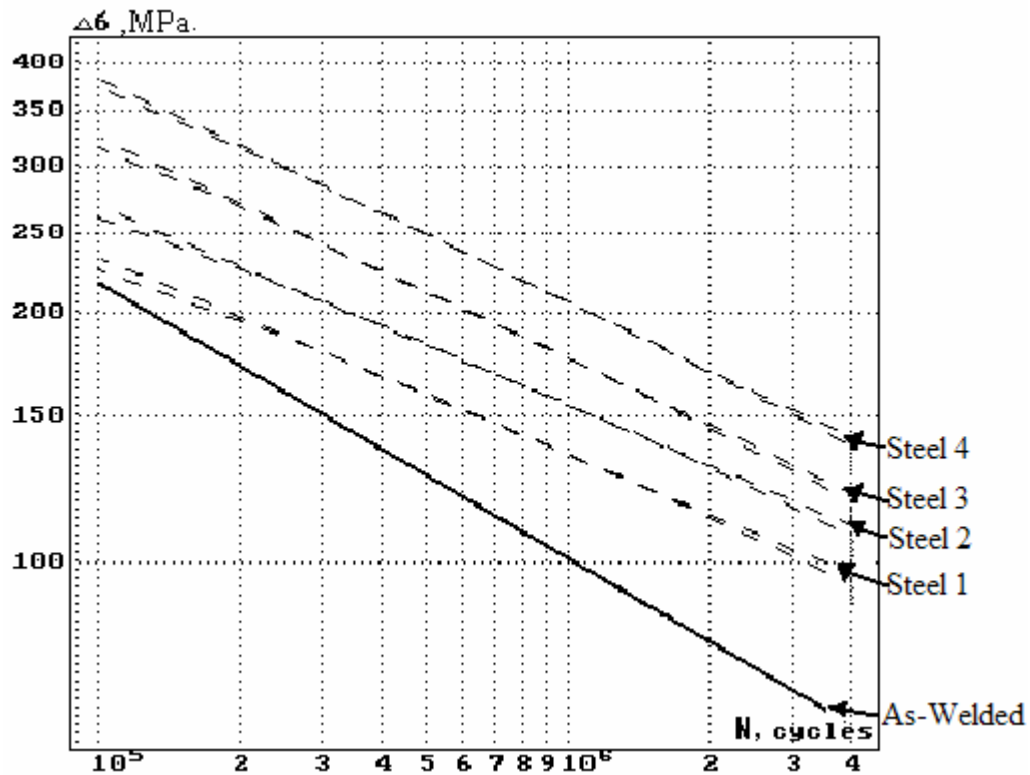


Figure C.5.1 Fatigue curves of non-load-carrying fillet welds. The solid line represents the as-welded condition for all steels, the dashed lines represent the 4 steels after UIT application [22]

Table C.5.1 Steel Specimens' Material Properties and Fatigue Life Increase After UIT Application [22]

Steel #	σ_y (MPa)	σ_u (MPa)	Fatigue Strength increase after UIT at $N=2 \times 10^6$ cycles (%)
1	270	410	42
2	370	470	64
3	615	747	83
4	864	897	112

These results show that UIT application on non-load-carrying fillet welded connections induces increasing fatigue strength improvements with increasing yield and ultimate strength of the parent material. As can be seen in Table C.5.1 and Figure C.5.1, steel with a yield strength of 270 MPa before UIT application has a 42% increase in fatigue strength after UIT application, while a steel with a higher yield strength of 864 MPa before UIT application has a 112% increase in fatigue strength after UIT application [22]. However, these results did not give any test parameters, and cannot be taken as conclusive evidence.

C.6 LONG VS SHORT LIFE

UIT gives consistently large increases in fatigue strength, particularly at long lives, for welded high strength steel specimens [3]. Fatigue strength is substituted for ultimate strength when a specimen is subjected to fatigue loading [25].

The results in Table C.6.1 indicate that UIT is more useful for fatigue strength enhancement when specimens are subjected to longer lives. For instance, the fatigue strength increase for Usiform 700 at 200,000 cycles is only 67.6%, but for 2,000,000 cycles is almost twice as much at 127.3%.

Table C.6.1 Fatigue Strengths of Fillet Welds Before and After UIT Application at Different Fatigue Lives [9]

Cycles	Usiform 355 ($\sigma_y = 355$ MPa, $\sigma_u = 500$ MPa)			Usiform 700 ($\sigma_y = 700$ MPa, $\sigma_u = 800$ MPa)		
	Stress (MPa)			Stress (MPa)		
	As-Welded	After UIT	Increase (%)	As-Welded	After UIT	Increase (%)
2,000,000	250	380	52	220	500	127.3
200,000	320	480	50	370	620	67.6

Also visible in Table C.6.1 is that increases in endurance limit for the higher strength Usiform 700 are greater than the increases in endurance limit for Usiform 355. For example, the fatigue strength increase for Usiform 700 (ultimate strength = 800 MPa) at 2×10^6 cycles is 127%, while the fatigue strength increase for Usiform 355 (ultimate strength = 500 MPa) at 2×10^6 cycles is only 52%.

C.7 FATIGUE CRACK INITIATION

C.7.1 As-Welded Steel Specimens

Fatigue cracks in the as-welded condition initiated at the weld toe in all steel specimens [11, 12, 16].

C.7.2 UIT Steel Specimens

Fatigue crack initiation began in two places for specimens prepared with UIT: in the base metal, and at the weld toe along the UIT application line. The deciding factor seemed to be the UIT pin diameter size.

Fillet welded Weldox 420 steel (Swedish specification) specimens treated with a 5 mm diameter pin in a multi-pin UIT tool had fatigue cracking initiation at the weld toe in all specimens [15, 16]. Likewise, fillet weld specimens that were peened using a 3 mm multi-pin tool also had fatigue crack initiation at the treated weld toes. The toe crack originated at the boundary of the HAZ and the weld metal right through the region treated by UIT. This pattern is typical for all weld toe cracks [5, 6, 12, 15]. However, fillet weld specimens that were originally treated with both a 5 mm diameter pin multi pin tool and a 3 mm diameter pin

multi-pin tool failed in the base metal outside the weld zone. Fatigue cracks in the base metal initiated at corrosive defects (cavities) on the rolled plate surface [16].

Fatigue cracks that initiated in the weld toe of ASTM A588-97B Grade 50W steel fillet welded specimens treated only with a 3 mm diameter pin multi-pin tool had a crack surface that indicates a classical two-stage crack growth pattern. Cracks initiated at multiple locations along the width of the metal specimen from microscopic defects due to the welding process, and coalesced soon after to form a long shallow crack [5].

Some reports did not specify pin size. In these cases, fatigue cracking initiated in both the weld toe and the base metal. In one such report, most UIT peened Q235B steel (Chinese specification) cruciform joints and butt joints had fatigue crack initiation occur in the base metal [11]. Another test also showed UIT peened butt-welded E690 steel (French specification) specimens that had fatigue crack initiation and propagation outside the weld in the parent metal [10].

Some tests that did not specify pin diameter had fillet welded specimens fail in the peened zone. The fatigue cracks generally initiated at the weld junction on the specimen side, then deviated into the parent metal. For some of the UIT peened E690 steel (French specification) butt joints, fatigue cracks also initiated at the weld toe, but after many more cycles than for the as-welded joint [10]. UIT peened butt-welded assemblies of Q235B steel (Chinese specification) also had some failure initiations occur at the weld toe [11].

C.8 UIT IN TEMPERATURE EXTREMES

C.8.1 Cool Temperatures

Decreasing the temperature of a weld specimen decreases fatigue strength. Two identical sets of welded T-joint specimens of 09G2S-grade steel (Russian specification) were tested under two different loading conditions and in two different environments. One set of specimens was tested under harmonic loading at room temperature. The second set of specimens was tested under harmonic loading at -60°C . The fatigue strength in the as-welded condition at -60°C and ramp loading is less than under conditions of harmonic loading at room temperature [1]. However, when the same welds are treated with UIT, under conditions of ramp loading at -60°C the fatigue strength is 20% higher than that of an untreated T-joint under conditions of harmonic loading at a room temperature. UIT increases the fatigue strength of a T-joint under ramp loading at -60° by 40% [1]. Reproductions of the same tests, but using butt joints in 14Kh2GMR and 12GN2MFAYu steel and T-joints in 15KhSND and 09G2S steels (Ukrainian specification) verified the same fatigue strength increases of specimens at -60°C subjected to ramp loading when compared to specimens at room temperature subjected to harmonic loading after UIT application [8].

Analysis of efficiency of other techniques for treatment of welded joints, such as mechanical treatment of a butt joint, and argon-arc welding of a T-joint, show conclusively UIT is the most efficient method for increase in fatigue strength of welded joints under conditions of ramp loading and low temperature [1]. Therefore, the UIT strengthening of welded joints is recommended to increase the durability of welded structures where temperatures of in the range -60°C are anticipated [1].

C.8.2 Heated Conditions

Research shows that when UIT is applied to butt joints in high strength steel and then heated to 300°C, there is practically no increase in fatigue life. The results of tests on original and treated samples occupy a single scatter region characteristic of several fatigue tests of such welds [7]. The increased temperature may have undone the UIT induced favorable residual compressive stresses in the surface layer of the samples. Similar negative results from heat are reported from tests on heat-applied galvanization repair after UIT application, to be discussed in Chapter 5.

C.9 UIT IN A CORROSIVE FATIGUE ENVIRONMENT

Welded low-carbon, low alloy, and high strength steel specimens were subjected to corrosion-fatigue tests involving 10^7 load reversal cycles in water containing 3% NaCl. The UIT specimens showed stable results of fatigue resistance increase between 1.4 to 1.8 times [1]. Fatigue performance also improved after UIT for testing in seawater. For example, the fatigue strength at 10^7 cycles increased from 80 MPa to 100 MPa for testing in seawater [19]. Therefore, UIT is effective at increasing fatigue resistance in a corrosive-fatigue environment

APPENDIX D

Literature Review – Part 3: Effect of UIT

D.1 INTRODUCTION

UIT increases fatigue performance of metals through a combination of effects. The most reported effects of UIT are weld toe geometry improvement [4, 5, 6, 7, 10, 11, 13] and introducing beneficial compressive residual stresses [4, 5, 10, 11, 20]. UIT also removes defects from the weld toe [4, 11], creates ultrasonic deformation of the treated metal surface [20, 23], and changes the microstructure of both the surface and subsurface [5, 23].

D.2 WELD TOE GEOMETRY IMPROVEMENT

Immediate deformation of the treated weld toe from UIT application produces a smooth, round, plastically deformed scarf along the treatment line, with a diameter at least equal to that of the working element of the tool [6, 7, 27]. Changes in weld toe geometry are visible after the first pass with the UIT tool, and subsequent passes do not show much further change in appearance [27]. The plastic deformation has a depth of up to 3-4 mm [7].

The toe angle, toe radius and undercut characterize the weld shape. A lower toe angle and a higher toe radius increase fatigue resistance. UIT increases the toe radius and introduces an undercut for softer metals [9]. UIT improvements on weld toes lower the stress concentration at the weld toe [19]. Results of UIT on weld toe characteristics are listed in Table D.2.1 and an example of an introduced undercut is shown in Figure D.2.1.

Table D.2.1 Weld Toe Characteristics Before and After UIT Application [9]

Grade	Type of Weld	Specimen No.	Toe angle (°)	Toe radius (mm)
Usiform 355	As-welded	8	63	-
		9	64	-
		11	80	-
		12	67	-
	UIT	14	63	0.95
		15	60	0.90
		17	69	0.80
		18	57	1.00
		20	63	0.80
		21	58	0.85
Usiform 700	As-welded	6 left	38	-
		6 right	40	-
	UIT	23	41	2.00
		24	40	2.10
		26	39	1.00
		27	44	0.85

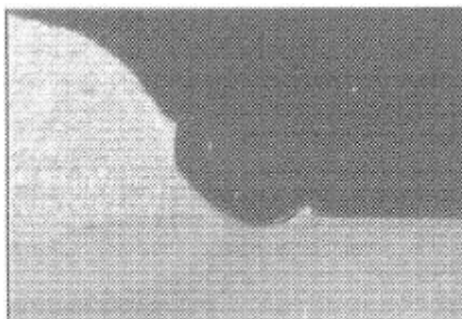


Figure D.2.1 Weld Toe After UIT Application (toe radius = 0.90 mm, undercut depth = 40 mm) [9]

UIT improves the weld geometry by mechanical cold working from the UIT tool pins [3, 9, 13, 19]. Ultrasonic vibrations of the UIT tool create plastic deformation at the instant of impact [23]. Regardless of the number of passes, a multi-pin UIT tool with 3 mm diameter pins operating at a frequency of 27 kHz produces a circularly-contoured groove 2-3 mm in width and ~0.25 mm in depth on A572 Gr.50 steel [13].

D.3 RESIDUAL STRESSES

High tensile residual stresses from welding are unfavorable because they lead to fatigue crack development. UIT induces compressive stresses in the treated surface and subsurface that may eliminate the tensile residual stresses from welding, or even induce compressive residual stresses at the point of treatment [1, 13, 17]. The effects of UIT, which decrease with depth, cause plastic deformations, which in turn induce residual compressive stresses in the surface layers of the treated metals [7, 13]. UIT introduces compressive residual stresses close to the yield strength of the base steel [1, 7, 22]. This compressive stress improvement affects the weld metal, and the heat affected zone (HAZ) of the base metal, which is where UIT is applied [6, 17].

Residual stresses in TY 428-61-grade steel (Russian specification) butt welds after UIT application were measured with a technique based on measuring deformation during model boring along an internal diameter from the specimen ends [1]. Results show that in the HAZ, UIT decreases residual stresses by 20% along the weld line, and 40% perpendicular to the weld line. In the weld metal, UIT decreases residual stresses by 45% along the weld line, and by 9 times perpendicular to the weld line [1].

For specimens of A572 Grade 50 steel (USA specification) with no welds, residual stresses were measured by X-ray diffraction together with a layer removal technique. UIT application with a 3 mm diameter pin in a multi-pin UIT tool induced a stress of -427 MPa parallel to the treatment line, which exceeded the nominal yield stress of A572 Grade 50 steel (345 MPa) [13].

D.3.1 Depth of Compressive Residual Stress

Application of UIT to U3-grade steel (Russian specification) induces residual compressive stresses in a depth of up to 1.4 mm. Residual stresses in U3 steel after UIT application was measured through the method of layered metal etch removal in 50% solution of nitric acid according to Davidenkov's formula transformed for flat plates of 120x35x6 mm in size were measured for residual stress through the method of electrochemical metal etch removal using automatic equipment [1].

The depth of compressive residual stress produced by UIT in A572 Grade 50 steel (USA specification) is 1.5 – 1.7 mm. Stresses were measured by X-ray diffraction together with layer removal technique [13]. For specimens of A572 Grade 50 steel with no welds, treated with a 3 mm diameter pin size multi-pin UIT tool, UIT introduces compressive stresses at the surface and subsurface in both directions. The depth of UIT induced compression layer was 1.47 mm for the stresses parallel (X-direction) to the treatment line. The depth of the UIT induced compression layer was ~ 1.65 mm (by extrapolation) perpendicular (Y-direction) to the treatment line [13]. The maximum compressive stress induced by UIT occurs beneath the treatment line. The maximum stress at the surface (nominal depth of 0.3 mm) was -418 ± 20 MPa in the parallel (X-) direction and –

458 \pm 20 MPa in the perpendicular (Y-) direction, which exceeded the compressive (nominal) yield stress of A572 Gr.50 steel [13].

The magnitude of the near-surface compressive stress decayed in width and disappeared about \pm 15 mm away from the UIT line. The UIT induced compressive stress perpendicular to the UIT line, which is normally in the direction of fatigue applied stress, was slightly less than stress parallel to the UIT line. The plastically deformed region from UIT is \sim 0.7 mm in depth and 1-1.5 mm from the UIT centerline, which covers the UIT groove itself. The compressive layer was about 1.6 mm deep for all three stress components [13].

The depth of the compressive residual stresses introduced by UIT appeared independent of plate thickness. [13]

D.3.2 Cause of Compressive Stresses

One theory is that ultrasonic wave vibration transfer causes residual stress improvement during UIT pin impact on the base metal being treated, and mechanical impact is not the cause of residual stress improvement [13]. It should be noted, however, that residual stress improvement that accompanies UIT application may more likely be from the extensively researched and documented plastic deformation induced by UIT.

D.3.3 Fatigue Crack Prevention

The compressive stresses introduced by UIT reduce the probability of the formation of cracks during the aging process [6]. However, the compressive stress layer of UIT is shallow, on the order of 1 mm deep, whereas the tensile weld residual stress layer is relatively deep [13]. Hence, once a fatigue crack initiates from the treated weld toe surface the beneficial compressive residual

stress is released and fatigue crack propagation is nearly the same as the original non-treated weld toe. Post-weld treatment effect has greater impact on fatigue crack initiation and early propagation rather than advanced fatigue crack propagation.

In Q235B steel (Chinese specimen) fillet and butt welded joints subjected to high stress ranges after UIT peening, fatigue cracks initiated at the weld toe after many more cycles than for the as-welded joints welded with E5015 (conventional) electrodes. However, for specimens subjected to low stress ranges, fatigue crack initiation occurred in the base metal. In such cases, the welded joints were no longer the critical locations [4].

D.4 STRUCTURE AND MECHANICAL PROPERTIES

Ultrasonic vibrations of the pins of the UIT tool create plastic deformation at the instant of impact. This is confirmed by a respective increase of the area and volume of indentation [23].

D.4.1 Grain Size Reduction

UIT reduces grain size. One batch of Steel 45 (Russian specification) specimens had a carburized layer of post-eutectoid composition, with an average pearlite grain size of 69.4 μm before UIT application. After UIT application, the batch of Steel 45 with a carburized layer of post-eutectoid composition had a finer grain size, with the average grain size of about 35 μm . The average grain size of pearlite was examined and measured using the optical (Neophot-21) and scanning (Cameca) microscopes. The grain size determination was done by the method of stereometric metallography [24].

D.4.2 Reduction in Grain Size Distribution

Metallographic investigations of specimen cross sections revealed that UIT application to the carburized layer of steel of eutectoid composition resulted in a reduction of grain size variation. Figure D.4.2.1 shows the grain size distribution in a carburized layer of Steel 45 (Russian specification) at a depth of 110, 400, and 1000 μm from the treated surface [24]. As is visible in Figure D.4.2.1, the grain size distribution increases with depth from the treated surface, and since UIT effects decrease with depth, this indicates that UIT decreases grain size distribution in steel.

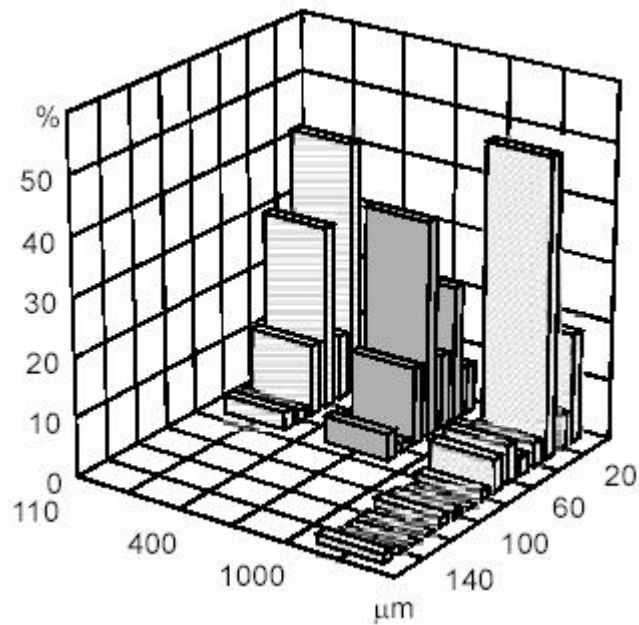


Figure D.4.2.1 Grain Size Distribution in a Carburized Layer of Steel 45 at Depths of 110, 400, and 1000 μm from the Surface [24]

D.4.3 Grain Elongation

UIT elongates treated base metals. Figure D.4.3.1 shows a 200x magnification of ASTM specification A588-97B Grade 50W steel after application of between 3 to 5 passes of 3 mm diameter pins in a multi-pin UIT tool, applied at a speed of 0.3 m/min and a frequency of 27 kHz [5]. As visible in Figure D.4.3.1, the grain shapes become progressively less elongated with depth below the surface and also along the surface away from the treated area. At the surface of the UIT application area the individual grains can barely be distinguished.

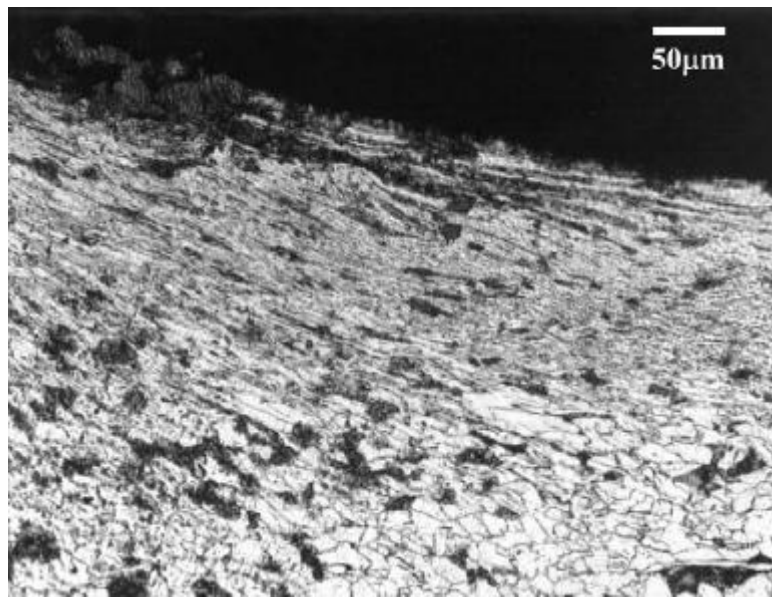


Figure D.4.3.1 Photomicrograph (200x) of UIT Application Area [15]

D.4.4 Creation of Cementite Along Pearlite Grain Boundaries

Carbon redistribution takes place during UIT, creating a cementite interlayer along pearlite grain boundaries for Steel 45 and 20 XH3A (Russian specification). Plastic deformations generally partially disintegrate cementite plates to form free carbon at sites of maximum defect density. UIT displaces the free carbon formed from cementite disintegration to the former and newly formed grain boundaries of pearlite colonies (sites of maximum defect density) to form a cementite network. When UIT stops, the free carbon re-forms into cementite at its new position at the grain boundaries of pearlite colonies. Figure D.4.4.1 shows this formation of a cementite network after UIT application. This formerly nonexistent cementite interlayer along the pearlite grain boundaries was revealed through metallographic investigation of the specimen cross section by the method of stereometric metallography [24].

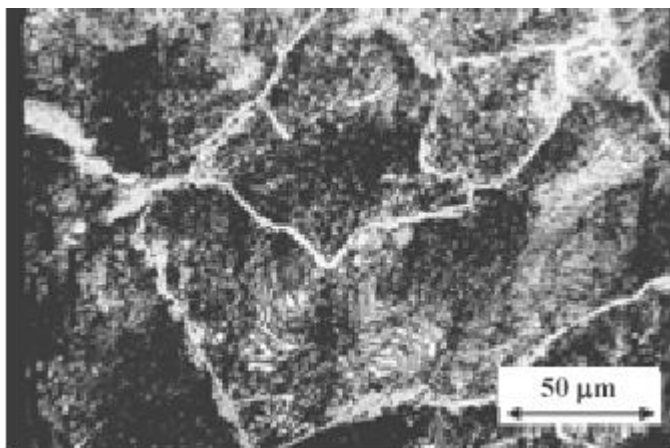


Figure D.4.4.1 Formation of Cementite Network After UIT Application [24]

However, UIT application to the carburized layer of Steel H3MA in the initial state induces a forced intrusion of carbon atoms into the ferrite lattice to form a deformation martensite structure. This is demonstrated by formation of white grains with high hardness, which is retained due to a non-equilibrium internal stress distribution [24]. The layer of white grains with high hardness is a deformation martensite structure. This white layer is shown in Figure D.4.4.2. The growth of the pearlite phase inside a martensite grain in this case is caused by weaker stresses upon termination of the impact [24].

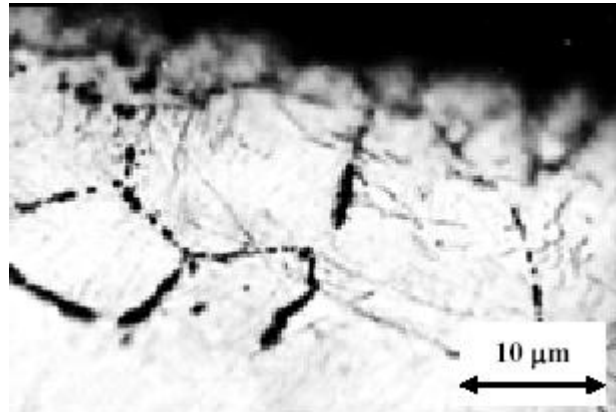


Figure D.4.4.2 Grain-Structure White Layer After UIT Application to Steel H3MA [24]

During cold plastic deformation, cementite disintegrates due to the ‘elongation’ of carbon in the stress dislocation field of ferrite in the deformed steel. Some researchers are of the opinion that while cold plastic deformation does disintegrate the cementite, it does not change the type of its crystal lattice. This theory is supported by no noticeable changes in cementite after UIT application and investigated by x-ray diffraction [24].

D.4.5 Steel Hardening

UIT application to the surface of 12Kh1MF steel (Russian specification) welded joints increases the surface hardness by 25-30% [6]. The structural changes in 12Kh1MF steel from UIT application were accompanied by a change in properties, which were investigated with metallography, ultrasonic and X-ray structure analysis. Investigations show that HAZ has the least surface hardness both in the original and the UIT applied states, as shown in Figure D.4.5.1. This is connected with the carbon depletion of the surface under strong heating during the welding process. There is a smooth transition to the level of hardness of the base metal and the weld. The weld metal was hardened to a depth of 60-70 μm , the base metal to 150 μm , and the HAZ to about 240 μm [6].

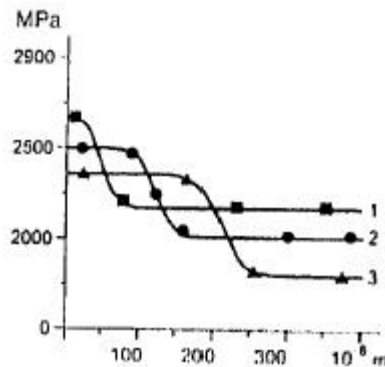


Figure D.4.5.1 Distribution of Microhardness in the Surface Layers of the Weld Zone of Low Carbon Ferrite-Pearlite Steel After UIT Application: 1) Weld; 2) Base Metal; 3) Heat Affected Zone (HAZ) [6]

UIT creates plastic deformation strain hardening in the surface layer. The depth of the cold-worked layer after the UIT can range from 0.5 mm to 0.7 mm deep [19].

The depth of plastic deformation due to UIT is manifested by the dense laminar structure extending up to about 0.2 mm from the surface [5].

APPENDIX E

Literature Review – Part 4: UIT vs. Other Methods of Weld Treatment

E.1 INTRODUCTION

Since UIT provides many weld improvements, such as weld toe geometry improvement, inducing compressive stresses and plastic cold working, UIT is comparable to many other weld improvement techniques.

Conventional post-weld treatment techniques include grinding, air hammer peening, shot peening, needle penning, and TIG (tungsten inert gas) remelting [13]. Other common weld improvements include sand blasting [8].

Comparison of all fatigue curves from different weld improvement treatments, shown in Figure E.1.1, indicates that UIT gives the greatest fatigue benefit when compared with TIG remelting, TIG followed by UIT, hammer peening, and shot peening. In Figure E.1.1, UIT 1 was treated with both a 5 mm and a 3 mm diameter pin in the multi-pin UIT tool, and UIT 2 was treated with only the 3 mm diameter pin in the multi-pin UIT tool. It should be noted that the benefit from UIT depends on the treatment parameters, such as pin diameter [15, 16].

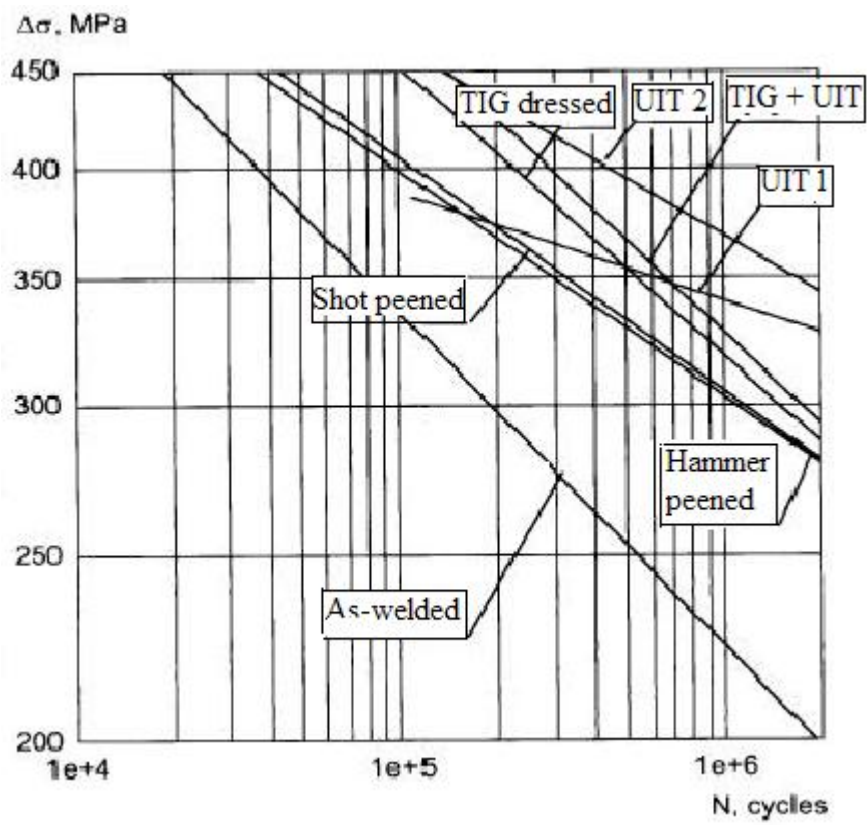


Figure E.1.1 Fatigue Curves for Weldox 420 Fillet Welds in the As-Welded and Improved Conditions [16]

This chapter gives an in-depth look at weld enhancement treatments in comparison to UIT.

E.2 HAMMER AND SHOT PEENING

The shot peening process is a cold working process in which the surface of metal material is bombarded with small spherical shot. Each piece of shot striking the material acts as a tiny peening hammer, imparting a small indentation or dimple to the surface. Overlapping dimples develop an even layer of metal with induced compressive stress and cold working on the surface, which increases fatigue life. Unlike UIT and air hammer peening in which treatment is focused locally along a weld toe, shot peening is focused on a surface of an area [13].

Air hammer peening works primarily by inducing a compressive residual stress, reducing the stress concentration by changing the weld toe profile, and decreasing the size of the small initial cracks at the weld toe. Air hammer peening can be focused locally along a weld toe [20].

Fatigue tests in NCHRP Report 206 demonstrated that a fatigue crack up to 3 mm (0.13 in) deep in coverplated details can be arrested by air hammer peening. However, this method is found to be dependant on the level of minimum stress. It was less effective at higher stress ranges, under high minimum stress, and with cracks deeper than 3 mm [20]. UIT shows similar dependencies on minimum stress and crack depths with arresting fatigue cracks.

E.2.1 Fatigue Crack Initiation from Hammer and Shot Peening

In hammer peened or shot peened specimens, fatigue cracks initiated at the weld toe [15, 16].

E.2.2 Extent of Compressive Layer for Hammer and Shot Peening

Post-weld treatments like UIT and shot peening introduce compressive residual stresses near the treatment surface. Material beneath the treatment is cold worked and plastically deformed, which causes work hardening of base material and heat affected zone (HAZ). The peak compressive stress occurs at or near the surface beneath the treatment and often exceeds the yield stress of the base metal. For UIT, it appears that stress in the direction perpendicular to the treatment line is slightly less than the stress in the parallel direction. For shot peening, the effect of treatment on both directions is almost identical. The depth of compressive stress layer in A572 Grade 50 steel (USA specification) was 1.5-1.7 mm for UIT and ~0.8mm for shot peening [13].

E.2.3 Fatigue Improvement from Hammer Peening

During the bridge retrofit of the Yellow Mill Pond Bridge on the Connecticut Turnpike in Bridgeport, specimens retrofitted by air hammer peening in 1976 achieved a significant improvement in fatigue strength even though the details had experienced an estimated 56 million cycles of truck traffic after their retrofit. The fatigue resistance of all weld toe details were improved to Category C from Category E'. This shows that air hammer peening can prevent reinitiation of fatigue cracks at treated weld toes. Measurements indicate that the stress cycle range was below 69 MPa (10 ksi). UIT application to the same welds details in 1997 and fatigue tested at a 10 ksi stress range improved the connections to Category B [20]. Hence, UIT application results in a higher fatigue category than hammer peening.

E.3 TIG REMELTING

TIG (tungsten inert gas) remelting is also known as GTA (gas tungsten arc) remelting. TIG was accomplished in 1976 by manually moving the nonconsumable tungsten electrode at a constant rate along the weld toe. This process removes small discontinuities such as slag inclusions and undercuts, as well as modifies the global profile of the fillet weld toe. TIG can be used to repair existing fatigue cracks.

When a cracked weld toe is repaired, a sufficient volume of weld and base metal adjacent to the weld toe must be melted to completely eliminate the preexisting crack during solidification. If the crack is not completely eliminated, the embedded crack will quickly propagate through the remelted zone. TIG can also stop developing fatigue cracks. Fatigue tests in NCHRP Report 206 demonstrated that TIG remelting was more effective and less dependant on minimum stress than air hammer peening at arresting fatigue cracks. However the TIG remelting required greater skill and better accessibility than air hammer peening, especially in fatigue crack repair [20].

TIG dressing procedures are selected according to IIW recommendations. TIG dressing is performed in one pass at room temperature without preheating when the strength of the material is not high [11].

E.3.1 Fatigue Crack Initiation from TIG Only

In Weldom 420 steel (Russian specification) welded specimens treated with TIG dressing, fatigue cracks initiated on the plate surface approximately 5 mm away from the TIG dressed area [15, 16].

E.3.2 Weld Toe Geometry Improvement from TIG Remelting

Table E.3.2.1 shows that TIG dressing is more effective at improving the weld toe geometry than UIT because the increase in ρ and the decrease in θ result in a reduction of the stress concentration factor.

Table E.3.2.1 Comparison of the Geometry Characteristics of Q235B Cruciform Joints [11]

Condition	Mean radius ρ (mm)	Mean obtuse angle θ	Mean weld height (mm)	Mean weld width (mm)
As-welded	0.35	47	8.5	8.8
UIT	2	47	8.5	8.8
TIG dressed	3.5	30.5	8.5	9.1

E.3.3 Hardness from TIG Remelting

Vickers hardness was measured under 10 kg for different zones of the as-welded, UIT peened, and TIG dressed joints [11]. In the crack initiation zone of Q235B (Chinese specification) welded and UIT peened butt joints, UIT increased the hardness by 7% (from 193 to 207). However, TIG dressing increased the hardness by 30% (from 193 to 251) [11]. Hence, TIG dressing was more beneficial than UIT to improve fatigue strength when only hardness was considered.

E.3.4 Residual Stresses of TIG Remelting

The blind hole-drilling method was used for measuring the residual stresses at the weld toes of the TIG dressed and UIT peened Q235B steel (Chinese specification) cruciform joint specimens. Results showed that TIG dressing

introduces tensile residual stresses (transverse stress value was 174 MPa) while UIT introduces compressive residual stresses (transverse stress value was -271 MPa) [11]. Thus, in the light of residual stresses, UIT was more effective than TIG dressing.

E.3.5 Fatigue Improvement from TIG Remelting

From Table E.3.5.1 it can be seen that, when compared with the as-welded joints, the fatigue strength at 2 million cycles of TIG dressed joints increased by 51% and that of UIT peened joints increased by 64% [11]. Since TIG improves weld profile and hardness more than UIT, the fact that UIT improves fatigue strength more than TIG can most likely be attributed to the compressive stresses induced by UIT, since TIG induces more harmful tensile stresses. Therefore, UIT is more effective than TIG at improving the fatigue strength of Q235B steel welded with a J422 electrode (China specification).

Table E.3.5.1 Comparison of Fatigue Limits of Q235B Cruciform Joints [11]

Condition	Fatigue strength (MPa) at 2×10^6 cycles	Improvement (%)
As-welded	143	-
UIT	234	64
TIG dressed	214.5	50.5

Other research shows that TIG improves fatigue strength of Weldox 420 steel (Swedish specification) with multi-pass welds at 2×10^6 cycles from as-welded by 41% to 51%, while UIT application with a 3 mm diameter pin in the multi-pin UIT tool improves the fatigue strength of the same specimens at 2×10^6

cycles from as-welded by 65% [16]. Therefore, UIT is more effective than TIG at improving the fatigue strength of Weldox 420 steel.

As visible in Table E.3.5.2, fatigue life improvement by TIG followed by UIT varies with stress range. In the high stress range (e.g., stress range = 308 MPa), the fatigue life of TIG dressed joints is longer than that of UIT peened joints. However, in the lower stress range (e.g., stress range = 182 MPa), the fatigue life of the UIT peened joints was longer than that of TIG joints [11]. Therefore UIT is more efficient than TIG for improving the fatigue life at lower stress ranges, but at higher stress ranges TIG dressing may be more efficient.

Table E.3.5.2 Comparison of Fatigue Life of Q235B Cruciform Joints [11]

Condition	Stress Range (MPa)	Life (cycles) x106	Improvement
As-welded	308	0.03	-
UIT	308	0.058	x 1.9
TIG dressed	308	0.185	x 6.2
As-welded	268	0.06	-
UIT	268	0.425	x 7.1
TIG dressed	268	0.423	x 7.1
As-welded	212	0.1	-
UIT	212	8.93	x 89.3
TIG dressed	212	1.02	x 10.2
As-welded	182	0.246	-
UIT	182	119	x 483.7
TIG dressed	182	10	x 40.7

E.4 TIG REMELTING FOLLOWED BY UIT

E.4.1 Fatigue Crack Initiation from TIG Followed by UIT

For the majority of the specimens treated with TIG dressing followed by UIT fatigue cracks initiated on the plate surface approximately 5 mm away from the TIG dressed area. Specimens were Weldox 420 and Weldox 700 (Swedish specification) fillet welds. A few specimens failed in the plate outside the weld zone [3, 15, 16]. One specimen had crack initiation at the root of the weld at the end of the attachment [3].

E.4.2 Fatigue Improvement from TIG Followed by UIT

The combined treatment of TIG dressing followed by UIT on Weldox 700 high strength steel (Swedish specification) fillet-welded joints gave the highest improvement out of as welded, UI-treated, TIG followed by UIT, and TIG dressing only. The fatigue strength at 2×10^6 cycles of Weldox 400 fillet welded specimens improved 135% for steel specimens treated with TIG followed by UIT [3].

The results indicate that there is some difference between specimens treated by UIT alone and specimens treated by TIG dressing followed by UIT. But in the long life region the difference is small and probably not statistically significant.

E.5 SAND BLASTING

Specimens were either subjected to sand blasting treatment by using cylindrical charges of a DShaA-12 explosive mounted along the welded joint on plasticine pads [8], or traditional sand blasting. The sand blasting operation gives a significant fatigue improvement by the introduction of residual stresses similar to shot peening [9].

E.5.1 Fatigue Strength Enhancement

The effect of hardening caused by blasting treatment remains practically constant within the entire range of loading cycles. UIT increases fatigue strength by 20% with each increasing range of cycles. Hence, UIT increases fatigue strength of 14Kh2GMR and 12GN2MFAYu steel T-joints and 15KhSND and 09G2S butt joints (Ukrainian specification) more efficiently with increasing number of fatigue cycles than sand blasting [8].

For Usiform 355 and 700 (French specification) fillet welds, UIT produces consistently higher fatigue strength than sand blasting at both low and high cycle fatigue parameters. As shown in Table E.5.1.1 and Table E.5.1.2, UIT gave consistently about twice as much improvement in fatigue strength as sand blasting.

Table E.5.1.1 Percentage of Improvement at 2,000,000 and 200,000 cycles [9]

Cycles	Usiform 355		Usiform 355	
	Improvement (%)		Improvement (%)	
	Sand Blasting	UIT	Sand Blasting	UIT
2,000,000	16	52	64	127
200,000	25	50	35	67

Table E.5.1.2 Endurance Limits for Usiform 355 and Usiform 700 (French specification) at 2,000,000 and 200,000 Cycles [9]

Cycles	Usiform 355			Usiform 355		
	Stress (MPa)			Stress (MPa)		
	As-welded	Sand Blasting	UIT	As-welded	Sand Blasting	UIT
2,000,000	250	290	380	220	360	500
200,000	320	400	480	370	500	620

E.6 LOW TRANSFORMATION TEMPERATURE ELECTRODES

Six kinds of low transformation temperature electrodes (LTTE) were considered for use. They were assessed on the basis of expansion strain measurements and the magnitude of the residual stress induced. LTTE3 was chosen because its maximum transformation expansion strain was 0.63% and M_s (the temperature at which the transformation from austenite to martensite begins) was 191°, which are desirable traits in comparison to LTTE 1 through 6 [12].

E.6.1 Fatigue Improvement from LTTE3

The increase in fatigue strength at 2 million cycles of the Q235B steel (Chinese specification) butt-welded joints after UIT application was 50%, while the increase in fatigue strength at 2×10^6 cycles for the fillet welded joints was 71%. However, the increases in fatigue strengths of the butt and fillet joints welded with LTTE3 were only 11% and 41% respectively [4].

A maximum fatigue life improvement from LTTE on any specimen was an improvement of 25 times was obtained for specimens with longitudinal gussets fillet welded with LTTE3 [4].

Between UIT and LTTE3, UIT is the more effective for improving the fatigue properties of transverse butt and longitudinal fillet welded joints in Q235B steel [4]. However, UIT does require the use of an extra process after welding. It may not be economically viable to apply a post-weld improvement technique to a very large welded structure. In view of this, the less effective but more economic option of using LTTE welding has merit, particularly in the case of longitudinal fillet welds operating in the high-cycle fatigue regime.

E.7 CONCLUSION

UIT effectively improves fatigue life, endurance limit, and fatigue strength of all steels and welds tested to date. UIT improves fatigue properties of steels and welds more efficiently than competitive conventional weld improvement techniques. UIT has potential to eliminate weld details as the weakest link in steel projects, opening the door for higher strength steels to be developed and for more possibilities in welded structures.

References

1. Statnikov ES. Applicatoinis of Operational Ultrasonic Impact Treatment (UIT) Technologies in Production of Welded Joints. IIW/IIS Document XIII-1667-97.
2. E. Sh. Statnikov et al., *Ultrasonic Impact tool for strengthening welds and reducing residual stresses*, New Physical Methods of Intensification of Technological Processes. 1977.
3. Haagensen PJ, Statnikov ES, Lopez-Martinez L. Introductory Fatigue Tests on Welded Joints in High Strength Steel and Aluminum Improved by Various Methods Including Ultrasonic Impact Treatment (UIT). IIW Doc. XIII-1748-98, 1998.
4. Lixing H, Dongpo W, Wenxian W, Yufeng Z. Ultrasonic Peening and Low Transformation Temperature Electrodes Used for Improving the Fatigue Strength of Welded Joints. *Welding in the World* 2004; 48(3-4): 34-39.
5. Roy S, Fisher JW, Yen BT. Fatigue Resistance of Welded Details Enhanced by Ultrasonic Impact Treatment (UIT). *International Journal of Fatigue* 2003; 25(9-11): 1239-1247.
6. Bezborodov VP, Klimenov VA, Pleshanov VS, Nekhoroshkov ON, Gorodishchenskii PA. Effect of Ultrasonic Treatment on the Structure and Properties of Welded Joints in 12Kh1MF Heat Resistant Steel. *Russian Ultrasonics (Svarochnoe Proizvodstvo)* 2000; 7(17-21): 117-125.
7. Mikheev PP, Nedoseka AY, Parkhomenko IV, Kuz'menko AZ, Statnikov ES, Senyukov VL, Chernetsov GP, Skvortsov VS. Effectiveness of Ultrasonic Treatment for Increasing the Fatigue Resistance of Welds. *Russian Ultrasonics* 1985; 15(4):70-75.
8. Degtyarev VA, Shul'ginov BS. Estimation of the Efficiency of Methods Aimed at Increasing the Fatigue Resistance of Welded Joints Under Impact Loading at Low Temperatures. *Strength of Materials* 2000; 32(6): 571-576.
9. Galtier A, Statnikov ES. The Influence of Ultrasonic Impact Treatment on Fatigue Behaviour of Welded Joints in High-Strength Steel. *Welding in the World* 2004; 48(5-6):1-66.

10. Janosch JJ, Koneczny H, Debiez S, Statnikov EC, Troufiakov VJ, Mikhee PP. Improvement of Fatigue Strength in Welded Joints (in HSS and in aluminum Alloys) by Ultrasonic Hammer Peening. *Welding in the World* 1996; 37(2): 72-83.
11. Lixing H, Dongpo W, Yufeng Z, Junmei C. Investigation on Improving Fatigue Properties of Welded Joints by Ultrasonic Peening Method. *Welding in the World* 2001; 45(3-4): 4-8.
12. Lihavainen VM, Marquis G, Statnikov ES. Fatigue Strength of a Longitudinal Attachment Improved by Ultrasonic Impact Treatment. *Welding in the World* 2004; 48(5-6): 67-73.
13. Cheng X, Fisher JW, Prask HJ, Gnaupel-Herold T, Yen BT, Roy S. Residual Stress Modification by Post-Weld Treatment and Its Beneficial Effect on Fatigue Strength of Welded Structures. *International Journal of Fatigue* 2003; 25(9-11): 1259-1269.
14. Fisher JW, Statnikov E, Tehini L. Fatigue Strength Enhancement by Means of Weld Design Change and the Application of Ultrasonic Impact Treatment. *Proceedings of the National Steel Bridge Alliance World Steel Bridge Symposium, Chicago, October 2001.*
15. Statnikov ES, Muktepavel VO, Trufyakov VI, Mikheev PP, Kuzmenko AZ, Blomqvist A. Efficiency Evaluation of Ultrasonic Impact Treatment (UIT) of Welded Joints in Weldox 420 Steel in Accordance with the IIW Program. *IIW/IIS Document XIII-1817-00.*
16. Statnikov ES, Muktepavel VO, Blomqvist A. Comparison of Ultrasonic Impact Treatment (UIT) and Other Fatigue Life Improvement Methods. *Welding in the World* 2002; 46(3-4): 20-32.
17. Statnikov ES. Guide for Application of Ultrasonic Impact Treatment Improving Fatigue Life of Welded Structures. *IIW/IIS Document XIII-1757-99.*
18. Rice L. Reviews of Acoustical Patents. *Journal of the Acoustical Society of America* 2003; 114(6): 2984.
19. Tryfyakov VI, Mikheev PP, Kudryavtsev YF. Ultrasonic Impact Peening Treatment of Welds and Its Effect on Fatigue Resistance in Air and Seawater. *Proceedings of the Annual Offshore Technology Conference, part 4, 1993: 183-187.*

20. Takamori H, Fisher JW. Tests of Large Girders Treated to Enhance Fatigue Strength. Transportation Research Record 1696, Transportation Research Board, 2000.
21. Fisher JW, Statnikov E, Tehini F. Fatigue Strength Improvement of Bridge Girders by Ultrasonic Impact Treatment (UIT). Welding in the World (Le Soudage Dans Le Monde) 2002; 46(9-10): 34-40.
22. Kudryavtsev Y. Optimum Application of Ultrasonic Peening. Integrity testing Laboratory Inc. www-tm.wbmt.tudelft.nl.
23. Statnikov ES, Vityazev VN, Korolkov OV. Study of Comparative Characteristics of Ultrasonic Impact and Optimization of Deformation Treatment Processes. Proceedings of the World Congress on Ultrasonics 2003, Paris, September 7-10, 2003.
24. Sizova OV, Kolubaev EA. Effect of Ultrasonic Treatment on Pearlite Structure and Properties. Russian Physics Journal 2003; 46(2): 133-137.
25. The Lincoln Electric Company, "The Procedure Handbook of Arc Welding". The Lincoln Electric Company, Cleveland, Ohio, 1973.
26. Trufiakov VI, Statnikov ES, Mikheev PP, Kuzmenko AZ. The Efficiency of Ultrasonic Impact Treatment for Improving the Fatigue Strength of Welded Joints. IIW Document XIII-1745-98.
27. Wright, W. Post-Weld Treatment of a Welded Bridge Girder by Ultrasonic Impact Treatment. FHWA, Turner-Fairbanks test report, September 29, 1996.
28. Koenigs, M.T.K. Fatigue Resistance of Traffic Signal Mast-Arm Connection Details. Masters of Science in Engineering Thesis, The University of Texas at Austin, May, 2003.
29. Freytag, D., Frank, K 2004. 'Fatigue Tests of Signal Mast Arms with Ultrasonic Impact Treated Welds', paper presented to the University of Texas at Austin.
30. Freytag, D., Frank, K 2004. 'Fatigue Tests of Signal Mast Arms', paper presented to the University of Texas of Texas at Austin.
31. Koenigs, M.T. 2003. 'Finite Element Analyses done on Mast Arm Connections', paper presented to the University of Texas at Austin.

VITA

Amanda Hope Palmatier was born in Summit, New Jersey on January 15, 1980 to Elizabeth and Richard Palmatier. Following graduation from Scotch Plains-Fanwood High School in June of 1998, Amanda matriculated to Rutgers University. After two years pursuing a BS in Biology, Amanda switched majors to Civil Engineering. During her time at Rutgers University, Amanda worked part time at the construction company of Conti Enterprises, Inc., in Piscataway, NJ, and at the geotechnical consulting company of Soilteknik in Piscataway, NJ. Amanda was also President of Chi Epsilon at Rutgers from Autumn of 2002 until Spring of 2003. Amanda graduated from the School of Engineering at Rutgers University in May of 2003 with her Bachelors of Science in Civil Engineering, with high honors. Amanda enrolled at the University of Texas at Austin in August of 2003.

Permanent Address: 2274 Jersey Ave
Scotch Plains, NJ 07076
amandapalmatier@yahoo.com

This thesis was typed by the author.